

CALIFORNIA INSTITUTE OF TECHNOLOGY
Pasadena, California

Antenna Laboratory
Technical Report No. 28

A THEORETICAL STUDY OF THE SCATTERING OF
ELECTROMAGNETIC IMPULSES BY FINITE OBSTACLES

W. P. Brown, Jr.

Research supported by
the U. S. Air Force Office of Scientific Research

June 1962

ABSTRACT

A general approach to the solution of pulse scattering by finite obstacles is formulated. The essential feature of this approach is the identification and separate treatment of the individual terms in a wavefront expansion of the transforms of the field vectors. It is demonstrated that the dispersive effect of a finite conductivity in the scattering obstacle can be neglected for all metals but that it may be significant for poorly conducting materials such as dry earth. The wavefront technique is employed to solve the problems of the transmission of a delta pulse through a conducting dielectric slab and the reflection and diffraction of a delta pulse from a perfectly conducting sphere. The transmission problem results provide a convenient example of the usefulness of the wavefront approach. The results for the sphere problem indicate that the nature of the waves observed at a given spatial point change in time. It is shown that the penumbra and the caustic region in the vicinity of the focal line $\theta = \pi$ are initially of zero extent. The rates of expansion of these regions with increasing time are obtained by a consideration of the error terms in the asymptotic expansions of the fields. The temporal behavior of the near and far field zones is obtained in a similar manner.

TABLE OF CONTENTS

ABSTRACT

I	INTRODUCTION	1
II	A GENERAL APPROACH TO THE PROBLEM OF PULSE DIFFRACTION	5
	2.1 The Laplace Transform of Maxwell's Equations and the Boundary Conditions	5
	2.2 Expression of the Transformed Field Quantities as a Series of Terms Determined by the Optical Wavefronts	9
	2.3 Behavior of the Fields in the Vicinity of the Wavefronts	12
	2.4 Behavior of the Fields when $t - T_m^0(\underline{r}) \gg 1$	14
III	THE DISPERSIVE EFFECT OF A FINITE CONDUCTIVITY	18
	3.1 Introduction	18
	3.2 The Reflection of a Delta Pulse from a Semi- Infinite Imperfect Dielectric	19
	3.3 Some General Conclusions about the Dispersive Effect of a Finite Conductivity	27
IV	A SIMPLE EXAMPLE OF THE METHOD OF SOLUTION WHEN MORE THAN ONE OPTICAL RAY IS PRESENT: THE TRANSMISSION OF A DELTA PULSE THROUGH A CONDUCTING DIELECTRIC SLAB	30
	4.1 Introduction	30
	4.2 Derivation of the Transforms of the Field Vectors	31
	4.3 A Discussion of the Alternative Methods Available for the Solution of the Inversion Integral	34
	4.4 Inversion of the First Term in the Wavefront Expansion when $\sigma \neq 0$	38
V	A COMPLICATED EXAMPLE OF THE METHOD OF SOLUTION WHEN MORE THAN ONE OPTICAL RAY IS PRESENT: REFLECTION AND DIFFRACTION OF A DELTA PULSE BY A PERFECTLY CONDUCTING SPHERE	45
	5.1 Introduction	45
	5.2 Derivation of the Transforms of the Field Vectors	47
	5.3 Investigation of the Properties of the Transforms for $s \gg 1$, $\text{Re}(s) > 0$	51
	5.4 Derivation of the Asymptotic Estimates of the Transforms for Large s	59

5.5	Behavior of the Fields in the Vicinity of the Wavefronts	103
5.6	Large Time Behavior of the Fields	110
VI	SUMMARY AND CONCLUSIONS	113
APPENDICES		
I	ASYMPTOTIC EXPANSIONS OF THE HANKEL FUNCTIONS $H_{\nu}^{(1,2)}(i\rho)$	116
II	AIRY INTEGRALS	134
III	ASYMPTOTIC EXPANSION OF THE ANGULAR FUNCTION $P_{\nu - \frac{1}{2}}^1(-\cos \theta)$	140
	REFERENCES	143

I. INTRODUCTION

Electromagnetic waves are seldom of a completely monochromatic character. The signals generated in the laboratory and by natural causes are predominantly of a transient nature. Quite often it is possible to adequately describe the interaction of these waves with matter by a steady state analysis. Sometimes, however, the departure from equilibrium may be significant. It might also be desired to employ a transient analysis in order to obtain more information than is available from a steady state theory. The distortion of a pulse returned from a scattering obstacle might possibly yield some additional information pertaining to the properties of the scatterer. The behavior of the leading edge of a scattered pulse usually indicates something about the composition of the body. The behavior of the trailing edge of a scattered pulse is related to the shape of the body and its radii of curvature.

In addition to the fact that practical problems are seldom of a steady state nature, there is a much more fundamental reason for the interest in transient electromagnetic theory. The pulse solution of a scattering problem yields a better understanding of the physics of the steady state problem. The existence of the generalized rays of geometric optics is easily demonstrated from a consideration of the transient scattering problem for a finite obstacle. Likewise, the coefficients in the familiar Kline-Luneberg expansion of steady state diffraction theory are intimately related to the solution of the corresponding pulse problem.

One of the earliest works related to solution of transient electromagnetic problems was written by Hadamard [1903]. In his book Lecons sur la propagation des ondes, Hadamard demonstrated that pulse fronts are characteristics of the wave equation. In subsequent papers a favorite topic was the scattering of pulses by a half plane or wedge. This problem was first considered by Sommerfeld [1901] and Lamb [1910]. Some more recent investigations of this problem have been performed by Friedlander [1941], Keller and Blank [1951], and Kay [1953]. Friedlander has made a rather comprehensive study of transient sound problems. In his book, Sound Pulses [1958], he discusses the solution of the scalar wave equation for waves reflected and diffracted by wedges, cylinders, and spheres. Friedlander's results are valid, however, only in the immediate vicinity of the wavefronts. The results obtained for the sphere and the cylinder do not include those for the transitional region between the shadow and the illuminated region. The transient problem for the sphere has also been considered by Levy and Keller [1957] and Weston (12)[1959]. Levy and Keller considered the propagation of a pulse around the surface of the earth. The results which they obtained are valid for short times after the arrival of the wavefront. Weston solved the problem of the backscattering of a pulse by a smooth sphere. His results are valid for all times but the solution is in such a form that the large time behavior is not at all evident.

The literature summarized in the above paragraph provides an excellent basis for the understanding of most of the fundamental aspects of transient electromagnetic theory. There are some problems, however, which merit additional attention. There is a need for the formulation of a general approach to the solution of pulse scattering from finite

obstacles. Quite often the straightforward obvious method does not yield results which are easily interpreted. In the present paper, the physics of the scattering process is employed to suggest a technique which should simplify the solution of these problems. It is also felt that some useful information can be obtained from a more detailed and systematic approach to the problem of pulse scattering by a sphere. The previous results for this problem have been restricted to particular time and spatial domains. This makes it very difficult to obtain a general over-all feeling for the physics of the transient scattering phenomena. The general method discussed in the initial portions of this paper will be employed to obtain the desired solution of the sphere problem.

The text of this paper is divided into four parts. Chapter II is devoted to a discussion of a general technique of solution for transient electromagnetic scattering problems of the type mentioned above. The crucial part of this technique involves the identification and separate consideration of the terms in the field transforms which correspond to the various rays in the generalized theory of diffraction. The dispersive effect of a finite conductivity in the scattering obstacle is investigated in Chapter III. The results for the reflection of a delta pulse from a semi-infinite conducting dielectric are employed to obtain some general conclusions about the significance of the signal distortion due to a finite conductivity. A simple example of the application of the technique developed in Chapter II is given in Chapter IV. The superiority of the wavefront approach is demonstrated by contrasting the solutions to the problem of the transmission of a delta pulse through a conducting slab obtained by the wavefront approach and by the conventional

approach. The results for the transmission problem are also of some practical significance. They are relevant to the problem of shielding equipment from non-monochromatic signals.

A very comprehensive investigation of the scattering of a delta pulse by a sphere is made in Chapter V . Results are obtained for all regions of space and for both large and small times. The change in the time behavior of the waves as the observer proceeds from the deep shadow to the penumbra to the illuminated region is demonstrated. In the process of obtaining these results, an asymptotic expansion of fields in the illuminated region was obtained by a saddle point integration. These results are valid in the near zone as well as the far zone. Analytic continuation of these results will provide an expansion which is useful in the steady state problem of near zone scattering.

II. A GENERAL APPROACH TO THE PROBLEM OF PULSE DIFFRACTION

2.1 The Laplace Transform of Maxwell's Equations and the Boundary Conditions.

The solution of non steady state problems in electromagnetic theory is facilitated if a transform type approach is employed. There is some latitude in the choice of the particular transform method to be used in a given problem. In some problems a Fourier transform is particularly convenient, whereas, in others, a Laplace transform must be employed. Since the Laplace transform is defined for a wider class of functions than the Fourier transform, it will be employed throughout this paper. Actually, since this paper is concerned with sources which have a delta function time dependence, the Fourier transform method could be used just as easily as the Laplace method. It is felt, however, that a Laplace transform formulation lends itself to an extension to more complicated source dependence better than the Fourier transform.

The Laplace transform of a function $F(t)$ is defined by the relation

$$\mathcal{L}[F(t)] = \int_0^{\infty} F(t) e^{-st} dt \equiv \mathcal{F}(s) \quad (2.1)$$

The inversion from the s domain to the t domain is accomplished by means of the relation

$$\mathcal{L}^{-1}[\mathcal{F}(s)] = \frac{1}{2\pi i} \int_{\Delta - i\infty}^{\Delta + i\infty} \mathcal{F}(s) e^{st} ds \quad , \quad (2.2)$$

where Δ is chosen such that $\mathcal{F}(s)$ is analytic for $\text{Re}(s) \geq \Delta$. The transform of $F^n(t)$ is given by

$$[F^n(t)] = s^n \mathcal{F}(s) - \sum_{\ell=0}^{n-1} s^{n-\ell-1} F^\ell(0) \quad (2.3)$$

In a region free of charge the electromagnetic field vectors satisfy the system of equations

$$\nabla \times \underline{E}(\underline{r}, t) = - \frac{\partial}{\partial t} \underline{B}(\underline{r}, t) \quad , \quad (2.3)$$

$$\nabla \times \underline{H}(\underline{r}, t) = \frac{\partial}{\partial t} \underline{D}(\underline{r}, t) + \underline{J}(\underline{r}, t) \quad (2.4)$$

$$\nabla \cdot \underline{B}(\underline{r}, t) = 0 \quad (2.5)$$

$$\nabla \cdot \underline{D}(\underline{r}, t) = 0 \quad (2.6)$$

$$\underline{B}(\underline{r}, t) = \mu \underline{H}(\underline{r}, t) \quad , \quad \underline{D}(\underline{r}, t) = \epsilon \underline{E}(\underline{r}, t) \quad . \quad (2.7)$$

In all of the work which follows it will be assumed that the medium in which the field vectors are defined is homogeneous, isotropic and non-dispersive. Also the current $\underline{J}(\underline{r}, t)$ will be assumed to be an induced conduction current $\sigma \underline{E}(\underline{r}, t)$. The Laplace transform of the set of equations which pertains to a medium of the type described above is given in the set of equations 2.8 - 2.12. In these equations the Laplace transform of a field vector is denoted by a script letter.

$$\nabla \times \underline{\xi}(\underline{r}, s) = - \mu s \underline{H}(\underline{r}, s) + \mu \underline{H}(\underline{r}, 0) \quad , \quad (2.8)$$

$$\nabla \times \underline{H}(\underline{r}, s) = (\sigma + \epsilon s) \underline{\xi}(\underline{r}, s) - \epsilon \underline{E}(\underline{r}, 0) \quad (2.9)$$

$$\nabla \cdot \underline{H}(\underline{r}, s) = 0 \quad (2.10)$$

$$\nabla \cdot \underline{\xi}(\underline{r}, s) = 0 \quad (2.11)$$

$$\underline{B}(\underline{r}, s) = \mu \underline{H}(\underline{r}, s) \quad , \quad \underline{D}(\underline{r}, s) = \epsilon \underline{\xi}(\underline{r}, s) \quad . \quad (2.12)$$

A vector wave equation can be derived from the relations 2.8, 2.9 by taking the curl of these equations. The result is simplified by using

equations 2.3 and 2.4 to express the curl of the initial values. The vector wave equation satisfied by the transformed field vector $\underline{\xi}(\underline{r}, s)$ is given by

$$\nabla \times \nabla \times \underline{\xi}(\underline{r}, s) + \frac{s^2}{c^2} \left(1 + \frac{\sigma}{\epsilon_B}\right) \underline{\xi}(\underline{r}, s) = \frac{s}{c^2} \left(1 + \frac{\sigma}{\epsilon_B}\right) \underline{E}(\underline{r}, 0) + \frac{1}{c^2} \frac{\partial}{\partial t} \underline{E}(\underline{r}, 0) \quad (2.13)$$

where $\mu\epsilon \equiv \frac{1}{c^2}$. The equation for the transformed magnetic field vector $\underline{H}(\underline{r}, s)$ is given by 2.13 with $\underline{\xi}$ replaced by \underline{H} and \underline{E} replaced by \underline{H} . If the quantity of interest is the scattered field, it is always possible to define the time origin such that the initial values of the scattered field are zero everywhere in space. Consequently, the transform of the field vector of the scattered electric field satisfies the homogeneous vector wave equation

$$\nabla \times \nabla \times \underline{\xi}^*(\underline{r}, s) + \frac{s^2}{c^2} \left(1 + \frac{\sigma}{\epsilon_B}\right) \underline{\xi}^*(\underline{r}, s) = 0 \quad (2.14)$$

where the superscript $*$ denotes the scattered component of the field vector.

The boundary conditions satisfied by the electromagnetic field vectors at the interface of two media are given by the familiar relations

a) Both media of finite conductivity:

$$\underline{n} \times (\underline{E}_2(\underline{r}, t) - \underline{E}_1(\underline{r}, t)) = 0 \quad (2.15)$$

$$\underline{n} \times (\underline{H}_2(\underline{r}, t) - \underline{H}_1(\underline{r}, t)) = 0. \quad (2.16)$$

b) Medium 1 being a perfect conductor:

$$\underline{n} \times \underline{E}_2(\underline{r}, t) = 0 \quad (2.17)$$

$$\underline{n} \times \underline{H}_2(\underline{r}, t) = \underline{K}(\underline{r}, t) = \text{surface current density.} \quad (2.18)$$

In these equations the vector \underline{n} is a unit vector normal to the interface

and directed from medium 1 into 2. When the Laplace transform of these equations is taken they assume the form

a) Both media finite conductivity:

$$\underline{n} \times (\underline{\mathcal{E}}_2(\underline{r},s) - \underline{\mathcal{E}}_1(\underline{r},s)) = 0 \quad (2.19)$$

$$\underline{n} \times (\underline{\mathcal{H}}_2(\underline{r},s) - \underline{\mathcal{H}}_1(\underline{r},s)) = 0 \quad . \quad (2.20)$$

b) Medium 1 being a perfect conductor:

$$\underline{n} \times \underline{\mathcal{E}}_2(\underline{r},s) = 0 \quad (2.21)$$

$$\underline{n} \times \underline{\mathcal{H}}_2(\underline{r},s) = \underline{K}(\underline{r},s) \quad . \quad (2.22)$$

The application of the approximate Leontovitch boundary conditions, $\underline{n} \times \underline{E}(\underline{r},t) = Z \underline{n} \times \underline{H}(\underline{r},t)$ where Z = surface impedance, to the problem of pulse diffraction must be approached with care. The error introduced by the application of the Leontovitch conditions in the solution of the diffraction of a monochromatic wave of wave number k by a curved obstacle of curvature ρ and refractive index n is of the order $(nk\rho)^{-1}$ (7). An analytic continuation of this result into the s plane indicates that the error introduced in the determination of the transformed field quantities by a Leontovitch boundary condition will be of the order $(n \frac{s\rho}{c})^{-1}$. It will presently be shown that the behavior of the scattered fields in the vicinity of the wavefronts is related to the asymptotic behavior of the transformed field quantities for large values of the transform variable s . It appears that the application of a Leontovitch type boundary condition introduces negligible error if the fields are desired in the vicinity of the wavefronts. The behavior of the fields a long time after the arrival of the wavefront, however, is related to the behavior of transform field quantities for small values of the transform variable s . Consequently, it appears that the application of a Leontovitch type boundary condition will lead to erroneous results for the field vectors when the time measured from the arrival of the wavefront is large.

2.2 Expression of the Transformed Field Quantities as a Series of Terms Determined by the Optical Wavefronts

In steady state electromagnetic theory it has been shown that the field scattered from an obstacle can be obtained by summing the contribution due to the various optical rays associated with the obstacle (8). When $k\rho \gg 1$, where k is the wave number of the incident field and ρ is the minimum value of the radius of curvature of obstacle, the series of optical contributions converges very rapidly. In this theory it is necessary to accept the existence of some rather unusual optical rays in addition to the conventional rays of geometric optics. The additional rays satisfy an extension of Fermat's principle. In order to simplify the discussion of these rays consider the ray system depicted in Figure 2.1. The ray O^r is the conventional geometric optics result where the position of the specular point τ is determined by the requirement that the optical distance measured from the reference plane to the obstacle to $P(x,y,z)$ is a minimum. The additional rays which appear in the generalized theory of geometrical optics are the rays S_{1m} and S_{2m} . These rays originate at the shadow boundaries S_1 and S_2 and travel along the surface of the obstacle and leave the surface at the points T_1 and T_2 determined by the two tangents from $P(x,y,z)$ to the surface of the obstacle. The m^{th} term in the sum $\sum_{n=0}^{\infty} S_{im}$ ($i=1,2$) is associated with the ray which undergoes m complete circulations around the obstacle and then travels to $P(x,y,z)$. The path on the obstacle taken by each of these rays is determined by the condition that the optical distance be a minimum.

It is known that the wavefronts of non-monochromatic waves satisfy geometrical optics. This fact, in conjunction with the above description

of the diffraction process, leads to the hypothesis that the solution of the pulse diffraction problem will be facilitated if the terms corresponding to the various monochromatic optical rays are identified and treated separately. A reasonable indication of the credibility of this hypothesis is the fact that at a finite time T after the arrival of the first signal at $P(x,y,z)$ there are only a finite number of possible optical ray contributions to the field. All of the rays which have time delays greater than T are absent. A direct inversion of the Laplace transform without taking the physics of the rays into consideration, will yield a correct answer. The work involved in deciphering the meaning of the result, however, will be considerable. The result usually is expressed in the form of an infinite sum of residue contributions and branch cut integrations. These individual contributions must then be summed in a manner such that the rays $\sum_{m=n}^{\infty} S_{im}$ ($i=1,2$) are absent for $t < T_n$. In all but the simplest of diffraction problems, this is a very difficult thing to accomplish. Consequently, it seems that the solution of the pulse diffraction problem can be handled most efficiently by treating each term in a wavefront expansion separately.

The solution of the vector wave equation 2.14 is obtained in the same manner as the solution of the vector wave equation for monochromatic fields. The transform of the field vector $\underline{\xi}^*(\underline{r},s)$ can be expressed as the result of some vector operations on two scalar functions which are solutions of a scalar wave equation. Consequently, in discussing the decomposition of the field into its optical components, it will suffice to investigate the behavior of a scalar function $\mathfrak{J}(\underline{r},s)$ which satisfies the scalar wave equation

$$\nabla^2 \mathfrak{J}(\underline{r},s) - \frac{s^2}{c^2} \left(1 + \frac{\sigma}{\epsilon_S}\right) \mathfrak{J}(\underline{r},s) = 0 . \quad (2.23)$$

It is desired to write the solution of 2.23 in the form of a sum of terms which can be identified with the optical wave fronts. The requirement that each of the terms be zero for time delays less than some specified minimum time necessitates that $\mathfrak{J}(\underline{r}, s)$ be expressible in the form

$$\mathfrak{J}(\underline{r}, s) = \sum_{n=0}^{\infty} \mathcal{U}_m(\underline{r}, s) e^{-s(1 + \frac{\sigma}{\epsilon s})^{1/2} T_m^0(\underline{r})} = \sum_{m=0}^{\infty} \mathfrak{J}_m(\underline{r}, s) . \quad (2.24)$$

When equation 2.24 is substituted in 2.23, the following relation is obtained

$$\sum_{m=0}^{\infty} \left[\nabla^2 - \frac{s^2}{c^2} \left(1 + \frac{\sigma}{\epsilon s} \right) \right] \mathfrak{J}_m(\underline{r}, s) = 0 , \quad (2.25)$$

and this requires that each term in the sum vanish separately. If the operator in the brackets in 2.25 is applied to $\mathfrak{J}_m(\underline{r}, s)$ and the result equated to zero, it is found that the functions $\mathcal{U}_m(\underline{r}, s)$ must satisfy the relation

$$s^2 \left(1 + \frac{\sigma}{\epsilon s} \right) \left[|\nabla T_m^0|^2 - \frac{1}{c^2} \right] \mathcal{U}_m(\underline{r}, s) - s \left(1 + \frac{\sigma}{\epsilon s} \right)^{1/2} \left[2 \nabla \mathcal{U}_m \cdot \nabla T_m^0 + \mathcal{U}_m \nabla^2 T_m^0 \right] + \nabla^2 \mathcal{U}_m(\underline{r}, s) = 0 . \quad (2.26)$$

In order to insure that the division given by equation 2.24 will yield waves whose fronts travel along the surfaces determined by geometric optics, we must choose the $T_m^0(\underline{r})$ such that they satisfy the Eikonal equation

$$|\nabla T_m^0(\underline{r})|^2 = \frac{1}{c^2} . \quad (2.27)$$

The functions $\mathcal{U}_m(\underline{r}, s)$ then satisfy the equation

$$\nabla^2 u_m(\underline{r}, s) - s(1 + \frac{\sigma}{\epsilon s})^{1/2} [2\nabla u_m \cdot \nabla T_m^0 + u_m \nabla^2 T_m^0] = 0 . \quad (2.28)$$

If s is replaced by $-i\omega$ and σ is equated to zero, equation 2.28 is identical with the equation satisfied by amplitudes of the geometrical optics waves in the asymptotic theory of diffraction.

2.3 Behavior of the Fields in the Vicinity of the Wavefronts

In this section it will be shown that the fields in the vicinity of the wavefronts can be obtained by considering the asymptotic behavior of the transform of the field vectors for large values of the complex frequency s . The Tauberian theorem which is employed to justify this procedure is obtained in an admittedly non-rigorous fashion from an Abel type theorem given in reference (9).

The Abel type theorem given in the above reference is stated in the following form:

Theorem: If a one-sided original is represented asymptotically as $t \rightarrow 0+$ by some power series of not necessarily integral exponents exceeding -1 , then the s series obtained by transposing the original term by term represents the image asymptotically as $s \rightarrow \infty$.

In this theorem the term original refers to the time function and the term image refers to the Laplace transform of the function. The inverse of this theorem, if it exists, will enable one to determine the asymptotic behavior of the original time function as $t \rightarrow 0+$ from the asymptotic representation of the image function as $s \rightarrow \infty$. It is not true in general that the inverse of an Abel theorem yields a correct Tauberian theorem. The conditions for the validity of a Tauberian theorem

are always more severe than those which guarantee the validity of an Abel theorem.

In order to justify the use of the Tauberian theorem which is inverse to the above Abel theorem, something must be said about the nature of the time functions which are likely to result from the inversion of the asymptotic representation of the image. A time function of the form

$$f(t) = \delta(t - t_0) + \mathcal{U}(t - t_0) \sum_{n=0}^{\infty} a_n t^{n-\alpha}, \quad (2.29)$$

has a Laplace transform if $\alpha > -1$. Formally applying the Laplace transform operator to both sides of 2.29 yields the result

$$\mathfrak{F}(\underline{r}, s) = e^{-st_0} \left[1 + \sum_{n=0}^{\infty} a_n \frac{\Gamma(n - \alpha + 1)}{s^{n - \alpha + 1}} \right], \quad \alpha > -1. \quad (2.30)$$

In the solution of pulse diffraction problems, the transform of the field vectors is obtained as a solution of a vector wave equation. There is no question about the existence of the Laplace transform when it is obtained in this manner. This implies that the inverse of the transform of a field vector must be representable in the form given in equation 2.29 in the vicinity of a wavefront. An application of the Abel theorem from (9) then indicates that the transform is representable in an asymptotic series for large s . Consequently, since we know that the inverse of the transform of the field vectors will yield a time function of the type 2.29, it is reasonable to assert that the asymptotic representation of the inverse of these transforms can be obtained by a term by term inversion of their asymptotic representation for large s .

With the assistance of the above Tauberian theorem, it is easily

demonstrated that the amplitudes of the waves at the wavefronts are determined by the laws of geometrical optics. As discussed in the preceding section, the solutions for the vector fields are derived from two scalar functions which satisfy the scalar wave equation 2.23. A solution of this equation was given in 2.24. For large values of s this equation can be written

$$\lim_{s \gg 1} \mathcal{J}(\underline{r}, s) = \sum_{m=0}^{\infty} \lim_{s \gg 1} \mathcal{U}_m(\underline{r}, s) \exp[-s(1 + \frac{1}{2} \frac{\sigma}{\epsilon s} - \frac{1}{8} (\frac{\sigma}{\epsilon s})^2 + \dots) T_m^0(\underline{r})] \quad (2.31)$$

The time function which corresponds to the m^{th} term in 2.31 will be zero for $t < T_m^0(\underline{r})$. Since $T_m^0(\underline{r})$ was chosen such that it satisfies the Eikonal equation, the equation $t = T_m^0(\underline{r})$ describes the arrival of the m^{th} wavefront at \underline{r} . The amplitude of the disturbance associated with this wavefront is given by $\lim_{s \rightarrow \infty} \mathcal{U}_m(\underline{r}, s)$. The function $\mathcal{U}_m(\underline{r}, s)$ satisfies the equation 2.28 and when $s \rightarrow \infty$ this equation can be approximated by the relation

$$2\nabla \mathcal{U}_m \cdot \nabla T_m^0 + \mathcal{U}_m \nabla^2 T_m^0 = 0 \quad (2.32)$$

The relation 2.32, however, is the equation satisfied by the amplitude of waves determined by geometrical optics (10). As a result, it is apparent that in pulse diffraction problems the amplitudes of the waves at the wavefronts are determined by geometrical optics.

2.4 Behavior of the Fields when $t - T_m^0(\underline{r}) \gg 1$

The inversion integral for the m^{th} term in the wavefront expansion given in 2.24 can be written

$$\mathcal{L}^{-1} [\mathcal{F}_m(\underline{r}, s)] = \frac{1}{2\pi i} \int_{\Delta-100}^{\Delta+100} \mathcal{U}_m(\underline{r}, s) e^{s(t - T_m^0(\underline{r}))} ds, \quad (2.33)$$

where it has been assumed that $\sigma = 0$. The fact that $t - T_m^0(\underline{r})$ is large suggests that it might be worthwhile to investigate the possibility of deforming the contour of integration in 2.33 into the left half plane where $\text{Re}(s) < 0$. A typical amplitude function $\mathcal{U}_m(\underline{r}, s)$ will in general have both poles and branch points in the region $\text{Re}(s) < \Delta$.

Figure 2.2 illustrates the deformation of the original contour into the left half plane for a typical distribution of singularities of $\mathcal{U}_m(\underline{r}, s)$.

If $t - T_m^0(\underline{r})$ is large, the most significant contribution to the value of the inversion integral is the one which results from the singularity which has the maximum real part. In the case depicted in Figure 2.2 the pole along the imaginary axis and the branch point at $s = 0$ are the significant singularities. The contribution from the pole on the imaginary axis is easily obtained by Cauchy's residue theorem. This will yield the steady state behavior of the time function associated with $\mathcal{F}_m(\underline{r}, s)$. The contribution which is obtained from the integration around the branch point at $s = 0$ will describe the deviation of $\mathcal{L}^{-1}[\mathcal{F}_m(\underline{r}, s)]$ from its steady state value.

An asymptotic expansion of the value of the integral around the branch point at $s = 0$ can be obtained by expanding the function $\mathcal{U}_m(\underline{r}, s)$ in a Laurent series about this point. The integrals which result from this procedure can, in principle, be solved. If the radius of convergence R of the Taylor series expansion of $\mathcal{U}_m(\underline{r}, s)$ about $s = 0$ is large enough that $[t - T_m^0(\underline{r})]R \gg 1$, it is not necessary to worry about the effect of the other singularities on the expansion of $\mathcal{U}_m(\underline{r}, s)$ about the

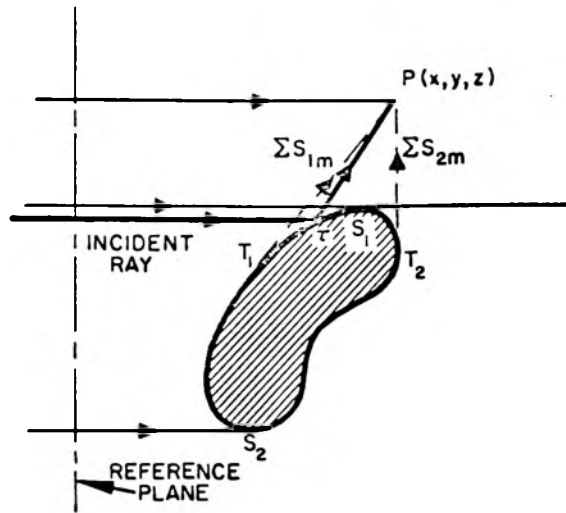


Fig. 2.1 Generalized ray system

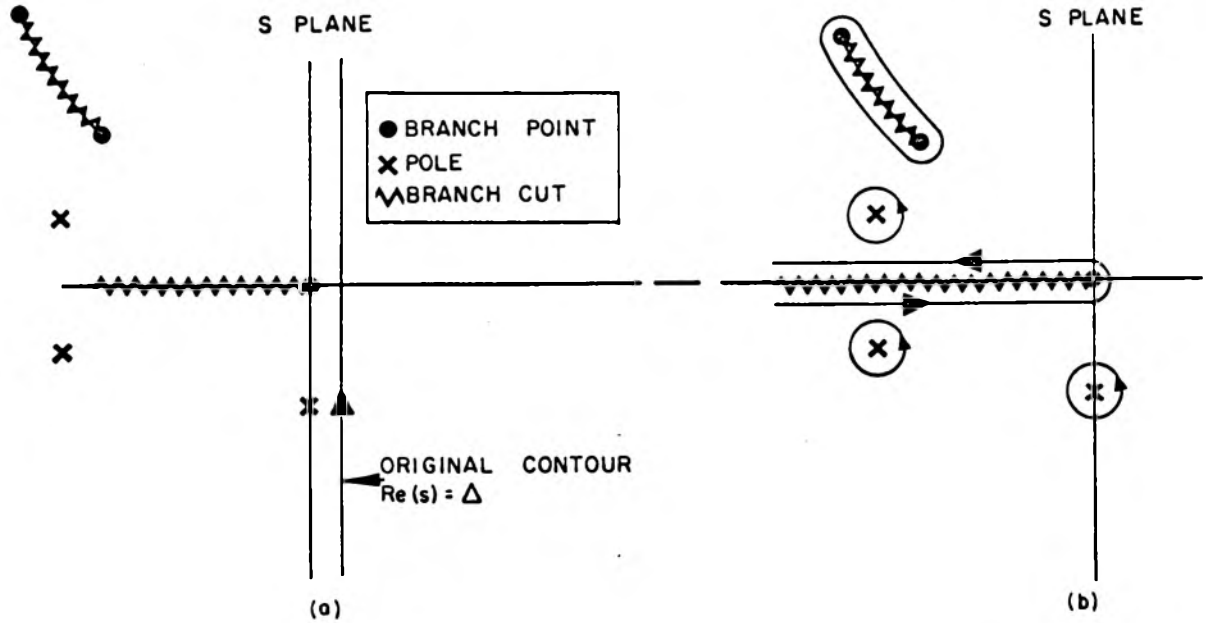


Fig. 2.2 Typical contour deformation

branch point. In this case the evaluation of the branch point integral with $U_m(\underline{r}, s)$ replaced by a Taylor series representation will yield an adequate asymptotic representation.

III. THE DISPERSIVE EFFECT OF A FINITE CONDUCTIVITY

3.1 Introduction

Although the constituent parameters μ , ϵ , and σ have been assumed to be individually of a non-dispersive nature, the fact that $\sigma \neq 0$ introduces a dispersive effect. This is easily demonstrated if equation 2.9 is written in the form

$$\nabla \times \underline{H}(\underline{r}, s) = \epsilon' s \underline{C}(\underline{r}, s) - \epsilon \underline{E}(\underline{r}, 0) , \quad (3.1)$$

where the effective dielectric constant ϵ' is defined by the relation

$$\epsilon' \equiv \epsilon \left(1 + \frac{\sigma}{\epsilon s} \right) . \quad (3.2)$$

In pulse diffraction problems the propagation process is of a secondary interest so that we will be concerned with situations in which a wave propagating in a non-conducting medium is scattered by a conducting obstacle. The question which naturally arises is, how significant is the dispersive effect predicted by equation 3.2?

The task of investigating the dispersion introduced by 3.2 is greatly simplified if we limit ourselves to a study of a problem in which the only source of dispersion is the fact that the scattering obstacle has a finite conductivity. The reflection of a pulse from a semi-infinite imperfect dielectric is a problem of this nature. This problem is solved in Section 3.2

It is apparent from equation 3.2 that $\lim_{s \rightarrow \infty} \epsilon' = \epsilon$. This fact, in conjunction with the knowledge that the behavior of a wave solution in the vicinity of its wavefront is determined by the limit of the transform of the field vector as $s \rightarrow \infty$, indicates that even a good conductor acts

like a dielectric in the immediate vicinity of the wavefronts. That is, at the wavefronts the reflection coefficient is determined by the dielectric constant of the metal and not by its conductivity. The length of time over which this dispersive effect is significant will be deduced from the results of the pulse reflection problem solved in Section 3.2.

3.2 The Reflection of a Delta Pulse from a Semi-Infinite Imperfect Dielectric

The problem which will be considered in this section is pictorially described in Figure 3.1. The incident field is chosen to be propagating in a direction normal to the surface of the dielectric. The case of non-normal incidence can also be solved but the solution of this problem is slightly more complicated and it does not add anything to the understanding of the dispersion phenomena. The transforms of the field vectors are obtained in a manner which is completely analogous to the procedure employed in the steady state problem. The crucial point in this procedure is the identification of the various types of wave solutions which exist in free space and in the dielectric. In the transient problem, it is useful to identify the exponential factors in the wave solutions with a time delay. A knowledge of the time delay associated with the reflected and transmitted signals enables one to correctly choose the proper form of the transform solutions.

3.2.1 Derivation of the transforms of the field vectors. The incident signal is assumed to be a delta pulse which moves through space as a plane wave. The wavefront of the incident signal is defined by the condition $t + \frac{z}{c} = 0$. If the electric field of this pulse is oriented in the x direction, the incident fields can be written

$$\underline{E}^i(z,t) = \underline{a}_x \delta\left(t + \frac{z}{c}\right) , \quad (3.3)$$

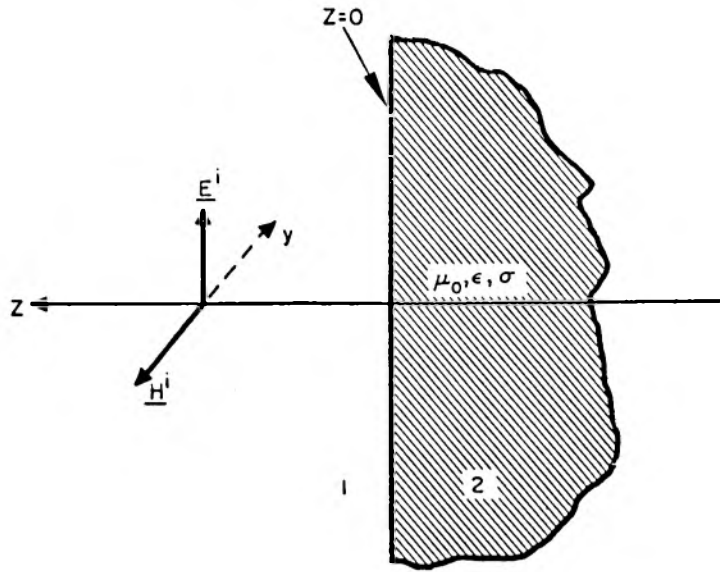


Fig. 3.1 Coordinate system and orientation of incident fields

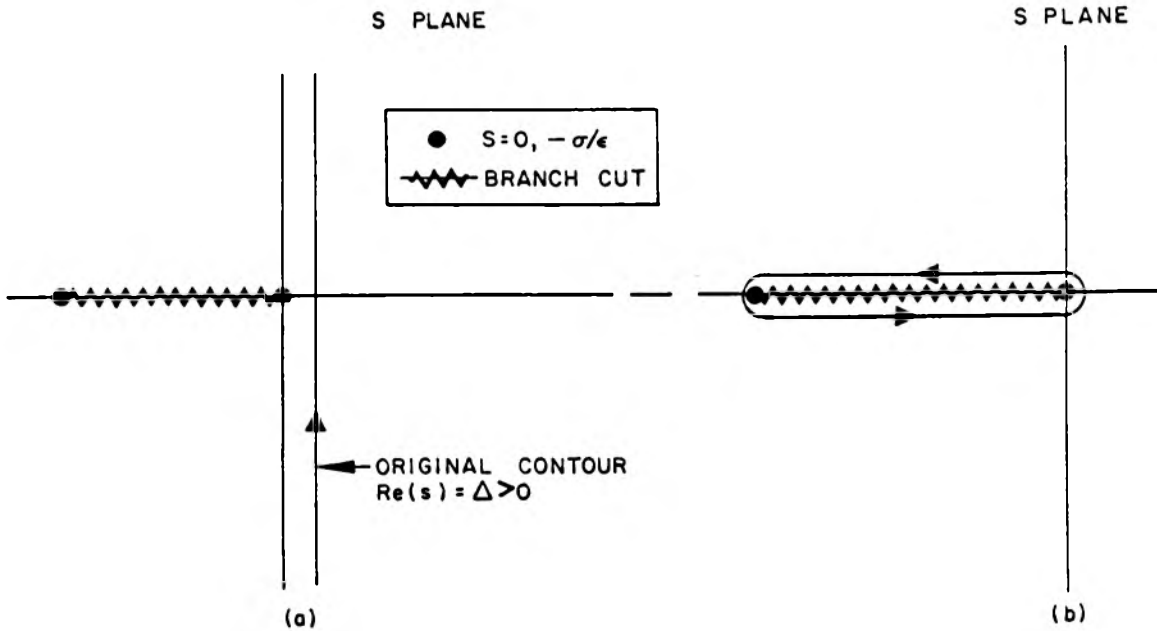


Fig. 3.2 Contour deformation

$$\underline{H}^i(z,t) = - \underline{a}_y \frac{1}{\mu_0 c} \delta(t + \frac{z}{c}) , \quad (3.4)$$

where \underline{a}_i denotes a unit vector in the i^{th} direction. When the Laplace transform operator defined by equation 2.1 is applied to the incident fields specified above, the following transform functions are obtained

$$\underline{E}^i(z,s) = \underline{a}_x e^{sz/c} \mathcal{U}(-z) , \quad (3.5)$$

$$\underline{H}^i(z,s) = - \underline{a}_y \frac{1}{\mu_0 c} e^{sz/c} \mathcal{U}(-z) . \quad (3.6)$$

The function $\mathcal{U}(-z)$ which appears in these equations is a Heaviside unit function which is zero for $z > 0$, unity for $z < 0$, and equal to the value $1/2$ for $z = 0$. The presence of this unit function necessitates that we apply the boundary conditions at the plane $z = 0^-$. An informal justification for considering the boundary value of the transform to be its limit as z approaches the boundary from the right can be obtained by appealing to the properties of the inversion integral 2.2 . When the Laplace transform of a function $f(t)$ is inverted the result is equal to $f(t)$ when $t > 0$, zero when $t < 0$, and $\frac{1}{2} f(0)$ at $t = 0$. Thus the inversion of the transform does not yield the true value of $f(t)$ at $t = 0$. At the plane $z = 0$ the incident signal specified by equations 3.3 and 3.4 is zero except at the time $t = 0$. But the time $t = 0$ is just exactly the time at which the inversion integral does not give the correct value for $f(t)$. For this reason, it is expected that a straightforward application of the transformed boundary conditions at $z = 0$ will not give a correct answer. At the plane $z = 0^-$ the incident signal is zero except at the time $t = 0^+$. In this case, however, the inversion of the Laplace transform of the incident signal yields the correct answer

since $t > 0$.

The time delay of the incident signal is $t + \frac{z}{c}$, that of the reflected signal $t - \frac{z}{c}$, and that of the transmitted signal $t + \frac{z}{c_2}$ where c_2 is the effective phase velocity in medium 2 . Since the incident signal has an exponential factor involving $+\frac{z}{c}$, the above information about the time delays suggests that the transform of the reflected signal should involve a factor $e^{-sz/c}$ and the transform of the transmitted signal a factor e^{+sz/c_2} . The transforms of the reflected and transmitted fields are thus written in the form

$$\underline{\mathcal{E}}^i(z,s) = \underline{a}_x R(s) e^{-sz/c} , \quad (3.7)$$

$$\underline{\mathcal{E}}^t(z,s) = \underline{a}_x [1 + R(s)] e^{sz/c_2} \quad (3.8)$$

$$\underline{\mathcal{H}}^i(z,s) = \underline{a}_y \frac{1}{\mu_0 c} R(s) e^{-sz/c} , \quad (3.9)$$

$$\underline{\mathcal{H}}^t(z,s) = -\underline{a}_y \frac{1}{\mu_0 c_2} [1 + R(s)] e^{sz/c_2} \quad (3.10)$$

where

$$\frac{c}{c_2} = n(1 + \frac{\sigma}{\epsilon_s})^{1/2} , \quad n = (\frac{\epsilon}{\epsilon_0})^{1/2} = \text{index of refraction of 2.} \quad (3.11)$$

The $\underline{\mathcal{E}}$ vectors have been chosen such that the boundary condition on the tangential components of total $\underline{\mathcal{E}}(z,t)$ is automatically satisfied. The $\underline{\mathcal{H}}$ vectors in equations 3.9 and 3.10 are obtained by a direct application of the curl relation 2.8 to the $\underline{\mathcal{E}}$ vectors in 3.7 and 3.8. The condition that $\underline{a}_z \times \underline{\mathcal{H}}(z,t)$ be continuous yields the relation

$$\frac{1}{\mu_0 c} [-1 + R(s)] = -\frac{1}{\mu_0 c_2} [1 + R(s)] ,$$

which, upon solving for $\mathcal{R}(s)$, can be written

$$\mathcal{R}(s) = \frac{1 - \frac{c}{c_2}}{1 + \frac{c}{c_2}} = \frac{1 - n(1 + \frac{\sigma}{\epsilon s})^{1/2}}{1 + n(1 + \frac{\sigma}{\epsilon s})^{1/2}} \quad (3.12)$$

The function $\mathcal{R}(s)$ is interpreted as the reflection coefficient in the s domain.

It will suffice to consider only the inversion of the reflected electric field transform. The other field quantities can easily be obtained in the same manner. When the value 3.12 for the reflection coefficient $\mathcal{R}(s)$ is substituted in 3.7 and the inversion integral 2.2 applied to the result, we obtain the following integral expression for the reflected electric field $\underline{E}(z,t)$

$$\underline{E}(z,t) = \frac{a-x}{2\pi i} \int_{\Delta-i\infty}^{\Delta+i\infty} \frac{1 - n(1 + \frac{\sigma}{\epsilon s})^{1/2}}{1 + n(1 + \frac{\sigma}{\epsilon s})^{1/2}} e^{s(t - \frac{z}{c})} ds \quad (3.13)$$

3.2.2 Evaluation of the inversion integral for the reflected electric field. The integral expression for $\underline{E}(\underline{r},t)$ can be evaluated asymptotically in the manner described in Sections 2.3 and 2.4. It is possible, however, to transform this integral into a form which will yield both of the asymptotic limits without making use of the Tauberian theorem given in Section 2.3. This provides a convenient check on the validity of this theorem. The approach to be employed here is also nice in that it yields an exact answer for the case $n = 1$.

The only singularities of the integrand in the integral 3.13 are the branch points at $s = 0, -\sigma/\epsilon$. Figure 3.2a illustrates the original contour and the choice of a branch cut along the negative real axis from

0 to $-\sigma/\epsilon$. Before deforming the contour of 3.13 into the left half plane, we must investigate the behavior of its integrand on the infinite arc in the left half plane.

$$\lim_{s \rightarrow \infty} \frac{1 - n(1 + \frac{\sigma}{\epsilon s})^{1/2}}{1 + n(1 + \frac{\sigma}{\epsilon s})^{1/2}} e^{s(t - \frac{z}{c})} = \frac{1 - n}{1 + n} e^{s(t - \frac{z}{c})}. \quad (3.14)$$

The integrand vanishes on the infinite arc if $t - \frac{z}{c} > 0$. If $t - \frac{z}{c} = 0$, however, the integrand does not disappear. In order to avoid this difficulty divide the integrand into two parts.

$$\frac{1 - n(1 + \frac{\sigma}{\epsilon s})^{1/2}}{1 + n(1 + \frac{\sigma}{\epsilon s})^{1/2}} = \frac{1 - n}{1 + n} + \frac{2n}{1 + n} \frac{1 - (1 + \frac{\sigma}{\epsilon s})^{1/2}}{1 + n(1 + \frac{\sigma}{\epsilon s})^{1/2}}. \quad (3.15)$$

The first term in 3.15 will yield a delta function return and the second term now vanishes on the infinite arc for all $(t - \frac{z}{c}) \geq 0$. When 3.15 is substituted in 3.13 the following expression is obtained for $\underline{E}(z,t)$.

$$\underline{E}(z,t) = \frac{a}{-x} \frac{1 - n}{1 + n} \delta(t - \frac{z}{c}) + \frac{a}{-x} \frac{1}{\pi i} \frac{n}{1 + n} \int_{\Delta - i\infty}^{\Delta + i\infty} \frac{1 - n(1 + \frac{\sigma}{\epsilon s})^{1/2}}{1 + n(1 + \frac{\sigma}{\epsilon s})^{1/2}} e^{s(t - \frac{z}{c})} ds \quad (3.16)$$

The integral in the second term of 3.16 will be designated as I in the calculations which follow. Since the integrand of I disappears on the infinite arc in the left half plane for all $t - \frac{z}{c} \geq 0$, it is possible to deform its contour into a new contour which surrounds the branch cut from $s = 0$ to $-\sigma/\epsilon$. This contour is depicted in Figure 3.2b. If the variable s is replaced by $\sigma/\epsilon w e^{\pm i\pi}$ (the plus sign is taken on the top side of the cut and the minus sign on the bottom side of the cut) and the results for the integration along the top and bottom side of the cut are added, it is found that I can be written

$$I = - \left[\frac{2i\sigma}{\epsilon} \frac{1+n}{n} \int_0^1 \frac{w^{1/2}(1-w)^{1/2}}{1 - (1-\frac{1}{n})w} e^{-\psi w} dw \right] \mathcal{U}(t - \frac{z}{c}), \quad (3.17)$$

where $\psi \equiv \frac{\sigma}{\epsilon}(t - \frac{z}{c})$. To the best of the writer's knowledge this integral cannot be solved exactly with the exception of the case $n = 1$.

When $n = 1$ the integral in 3.17 assumes the form of an integral representation of a confluent hypergeometric function.

$$\int_0^1 w^{1/2}(1-w)^{1/2} e^{-\psi w} dw = \frac{\pi}{8} {}_1F_1\left(\frac{3}{2}; 3; \psi\right). \quad (3.18)$$

The confluent hypergeometric function in 3.18 can be shown to be equal to the following combination of well-known functions.

$${}_1F_1\left(\frac{3}{2}; 3; \psi\right) = \frac{4}{\psi} e^{\psi/2} I_1\left(\frac{\psi}{2}\right), \quad (3.19)$$

where I_1 denotes a modified Bessel function of order one. Thus when $n = 1$, the exact expression for the reflected electric field can be written

$$\underline{E}(z, t) \Big|_{n=1} = - \frac{a}{x} \frac{I_1\left(\frac{\sigma}{2\epsilon_0}(t - \frac{z}{c})\right)}{(t - \frac{z}{c})} e^{-\frac{\sigma}{2\epsilon_0}(t - \frac{z}{c})} \mathcal{U}(t - \frac{z}{c}). \quad (3.20)$$

The behavior of equation 3.20 is plotted in Figure 3.3.

If $n \neq 1$, asymptotic approximations to I can be obtained for the two extremes $\psi \ll 1$, and $\psi \gg 1$. In the case $\psi \ll 1$ an asymptotic expansion can be obtained by expanding the exponential function $e^{-\psi w}$ in a Taylor series about $\psi w = 0$.

$$\lim_{\psi \ll 1} I \sim - \frac{2i\sigma}{\epsilon} \frac{1+n}{n} \int_0^1 \frac{w^{1/2}(1-w)^{1/2}}{1 - rw} \left[1 - \psi w + \frac{\psi^2}{2} w^2 + \dots \right] dw \mathcal{U}(t - \frac{z}{c}), \quad (3.21)$$

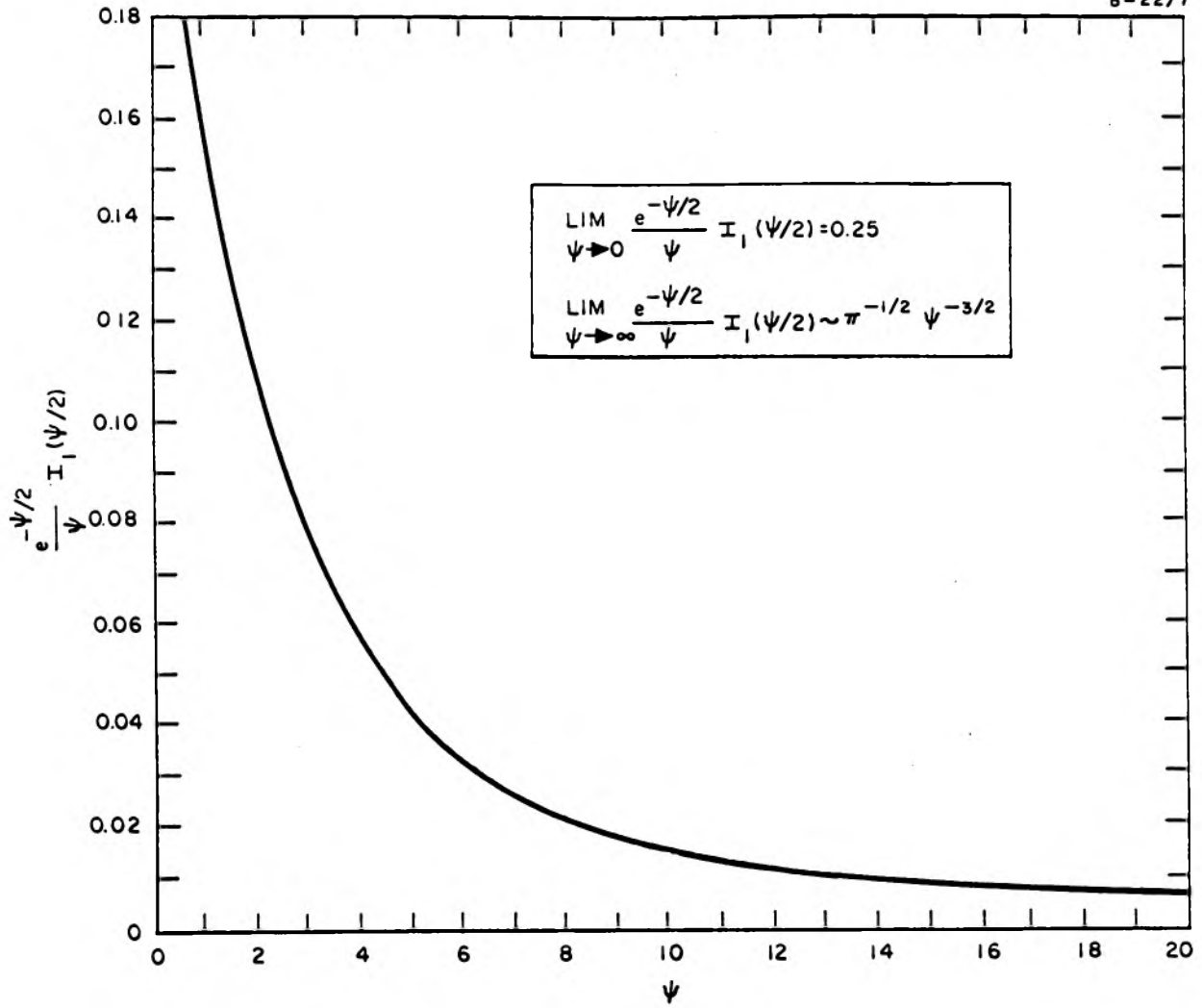


Fig. 3.3 Behavior of the function $\frac{e^{-\psi/2}}{\psi} I_1\left(\frac{\psi}{2}\right)$

where $r \equiv 1 - \frac{1}{n}$. This procedure yields the following series expansion valid in the vicinity of $\psi \sim 0$.

$$I \sim - \frac{2i\sigma}{\epsilon} \frac{1+n}{n} \sum_{m=0}^N a_m(r) \psi^m \mathcal{U}(t - \frac{z}{c}), \quad (3.22)$$

where

$$a_m = \int_0^1 \frac{w^{\frac{2m+1}{2}}(1-w)^{1/2}}{1-rw} dw = \frac{\Gamma(\frac{3}{2})\Gamma(\frac{2n+3}{2})}{\Gamma(n+3)} {}_2F_1(1, \frac{2n+3}{2}; n+3; r). \quad (3.23)$$

The asymptotic expansion of $\underline{E}(z, t)$ has also been calculated using the Tauberian theorem given in Section 2.3. The results from these two methods coincide. A point in favor of the Tauberian theorem results is the fact that they do not require the evaluation of complicated coefficients such as 3.23.

The asymptotic approximation to I for the case $\psi \gg 1$ can be obtained by expanding the integrand in 3.17 about $w = 0$. It is also asymptotically correct to replace the upper integration limit by ∞ . When these things are done we obtain

$$\begin{aligned} \lim_{\psi \gg 1} I &\sim - \frac{2i\sigma}{\epsilon} \frac{1+n}{n} \int_0^{\infty} w^{1/2} (1 - \frac{1}{2}w - \frac{1}{8}w^2 + \dots) (1 + rw + r^2w^2 + \dots) \\ &\quad \times e^{-\psi w} dw \mathcal{U}(t - \frac{z}{c}) \\ &= - \frac{\pi^{1/2} i\sigma}{\epsilon} \frac{1+n}{n} \psi^{-3/2} \left[1 + \frac{3}{2}(r - \frac{1}{2})\psi^{-1} + \frac{15}{4}(r^2 - \frac{r}{2} - \frac{1}{8})\psi^{-2} + \mathcal{O}(\psi^{-3}) \right] \mathcal{U}(t - \frac{z}{c}). \end{aligned} \quad (3.24)$$

3.3 Some General Conclusions about the Dispersive Effect of a Finite Conductivity

The physical process which causes a conductor to be dispersive is the excitation of eddy currents. If $\sigma = 0$ there cannot be any current

flow so there is no dispersion. It appears that a significant parameter in the assessment of the magnitude of the dispersive effect is the relaxation time $(\sigma/\epsilon)^{-1}$ of the material of which the scattering obstacle is composed. When $\sigma = \infty$ the relaxation time is zero. This implies that the currents induced in a perfect conductor attain their equilibrium value instantaneously. Consequently, it should be expected that a perfect conductor would be non-dispersive. This, of course, is true.

Another important consideration in the assessment of the significance of the dispersive effect is the bandwidth of the incident signal. It is obvious that a narrow-band signal is distorted much less than a wide-band signal. The bandwidth of a signal with a delta function time dependence is infinite. Consequently the dispersive effect of a finite conductivity can be maximized by considering the solution of a delta source problem. It is reasonable to assume that if the dispersion is negligible for a delta source, it will be negligible for all signals.

The conditions in the problem solved in the preceding section were chosen such that the only source of dispersion was the fact that $\sigma \neq 0$. The distortion of the reflected signal can thus be attributed solely to the dispersive effect of a finite conductivity. Also the incident signal has a delta function time dependence so that, according to the reasoning given above, we should expect that the distortion in the reflected signal will be maximized. The exact results for the case $n = 1$ provide a convenient means of estimating the significance of the effect when $\sigma \neq 0$. The plot of the time behavior of the reflected signal given in Figure 3.3 indicates that the signal rapidly approaches its steady state value in a few relaxation periods $(\sigma/\epsilon)^{-1}$. This is physically reasonable since, as mentioned above, the dispersion is caused

by the flow of eddy currents in the scatterer and it is known that these currents decay in a time of the order of a few relaxation periods. Thus it appears that a sufficient criterion for neglecting the dispersive effect due to a finite conductivity is the condition $\sigma/\epsilon \gg f_m$. The frequency f_m is determined by the high frequency cutoff of the equipment which is employed to detect the scattered signal. If $\sigma/\epsilon \gg f_m$ the distortion in a received signal is undetectable.

Almost all metallic conductors satisfy the condition $\sigma/\epsilon > 10^{18}$. This corresponds to a frequency which is many times larger than the upper limit of the best receivers available at the present time and in the foreseeable future. Consequently it is reasonable to neglect the dispersive effect of a finite conductivity when the scattering obstacle is composed of a metallic material. There can be a significant detectable distortion due to a finite conductivity when a signal is scattered by an obstacle whose composition is somewhat like dry earth. In this case $\sigma/\epsilon \sim 10^7$ and this frequency is well within the upper cutoff frequency of a good receiver. It is reasonable to expect, for instance, that a signal scattered by one of the planets or our moon would be distorted as a result of their finite conductivity.

IV. A SIMPLE EXAMPLE OF THE METHOD OF SOLUTION WHEN MORE THAN ONE
OPTICAL RAY IS PRESENT: THE TRANSMISSION OF A DELTA PULSE
THROUGH A CONDUCTING DIELECTRIC SLAB

4.1 Introduction

The virtues of the method of solution for pulse scattering problems which was described in Chapter II are not readily obvious until the method has been tested on a typical problem. The choice of a particular problem to illustrate the method is influenced by two factors. First, the physics of the problem should predict the presence of more than one optical ray at the observation point. This is a rather obvious requirement since the crux of the wavefront approach is the fact that pulse scattering problems are solved most efficiently if the effects of the various wavefronts are considered separately. If there is only one wavefront, the method of Chapter II and the conventional approach are identical. Secondly, the solution of the problem which is chosen should be simple enough that the value of the pulse scattering method is readily apparent. If the problem were not of a simple nature, the advantages of the wavefront approach might be masked by the complexity of the solution. For these reasons it was decided to use the problem of the transmission of a delta pulse through a conducting dielectric slab as an example of the wavefront expansion technique.

The problem which is solved in this chapter is actually slightly more complicated than it need be to demonstrate the solution technique. For the purposes of the demonstration, it would have been sufficient to consider the transmission through a nonconducting slab. It is felt, however, that the added complexity is compensated by the fact that the solution to the problem with non-zero conductivity is of reasonable practical

significance. The results of this problem are relevant to the problem of shielding equipment from unwanted non-monochromatic signals.

4.2 Derivation of the Transforms of the Field Vectors

The scattering problem which will be solved in this chapter is depicted in Figure 4.1. The media in regions 1 and 3 are assumed to be vacuums and the magnetic permeability of medium 2 is taken to be the same as that in 1 and 3. The incident field is again chosen to be a plane delta wave which moves in the negative z direction with a wave-front determined by the condition $t + z/c = 0$. The orientation of the incident field vectors is indicated in Figure 4.1. The equations which describe the incident field and its Laplace transform are identical with equations 3.3-3.6 of Chapter III. For the sake of convenience, those equations are repeated below:

$$\underline{E}^i(z,t) = \underline{a}_x \delta(t + \frac{z}{c}) \quad , \quad (4.1)$$

$$\underline{H}^i(z,t) = - \underline{a}_y \frac{1}{\mu_0 c} \delta(t + \frac{z}{c}) \quad , \quad (4.2)$$

$$\underline{E}^i(z,s) = \underline{a}_x e^{sz/c} \mathcal{U}(-z) \quad , \quad (4.3)$$

$$\underline{H}^i(z,s) = - \underline{a}_y \frac{1}{\mu_0 c} e^{sz/c} \mathcal{U}(-z) \quad , \quad (4.4)$$

where \underline{a}_i denotes a unit vector in the i^{th} direction.

The appropriate forms for the vector field transforms of the reflected and transmitted signals are obtained in the same way, by the same technique, that was employed in the solution of the problem in Chapter III. The exponent of the exponential factor in the transform of a field vector is determined by a consideration of the time delay associated with the field vector. The reflected signals have time delays of the form

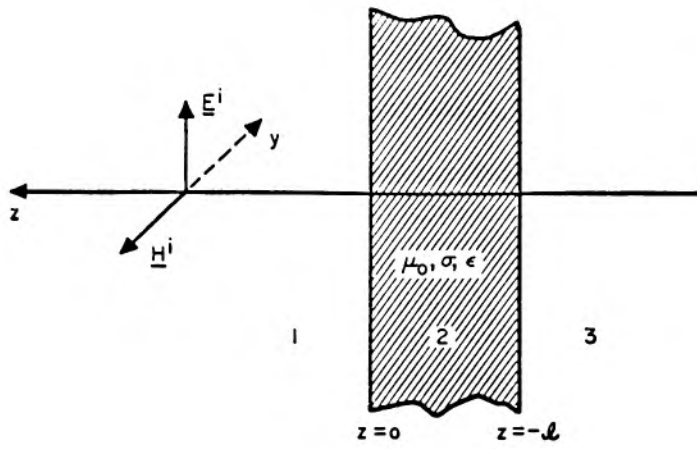


Fig. 4.1 Coordinate system and orientation of incident fields

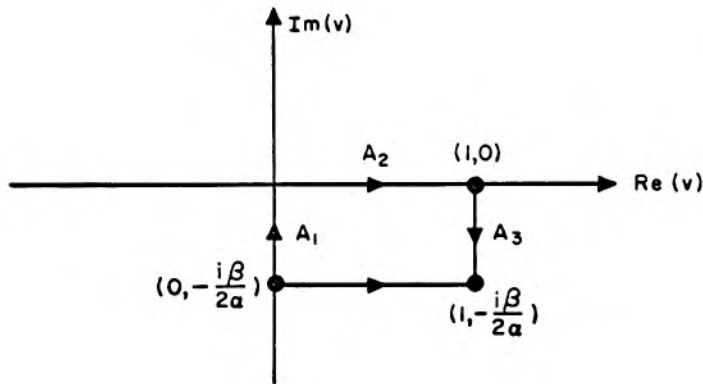


Fig. 4.2 Contours of integration

$t - \frac{z}{c_1}$ ($i = 1, 2, 3$) and the delay for a transmitted signal is of the form $t + \frac{z}{c_1}$ ($i = 1, 2, 3$). This indicates that the transforms of the reflected and transmitted fields can be written

$$\underline{E}_1^o(z, s) = \underline{a}_x R_1(s) e^{-sz/c} \quad (4.5)$$

$$\underline{E}_2(z, s) = \underline{a}_x \left[J_2(s) e^{sz/c_2} + R_2(s) e^{-sz/c_2} \right], \quad (4.6)$$

$$\underline{E}_3(z, s) = \underline{a}_x J(s) e^{sz/c}, \quad (4.7)$$

$$\underline{H}_1^o(z, s) = \underline{a}_y \frac{1}{\mu_0 c} R_1(s) e^{-sz/c} \quad (4.8)$$

$$\underline{H}_2(z, s) = \underline{a}_y \frac{1}{\mu_0 c_2} \left[-J_2(s) e^{sz/c_2} + R_2(s) e^{-sz/c_2} \right], \quad (4.9)$$

$$\underline{H}_3(z, s) = -\underline{a}_y \frac{1}{\mu_0 c} J(s) e^{sz/c}, \quad (4.10)$$

where

$$\frac{c}{c_2} = n \left(1 + \frac{\sigma}{\epsilon s} \right)^{1/2}, \quad n = \text{index of refraction of 2}. \quad (4.11)$$

The continuity of the tangential components of the transformed vector fields at the boundaries $z = 0, -l$ yields a set of four equations involving the quantities $R_1(s)$, $J_2(s)$, $R_2(s)$, and $J(s)$. These equations can be represented conveniently by the matrix relation

$$\begin{bmatrix} -1 & 1 & 1 & 0 \\ 0 & e^{-sl/c_2} & e^{sl/c_2} & -e^{-sl/c_2} \\ 0 & 1 + c/c_2 & 1 - c/c_2 & 0 \\ 0 & -\frac{c}{c_2} e^{-sl/c_2} & \frac{c}{c_2} e^{sl/c_2} & e^{-sl/c} \end{bmatrix} \begin{bmatrix} R_1(s) \\ J_2(s) \\ R_2(s) \\ J(s) \end{bmatrix} = \begin{bmatrix} 1 \\ 0 \\ 2 \\ 0 \end{bmatrix} \quad (4.12)$$

Each of the coefficients which appear in equations 4.5 - 4.10 can easily be obtained from the above matrix equation. The result for the transmission coefficient $J(s)$ can be written

$$J(s) = \frac{4 \frac{c}{c_2} e^{s l / c}}{\left(1 + \frac{c}{c_2}\right)^2 e^{s l / c_2} - \left(1 - \frac{c}{c_2}\right)^2 e^{-s l / c_2}} \quad (4.13)$$

An integral representation of the transmitted electric field $\underline{E}_3(z, t)$ can now be obtained by applying the inversion operator defined in 2.2 to equation 4.7 with $J(s)$ replaced by 4.13.

$$\underline{E}_3(z, t) = \frac{a_x}{-x} \frac{1}{2\pi i} \int_{\Delta - i\infty}^{\Delta + i\infty} \frac{4 \frac{c}{c_2} e^{s(t + \frac{z+l}{c})}}{\left(1 + \frac{c}{c_2}\right)^2 e^{s l / c_2} - \left(1 - \frac{c}{c_2}\right)^2 e^{-s l / c_2}} ds \quad (4.14)$$

4.3 A Discussion of the Alternative Methods Available for the Solution of the Inversion Integral

The integrand of the integral in 4.14 is a single-valued function of s . This is not immediately obvious since the function c/c_2 is a multiple-valued function with branch points at $s = 0, -\sigma/\epsilon$. It is noted, however, that the integrand is unchanged if c/c_2 is replaced by $-c/c_2$. Consequently, even though c/c_2 changes sign as s passes from the top side of its branch out to the bottom side, the integrand remains unchanged. It is also apparent that the integrand in 4.14 has an infinite number of poles in the left half of the s plane. These poles are located at the values of s which satisfy the relation

$$\frac{s\ell}{c_2} = - \ln \left(\frac{\frac{c}{c_2} + 1}{\frac{c}{c_2} - 1} \right) \pm i m \pi \quad , \quad m = 0, 1, 2, \dots \quad (4.15)$$

An obvious way to evaluate $\underline{E}_3(z,t)$ is to apply Cauchy's residue theorem and express the integral in 4.14 as an infinite sum of residue terms.

The method which has been expounded in this paper involves a decomposition of the field $\underline{E}_3(z,t)$ into a series of terms which are determined by the optical wavefronts. An approach which is, in general, quite successful in the determination of the desired wavefront expansion is to investigate the behavior of the transform of the field vector on the infinite arc in the right half of the s plane. When the transform is expanded in an asymptotic series, it is usually found that the wavefront terms are easily recognized. An asymptotic expansion of the integrand in 4.14 for large values of s where $\text{Re}(s) > 0$ yields the result

$$\begin{aligned} & \lim_{\substack{s \gg 1 \\ \text{Re}(s) > 0}} \frac{4 \frac{c}{c_2} e^{s(t + \frac{z+\ell}{c})}}{\left(1 + \frac{c}{c_2}\right)^2 e^{s\ell/c_2} - \left(1 - \frac{c}{c_2}\right)^2 e^{-s\ell/c_2}} \sim \\ & \sim \sum_{m=0}^{\infty} \frac{4n}{(n+1)^2} \left(\frac{n-1}{n+1}\right)^{2m} \cdot \left[1 + \mathcal{O}(s^{-1})\right] e^{s(t + \frac{z+\ell}{c}) - (2m+1)\frac{\ell n}{c}} \quad (4.16) \end{aligned}$$

The quantity $(t + \frac{z+\ell}{c} - (2m+1)\frac{\ell n}{c})$ which appears in the exponent of each term in 4.16 can be interpreted as the time delay associated with a wave which has been internally reflected $2m$ times inside of the dielectric slab. Likewise, the coefficient $\frac{4n}{(n+1)^2} \left(\frac{n-1}{n+1}\right)^{2m}$ is the transmission coefficient of a wave which is internally reflected $2m$ times in a dielectric slab whose refractive index is n . The expansion 4.16 was obtained by expanding the denominator on the left hand side in a geometric series

and then taking the limit as $s \gg 1$. As a result, it appears that the desired wavefront expansion of the field $\underline{E}_3(z,t)$ can be obtained by expanding the denominator of the integrand in 4.14 in a geometric series. The geometric series obtained in this way is convergent everywhere to the right of the singularities of the integrand. The field $\underline{E}_3(z,t)$ can thus be written in the form

$$\underline{E}_3(z,t) = \frac{a}{-x} \frac{2}{\pi i} \sum_{m=0}^{\infty} \int_{\Delta-1\infty}^{\Delta+1\infty} \frac{c/c_2}{(1 + \frac{c}{c_2})^2} \left(\frac{1 - \frac{c}{c_2}}{1 + \frac{c}{c_2}} \right)^{2m} e^{s(t + \frac{z+l}{c} - (2m+1)\frac{l}{c_2})} ds . \quad (4.17)$$

The task of comparing the relative merits of the two approaches discussed in the preceding two paragraphs is considerably simplified if we restrict ourselves to the case $\sigma = 0$. This choice makes the solution of 4.17 almost trivial since the function c/c_2 is then equal to the constant value n . The integrals which remain are easily shown to be expressible in the form of delta functions. The result for $\underline{E}_3(z,t)$ can be written

$$\underline{E}_3(z,t) = \frac{a}{-x} \frac{4n}{(n+1)^2} \sum_{m=0}^{\infty} \left(\frac{n-1}{n+1} \right)^{2m} \delta(t + \frac{z+l}{c} - (2m+1)\frac{ln}{c}) . \quad (4.18)$$

The answer given in 4.18 is exactly that which is predicted by the physics of the problem. The transmitted signal is expressed in the form of a series of discrete delta signals received at time delays which correspond to the optical wavefronts. The magnitude of each signal is also in accordance with the physical interpretation.

When $\sigma = 0$ the locations of the poles in the integrand of 4.14 are given by the relation

$$s_m \frac{n\ell}{c} = -\ln\left(\frac{n+1}{n-1}\right) \pm im\pi, \quad m = 0, 1, 2, \dots \quad (4.19)$$

The integral along the contour $\text{Re}(s) = \Delta$ is equal to $2\pi i$ times the sum of the residues at these poles if the integrand of 4.14 vanishes on the infinite arc in the left half plane. The asymptotic limit of the integrand as $s \rightarrow \infty$ with $\text{Re}(s) < 0$ is given by

$$\lim_{\substack{s \rightarrow \infty \\ \text{Re}(s) < 0}} \frac{4n e^{s(t + \frac{z+\ell}{c})}}{(n+1)^2 e^{s\ell n/c} - (n-1)^2 e^{-s\ell n/c}} \sim \mathcal{O}\left(e^{s(t + \frac{z+\ell}{c} + \frac{\ell n}{c})}\right). \quad (4.20)$$

Therefore, if $(t + \frac{z+\ell}{c} + \frac{\ell n}{c}) > 0$, the integrand of 4.14 vanishes on the infinite arc in the left half plane. It is also known, from a consideration of the behavior of the integrand in the right half plane, that the integral in 4.14 is zero for $(t + \frac{z+\ell}{c} - \frac{\ell n}{c}) < 0$. When $(t + \frac{z+\ell}{c} - \frac{\ell n}{c}) > 0$ the condition obtained from 4.20 is satisfied and we can then express the integral in 4.14 as a sum of residue terms. The expression which is obtained for $\underline{E}_3(z, t)$ can be written

$$\underline{E}_3(z, t) = \frac{a}{x} \frac{4n}{(n+1)^2} \frac{(r)^{T/\tau}}{2r\tau} \sum_{m=-\infty}^{\infty} e^{im\pi(1 - \frac{T}{\tau})} \mathcal{U}(T - \tau), \quad (4.21)$$

where

$$r \equiv \frac{n-1}{n+1}; \quad \tau \equiv \frac{n\ell}{c}; \quad T \equiv t + \frac{z+\ell}{c}.$$

The result given in 4.21 shows little resemblance to the wavefront expansion given in 4.18. As a matter of fact, it is not even apparent that return is of the discrete nature indicated by physical reasoning.

The equivalence of equations 4.21 and 4.18 can be demonstrated if the following relation is employed (11)

$$\frac{1}{2u} \sum_{m=-\infty}^{\infty} e^{im\pi z/u} = \sum_{m=-\infty}^{\infty} \delta(z - 2mu) . \quad (4.22)$$

With the assistance of 4.22 the product of the summation and the unit function in 4.21 can be written in the form

$$\begin{aligned} \sum_{m=-\infty}^{\infty} e^{im\pi(1 - \frac{T}{\tau})} \mathcal{U}(T - \tau) &= 2 \sum_{m=-\infty}^{\infty} \delta(1 - \frac{T}{\tau} - 2m) \mathcal{U}(T - \tau) \\ &= 2\tau \sum_{m=0}^{\infty} \delta(T - (2m+1)\tau) . \end{aligned} \quad (4.23)$$

If 4.23 is substituted in 4.21 and it is recognized that

$$r^{T/\tau} \delta(T - (2m+1)\tau) = r^{2m+1} \delta(T - (2m+1)\tau) ,$$

the expressions in 4.21 and 4.18 can be shown to be equivalent. The important point to be noted here is that in order to obtain each term in the result predicted by the physics of the problem an infinite number of residue terms must be summed. In the above example this did not cause too much hardship since the residue series could be summed exactly. It is not always so simple. The sum of the residue series obtained from 4.14 when $\sigma \neq 0$ is not so easily obtained.

4.4 Inversion of the First Term in the Wavefront Expansion when $\sigma \neq 0$

The results for the transmission of a delta pulse through a conducting slab are of interest if it is desired to assess the ability of a thin sheet to shield a region from unwanted transient signals. The shielding properties of a metallic sheet are easily obtained if the

incident signal has a very narrow spectrum. In this case, the steady state behavior of the signal transmitted at the frequency corresponding to the maximum in the incident signal spectrum will yield a very good indication of the over-all shielding capabilities. When the signal has a relatively wide bandwidth, however, the steady state theory may not yield a result which is sufficiently accurate. In this case it is useful to appeal to the impulse response results given in this section. The signal transmitted when the incident signal has an arbitrary time dependence can be obtained from the impulse response by means of the convolution integral.

It will suffice to consider the inversion of the first term in the wavefront expansion since magnitudes of the higher order terms are significantly reduced because of the attenuating effect of the conductivity of the slab. If it should prove necessary to include the higher order terms in a particular problem, they can be evaluated in the same manner as the first term. The various terms in the wavefront expansion are represented in integral form in equation 4.17. If the first term is designated by $\underline{E}_{30}(z,t)$, we can write

$$\underline{E}_{30}(z,t) = \underline{a}_x \frac{2}{\pi i} \int_{\Delta-100}^{\Delta+100} \frac{c/c_2}{(1 + \frac{c}{c_2})^2} e^{s(t + \frac{z+l}{c} - \frac{l}{c_2})} ds \quad . \quad (4.24)$$

The magnitude of the field in the vicinity of the wavefront will be obtained by applying the Tauberian theorem given in Chapter II, Section 2.3. This requires that the integrand of 4.24 be expanded in an asymptotic series valid for $s \rightarrow \infty$. The asymptotic expansions of the factors in the integrand are given below

$$\lim_{s \rightarrow \infty} \frac{c/c_2}{(1 + \frac{c}{c_2})^2} = \frac{n}{(n+1)^2} \left[1 - \frac{n-1}{2(n+1)} \frac{\sigma}{\epsilon s} + \left(\frac{2n^2 - n}{4(n+1)^2} - \frac{1}{8} \right) \left(\frac{\sigma}{\epsilon s} \right)^2 + \mathcal{O} \left(\frac{\sigma}{\epsilon s} \right)^3 \right] \quad (4.25)$$

$$\lim_{s \rightarrow \infty} e^{s(t + \frac{z+l}{c} - \frac{l}{c_2})} = e^{sT_0 - \frac{\sigma}{2\epsilon} \cdot \frac{nl}{c}} \left[1 + \frac{1}{8} \left(\frac{\sigma}{\epsilon} \cdot \frac{nl}{c} \right) \frac{\sigma}{\epsilon s} + \frac{1}{128} \cdot \frac{\sigma}{\epsilon} \frac{nl}{c} \left(\frac{\sigma}{\epsilon} \cdot \frac{nl}{c} - 8 \right) \left(\frac{\sigma}{\epsilon s} \right)^2 + \mathcal{O} \left(\frac{\sigma}{\epsilon s} \right)^3 \right] \quad (4.26)$$

where $T_0 \equiv (t + \frac{z+l}{c} - \frac{ln}{c})$ = time measured from the arrival of the wavefront. (4.27)

When equations 4.25 and 4.26 are substituted in 4.24 and the result inverted term by term, the following expression is obtained for the transmitted electric field in the vicinity of the first wavefront

$$\lim_{T_0 \ll 1} \underline{E}_{30}(z,t) \sim \frac{a}{x} \frac{4n}{(n+1)^2} e^{-\frac{\sigma}{2\epsilon} \cdot \frac{nl}{c}} \left\{ \delta(T_0) - \frac{\sigma}{\epsilon} \left[\frac{n-1}{2(n+1)} - \frac{1}{8} \left(\frac{\sigma}{\epsilon} \cdot \frac{nl}{c} \right) \right] \mathcal{U}(T_0) + \frac{\sigma}{\epsilon} \left[\frac{2n^2 - n}{4(n+1)^2} - \frac{1}{8} + \frac{1}{128} \left(\frac{\sigma}{\epsilon} \cdot \frac{nl}{c} \right) \left(\frac{\sigma}{\epsilon} \cdot \frac{nl}{c} - \frac{16n}{n+1} \right) \right] \frac{\sigma}{\epsilon T_0} \mathcal{U}(T_0) + \mathcal{O} \left(\frac{\sigma}{\epsilon} \left(\frac{\sigma}{\epsilon} T_0 \right)^2 \right) \right\} \quad (4.28)$$

It is apparent that 4.28 is valid when $\frac{\sigma}{\epsilon} T_0 \ll 1$. In other words, the expression obtained above yields an asymptotic estimate of $\underline{E}_{30}(z,t)$ for times much smaller than the relaxation time $(\sigma/\epsilon)^{-1}$ of material of which the slab is composed. The exponential factor in 4.28 describes

the attenuation sustained by the incident signal in passing through the slab. It is rather interesting to equate this attenuation to that which a monochromatic signal would experience in passing through the same slab. It is found that a monochromatic signal of angular frequency $\sigma/2\epsilon$ satisfies the above condition.

The value of $\underline{E}_{30}(z,t)$ for large values of T_0 will be obtained by deforming the contour of integration in 4.24 into a new contour which surrounds the branch cut connecting the points $s = 0, -\sigma/\epsilon$. The information pertinent to this contour deformation is contained in Figure 3.2. In order to insure that the contour deformation is valid for $T_0 = 0$, the integrand of 4.24 must be expressed as the sum of two terms. The first term is the asymptotic limit of the integrand on the infinite arc in the left half plane, and the second term is the remainder of the integrand. When this split is performed the integral expression for $\underline{E}_{30}(z,t)$ assumes the form

$$\underline{E}_{30}(z,t) = \frac{a_x}{(n+1)^2} e^{-\frac{\sigma}{2\epsilon} \cdot \frac{n\ell}{c}} \delta(T_0) + \frac{a_x}{\pi i(n+1)^2} I(z,t) \quad (4.29)$$

where

$$I(z,t) = \int_{\Delta-i\infty}^{\Delta+i\infty} \frac{-1 + (1+n^2)(1 + \frac{\sigma}{\epsilon s})^{1/2} - n^2(1 + \frac{\sigma}{\epsilon s})}{1 + n(1 + \frac{\sigma}{\epsilon s})^{1/2}} e^{s(T'_0 - \frac{n\ell}{c}(1 + \frac{\sigma}{\epsilon s})^{1/2})} ds$$

$$T'_0 \equiv T_0 + \frac{n\ell}{c} \quad (4.30)$$

The integrand of the integral $I(z,t)$ vanishes on the infinite arc in the left half plane for $T_0 \geq 0$. Consequently the path of integration

along the line $\text{Re}(s) = \Delta$ can be deformed into the path C which is indicated in Figure 3.2b. On C it is convenient to replace the variable s by $e^{\pm i\pi} \frac{\sigma}{\epsilon} w$. When this is done and the contributions from the top and bottom sides of the cut are added, the following expression is obtained for the integral in 4.29

$$I(z, t) = - \frac{2i\sigma}{\epsilon} \text{Im} \int_0^1 \frac{n^2 - (1+n^2)w + i(1+n^2)w^{1/2}(1-w)^{1/2}}{n^2 - (1+n^2)w - i2nw^{1/2}(1-w)^{1/2}} e^{-\alpha w + i\beta w^{1/2}(1-w)^{1/2}} dw, \quad (4.31)$$

where

$$\alpha \equiv \frac{\sigma}{\epsilon} T'_0, \quad \beta \equiv \frac{\sigma}{\epsilon} \cdot \frac{n\ell}{c},$$

and Im signifies that the imaginary part of the integral is to be taken.

The integral given in 4.31 can be solved asymptotically for large values of α by expanding the integrand in a Taylor series about the origin. This expansion is divergent at $w = 1$ but the results will be asymptotically correct if α is sufficiently large. The appropriate expansions are

$$\frac{n^2 - (1+n^2)w + i(1+n^2)w^{1/2}(1-w)^{1/2}}{n^2 - (1+n^2)w - i2nw^{1/2}(1-w)^{1/2}} = 1 + i \frac{(1+n)^2}{n^2} w^{1/2} - \frac{2(1+n)^2}{n^3} w + \mathcal{O}(w^{3/2}), \quad (4.32)$$

$$e^{i\beta w^{1/2}(1-w)^{1/2}} = e^{i\beta w^{1/2}} [1 + \mathcal{O}(w^{3/2})]. \quad (4.33)$$

The integral which results when 4.32 and 4.33 are substituted in 4.31 can be solved by completing the square in the exponent. If a new

variable $v = w^{1/2} - i \frac{\beta}{2\alpha}$ is introduced, this integral assumes the form

$$\lim_{\alpha \gg 1} I(z,t) \sim -\frac{4i\sigma}{\epsilon} e^{-\frac{\beta^2}{4\alpha}} \operatorname{Im} \int_{-i \frac{\beta}{2\alpha}}^{1 - \frac{i\beta}{2\alpha}} e^{-\alpha v^2} \left[\left(v + \frac{i\beta}{2\alpha}\right) + i \frac{(1+n)^2}{n^2} \left(v + i \frac{\beta}{2\alpha}\right)^2 - 2 \frac{(1+n)^2}{n^3} \left(v + i \frac{\beta}{2\alpha}\right)^3 + \mathcal{O}(v^4) \right] dv. \quad (4.34)$$

The values of three integrals required in the solution of 4.34 are given in the following equations

$$\int_{i \frac{\beta}{2\alpha}}^{1 - i \frac{\beta}{2\alpha}} e^{-\alpha v^2} dv = \left(\frac{\pi}{2\alpha}\right)^{1/2} + i \frac{\beta}{2\alpha} + \mathcal{O}\left(\frac{\beta^3}{\alpha^2}\right), \quad (4.35)$$

$$\int_{-i \frac{\beta}{2\alpha}}^{1 - i \frac{\beta}{2\alpha}} e^{-\alpha v^2} v dv = \frac{1}{2\alpha} e^{\beta^2/4\alpha} + \mathcal{O}(e^{-\alpha}), \quad (4.36)$$

$$\int_{-i \frac{\beta}{2\alpha}}^{1 - i \frac{\beta}{2\alpha}} e^{-\alpha v^2} v^2 dv = \frac{\pi^{1/2}}{(2\alpha)^{3/2}} + \mathcal{O}\left(\frac{\beta^3}{\alpha^2}\right). \quad (4.37)$$

These integrals are evaluated by changing the contour as indicated in Figure 4.2 and solving the integrals along R_1 , R_2 , and R_3 separately. When 4.35 - 4.37 are substituted in 4.34, an asymptotic expansion of $I(z,t)$ is obtained. The result for the transmitted electric field can then be written

$$\begin{aligned}
 \lim_{\frac{\sigma}{\epsilon T'_0} \gg 1} \underline{E}_{30}(z, t) &\sim \frac{a_x}{-x} \frac{4n}{(n+1)^2} e^{-\frac{\sigma}{2\epsilon} \cdot \frac{nl}{c}} \delta(T_0) - \frac{a_x}{(2\pi)^{1/2}} \frac{\sigma}{\epsilon} x \\
 &\sim \frac{4n}{(n+1)^2} \left(\frac{\sigma}{\epsilon} \cdot \frac{nl}{c}\right) \frac{e^{-\frac{\sigma}{4\epsilon} \cdot \frac{nl}{c} \left(\frac{nl}{cT'_0}\right)}}{\left(\frac{\sigma}{\epsilon} T'_0\right)^{3/2}} \left[1 + \frac{(1+n)^2}{n^2} \left(\frac{\sigma}{\epsilon} \frac{nl}{c}\right)^{-1} + \mathcal{O}\left(\frac{nl}{cT'_0}\right)\right] .
 \end{aligned}
 \tag{4.38}$$

V. A COMPLICATED EXAMPLE OF THE METHOD OF SOLUTION WHEN MORE THAN ONE OPTICAL RAY IS PRESENT: REFLECTION AND DIFFRACTION OF A DELTA PULSE BY A PERFECTLY CONDUCTING SPHERE

The approach to the solution of pulse scattering problems which is discussed in the earlier portions of this paper was evolved in an attempt to obtain a satisfactory solution to the problem of pulse scattering from a sphere. The idea of treating each wavefront term separately was conceived in the process of interpreting some of the results of V. H. Weston on the backscattering from a sphere (12). Weston obtains results for the large time behavior of the fields scattered when a square wave modulated carrier signal strikes a sphere. These results are expressed in the form of an infinite sum of residues. The leading term in the residue series is the steady state behavior and the other terms are those associated with the transient behavior. It is found that the transient portion of the residue series does not converge rapidly when $ka \gg 1$. This difficulty can be interpreted as resulting from the fact that, at a finite time T , the wavefronts with delays greater than T are absent. Consequently, the sum of the transient terms must be large enough to eliminate those terms from the steady state term. This leads to the hypothesis that a more desirable formulation of the problem can be obtained by separately considering each term in the wavefront expansion of the transforms of the field vectors.

The wavefront expansion for the problem of pulse scattering by a sphere is obtained with the same technique as was employed in the problem discussed in Chapter IV. The behavior of the transforms of the field vectors in the right half of the z plane is investigated for large values of s . It is well known from the work in steady state diffraction theory, that the harmonic series converges very slowly when $s \gg 1$. One of the most important contributions of the researches in steady state diffraction theory performed in the first half of this century was the evolution of a technique by which a slowly convergent harmonic series can be transformed to a rapidly convergent representation of the field vector transforms when $s \gg 1$. When the field vector transforms are expressed in this form, the identification of the various terms in the wavefront expansion is easily obtained by noting the time delay associated with each term.

The technique employed for the evaluation of the various terms in the wavefront expansion is dependent upon the time at which the signal is desired and the region in space at which the observation is made. The wave behavior in the vicinity of the wavefronts is obtained by applying the Tauberian theorem given in Chapter II, Section 2.3. The integral expressions for the asymptotic values of the field transforms are then treated differently depending on the angular domain within which the observation point is located. The wavefront terms which correspond to

the diffracted rays can be evaluated by the Watson residue series technique. The first term in the wavefront expansion, however, cannot always be evaluated in this manner. The residue series expansion of the first term is adequate in the deep shadow zone. This region is defined by the interior of the cone generated by the tangents to the sphere at the points $(r, \theta, \phi) = (a, \frac{\pi}{2} + (\frac{\rho}{2})^{1/3}, \phi)$. In the illuminated region the appropriate technique of solution is the saddle point method. This region is defined by the tangents to the surface of the sphere at the points $(r, \theta, \phi) = (a, \frac{\pi}{2} - (\frac{\rho}{2})^{-1/3}, \phi)$. In correspondence with the steady state theory, the transition region between the deep shadow and the illuminated region is termed the penumbra. The asymptotic values of the field transforms in this region are obtained by expressing the integral representation in a form which contains Fok type integrals. These integrals are tabulated by Logan (13). The behavior of the waves at large times is obtained in essentially the same manner for all of the wavefront terms.

5.2 Derivation of the Transforms of the Field Vectors

The scattering problem which will be considered in this chapter is depicted in Figure 5.1. The incident wave is a delta pulse which moves along the plane wavefront defined by the condition $t + \frac{z-a}{c} = 0$. The time delay of the incident field is chosen such that the initial values of the scattered field are zero. The incident field vectors and their Laplace transforms can be written

$$\underline{E}^i(z, t) = \frac{a}{-x} \delta(t + \frac{z-a}{c}) \quad , \quad (5.1)$$

$$\underline{H}^i(z, t) = - \frac{a}{-y} \frac{1}{\mu_0 c} \delta(t + \frac{z-a}{c}) \quad , \quad (5.2)$$

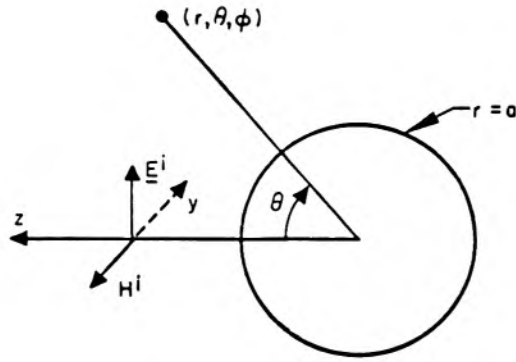


Fig. 5.1 Coordinate system and orientation of incident fields

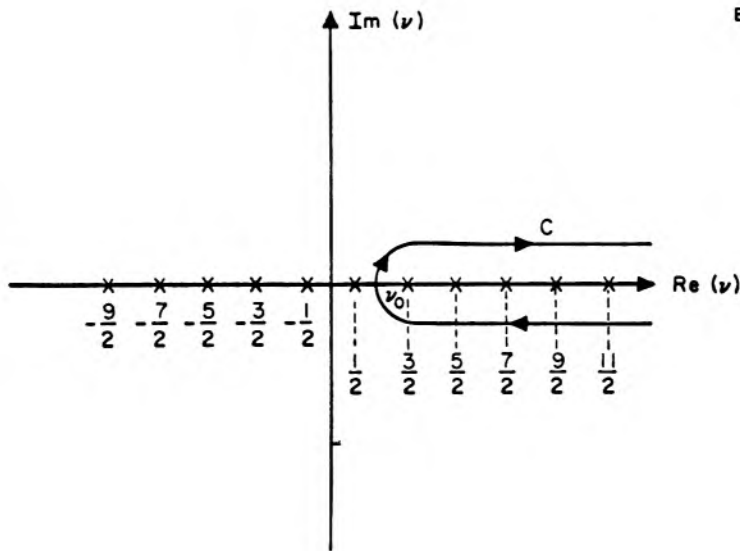


Fig. 5.2 Initial contour

$$\underline{\xi}^i(z, s) = \frac{a}{x} e^{\frac{s}{c}(z-a)} \mathcal{U}(a-z) \quad , \quad (5.3)$$

$$\underline{H}^i(z, s) = -\frac{a}{y} \frac{1}{\mu_0 c} e^{\frac{s}{c}(z-a)} \mathcal{U}(a-z) \quad . \quad (5.4)$$

The transforms of incident field can be written in a more useful form by referring to the work of Stratton which pertains to the expansion of a steady state vector plane wave in spherical coordinates (14). An analytic continuation of the complex conjugate of Stratton's plane wave results yields the expressions

$$\underline{\xi}^i(\underline{r}, s) = e^{-\frac{sa}{c}} \sum_{n=1}^{\infty} (-1)^n \frac{2n+1}{n(n+1)} \left[\frac{m^{(1)}(\underline{r}, s)}{o_{ln}} + i \frac{n^{(1)}(\underline{r}, s)}{e_{ln}} \right] \mathcal{U}(a-z) \quad , \quad (5.5)$$

$$\underline{H}^i(\underline{r}, s) = -\frac{1}{\mu_0 c} e^{-\frac{sa}{c}} \sum_{n=1}^{\infty} (-1)^n \frac{2n+1}{n(n+1)} \left[\frac{m^{(1)}(\underline{r}, s)}{e_{ln}} - i \frac{n^{(1)}(\underline{r}, s)}{o_{ln}} \right] \mathcal{U}(a-z) \quad (5.6)$$

where

$$\frac{m^{(1)}(\underline{r}, s)}{o_{ln}} = \pm j_n(iR) \frac{P_n^1(\cos \theta)}{\sin \theta} \cos \phi \frac{a}{\rho} - j_n(iR) \frac{\partial}{\partial \theta} P_n^1(\cos \theta) \frac{\sin \phi}{\cos \theta} \frac{a}{\rho} \quad (5.7)$$

$$\frac{n^{(1)}(\underline{r}, s)}{e_{ln}} = \frac{n(n+1)}{iR} j_n(iR) P_n^1(\cos \theta) \frac{\sin \phi}{\cos \theta} \frac{a}{r} + \frac{1}{iR} [iR j_n(iR)]' \frac{\partial}{\partial \theta} P_n^1(\cos \theta) \frac{\sin \phi}{\cos \theta} \frac{a}{\rho} \pm \frac{1}{iR} [iR j_n(iR)]' \frac{P_n^1(\cos \theta)}{\sin \theta} \cos \phi \frac{a}{\rho} \quad (5.8)$$

and the prime denotes a differentiation with respect to $\frac{isr}{c} \equiv iR$.

The transforms of the scattered fields satisfy the vector wave equation 2.14 with $\sigma = 0$. This equation becomes identical with the steady state vector wave equation if s is replaced by $-ik$, where k is the wave number of a steady state wave. This indicates that the transforms of the scattered field vectors can also be obtained from Stratton's results on plane wave scattering by analytic continuation. The transforms of the scattered electromagnetic fields obtained in this way are

$$\underline{\underline{\xi}}^{\Delta}(\underline{r}, s) = e^{-\frac{sa}{c}} \sum_{n=1}^{\infty} (-1)^n \frac{2n+1}{n(n+1)} \left[a_n^{\Delta} \frac{m^{(3)}(\underline{r}, s)}{o_{ln}} + i b_n^{\Delta} \frac{n^{(3)}(\underline{r}, s)}{e_{ln}} \right] \quad (5.9)$$

$$-u_c \underline{\underline{H}}^{\Delta}(\underline{r}, s) = e^{-\frac{sa}{c}} \sum_{n=1}^{\infty} (-1)^n \frac{2n+1}{n(n+1)} \left[b_n^{\Delta} \frac{m^{(3)}(\underline{r}, s)}{e_{ln}} - i a_n^{\Delta} \frac{n^{(3)}(\underline{r}, s)}{o_{ln}} \right] \quad (5.10)$$

where $\frac{m^{(3)}}{e_{ln}}$ and $\frac{n^{(3)}}{o_{ln}}$ are the same respectively as the superscript (1) quantities, except that $j_n(iR)$ is replaced by $h_n^{(1)}(iR)$ throughout.

For a perfectly conducting sphere

$$a_n^{\Delta} = - \frac{j_n(i\rho)}{h_n^{(1)}(i\rho)}, \quad (5.11)$$

$$b_n^{\Delta} = - \frac{[i\rho j_n(i\rho)]'}{[i\rho h_n^{(1)}(i\rho)]'} \quad (5.12)$$

where $\frac{sa}{c} \equiv \rho$. The explicit forms of the transverse components of the transforms of the electric field scattered by a perfectly conducting sphere are

$$\begin{aligned} \xi_{\theta}^{\circ}(\underline{r}, s) = & - e^{-\frac{sa}{c}} \sum_{n=1}^{\infty} (-i)^n \frac{2n+1}{n(n+1)} \left[\frac{j_n(i\rho)}{h_n^{(1)}(i\rho)} h_n^{(1)}(iR) \frac{P_n^1(\cos \theta)}{\sin \theta} + \right. \\ & \left. + \frac{1}{R} \frac{[i\rho j_n(k\rho)]'}{[i\rho h_n^{(1)}(i\rho)]'} [iR h_n^{(1)}(iR)]' \frac{\partial}{\partial \theta} P_n^1(\cos \theta) \right] \cos \phi \quad (5.13) \end{aligned}$$

$$\begin{aligned} \xi_{\phi}^{\circ}(\underline{r}, s) = & e^{-\frac{sa}{c}} \sum_{n=1}^{\infty} (-i)^n \frac{2n+1}{n(n+1)} \left[\frac{j_n(i\rho)}{h_n^{(1)}(i\rho)} h_n^{(1)}(iR) \frac{\partial}{\partial \theta} P_n^1(\cos \theta) + \right. \\ & \left. + \frac{1}{R} \frac{[i\rho j_n(i\rho)]'}{[i\rho h_n^{(1)}(i\rho)]'} [iR h_n^{(1)}(iR)]' \frac{P_n^1(\cos \theta)}{\sin \theta} \right] \sin \phi \quad (5.14) \end{aligned}$$

5.3 Investigation of the Properties of the Transforms for $s \gg 1, \text{Re}(s) > 0$

The form of the wavefront expansion for the scattering from a sphere is not at all obvious from the results derived in the last section. In order to discover the correct way to decompose the field, we must appeal to the approach employed in the simple problem of Chapter IV. It has been shown that the behavior of a scattered wave in the vicinity of its wavefronts can be obtained by considering the asymptotic behavior of its transform in the right half of the s plane. Consequently, it is reasonable to assume that an investigation of the asymptotic behavior of ξ_{θ}° and ξ_{ϕ}° in the right half plane will give an indication of the way in which these transforms should be written in order to accomplish the desired wavefront expansion.

5.3.1 The transformation from the harmonic series to an equivalent integral form. When $s \gg 1$ the harmonic series representations given in Section 5.2 do not converge very rapidly. Basically, the reason for the poor convergence is the fact that the Bessel function $j_n(i\rho)$ has

its maximum value in the vicinity of $n \sim ip$. Consequently, when $s \gg 1$ a large number of terms must be included when the harmonic series are summed. A reasonably accurate result can be obtained if the number of terms retained is of the order 2ρ (15). The slow convergence of the harmonic series was a major hurdle to the development of the theory of the diffraction of monochromatic waves by a sphere. This difficulty was eventually circumvented by the application of a summation technique in which the harmonic series was transformed into a new series which was rapidly convergent for large ka . One of the first papers on this transformation of the harmonic series was written by Watson (16). As a result, the transformation of a harmonic series to a new series which is more rapidly convergent is quite often termed a Watson transformation. The Watson transformation is accomplished by transforming the harmonic series into an equivalent integral representation and then evaluating the integral by the calculus of residues. The result of this operation is commonly referred to as a Watson residue series. In the present section we will perform the first part of a Watson transformation. The harmonic series representations of the transverse fields will be transformed into equivalent integral representations.

In the attempt to uncover the proper decomposition of the transforms of the field vectors, it is convenient to consider the total field rather than the scattered field alone. It also simplifies matters if the transforms of the transverse components are defined in terms of two scalar functions $V_1(\underline{r}, s)$ and $V_2(\underline{r}, s)$. These functions will be defined by the following equations:

$$V_1(\underline{r}, s) = \sum_{n=1}^{\infty} (-1)^n \frac{2n+1}{n(n+1)} \left[j_n(iR) - \frac{j_n(i\rho)}{h_n^{(1)}(i\rho)} h_n^{(1)}(iR) \right] P_n^1(\cos \theta) \quad (5.15)$$

$$V_2(\underline{r}, s) = \frac{1}{R} \sum_{n=1}^{\infty} (-1)^n \frac{2n+1}{n(n+1)} \left[[iR j_n(iR)]' - \frac{[i\rho j_n(i\rho)]'}{[i\rho h_n^{(1)}(i\rho)]'} [iR h_n^{(1)}(iR)] \right] \times \\ \times P_n^1(\cos \theta) . \quad (5.16)$$

In terms of these functions, the transverse electric fields are given by the relations

$$\mathcal{E}_\theta(\underline{r}, s) = e^{-\frac{sa}{c}} \left[\frac{V_1(\underline{r}, s)}{\sin \theta} + \frac{\partial}{\partial \theta} V_2(\underline{r}, s) \right] \cos \phi \quad (5.17)$$

$$\mathcal{E}_\phi(\underline{r}, s) = -e^{-\frac{sa}{c}} \left[\frac{\partial}{\partial \theta} V_1(\underline{r}, s) + \frac{V_2(\underline{r}, s)}{\sin \theta} \right] \sin \phi . \quad (5.18)$$

The transverse components of the transforms of the field vectors are obviously completely determined by the scalar functions $V_1(\underline{r}, s)$ and $V_2(\underline{r}, s)$. The radial field quantities are not determined by the same functions but instead by the function

$$V_3(\underline{r}, s) = \frac{1}{R} \sum_{n=1}^{\infty} (-1)^n (2n+1) \left[j_n(iR) - \frac{[i\rho j_n(i\rho)]'}{[i\rho h_n^{(1)}(i\rho)]'} h_n^{(1)}(iR) \right] \times \\ \times P_n^1(\cos \theta) . \quad (5.19)$$

The transform of the radial electric field is given by the relation

$$\xi_{\underline{r}}(\underline{r}, s) = e^{-\frac{sa}{c}} V_3(\underline{r}, s) \cos \phi . \quad (5.20)$$

In the work which follows we will consider only the functions $V_1(\underline{r}, s)$ and $V_2(\underline{r}, s)$ since the transverse fields are usually the quantities of physical interest. Also the results for $V_2(\underline{r}, s)$ will be deduced from those derived for $V_1(\underline{r}, s)$.

The series representation of $V_1(\underline{r}, s)$ can be changed into an equivalent integral form by means of a "trick" often employed in problems of this type. Consider the value of an integral with respect to a variable τ whose integrand is equal to the product of the n^{th} term in 5.15 with n replaced by τ , the function $(\sin \pi \tau)^{-1}$, and an, as yet, unspecified function $B(\tau)$.

$$V_1(\underline{r}, s) = \int_C (-1)^\tau \frac{2\tau+1}{\tau(\tau+1)} \left[j^\tau(iR) - \frac{j_\tau(i\rho)}{h_\tau^{(1)}(i\rho)} h_\tau^{(1)}(iR) \right] \times \\ \times P_\tau^1(-\cos \theta) \frac{(-1)^{\tau+1} B(\tau)}{\sin \pi \tau} d\tau . \quad (5.21)$$

The contour C is illustrated in Figure 5.2. In writing 5.21, the relation

$$P_n^1(\cos \theta) = (-1)^{n+1} P_n^1(-\cos \theta) \quad (5.22)$$

is employed. This is necessitated by the fact that the associated Legendre function of non-integral order, $P_\tau^1(\cos \theta)$ is singular along the line $\theta = \pi$. Since it is desired to obtain a representation which is valid along this line, the relation 5.22 is employed. A rather confusing point about the representation given in 5.21 is the fact that, in its final form when the wavefront terms have been separated, the results

obtained along the line $\theta = 0$ are correct. This is not predicted by the form of 5.21 since $P_{\tau}^1(-\cos \theta)$ is singular along the line. When Cauchy's residue theorem is applied to 5.21 and the result is equated to the series 5.15, it is found that $B(\tau) = 1/2i$.

The integral representation of $V_1(\underline{r}, s)$ derived above is not yet in a form in which the wavefront terms are evident. The direction in which to proceed at this point, however, is indicated by the results from steady state diffraction theory. In the steady state theory the integral representation of the field for short wavelength involves an integral of the type given in 5.21 but the path usually runs along a straight line above or below the real axis from $-\infty$ to ∞ . The result 5.21 can be put in this form by first replacing the variable τ by a new variable $\nu - \frac{1}{2}$. When this is done, it is found that the integrand of the new integral is an even function of ν . The lower portion of the path C can then be replaced by a path along the top of the negative real axis. This path is obtained by a reflection of the lower portion of C through the origin. The resultant contour of integration, D_0 , is illustrated in Figure 5.3a. This is still not quite what is required, since a continuous path from $-\infty$ to ∞ is desired. The path D_0 is equal to a continuous path D plus a short path E running from ν_0 to $-\nu_0$ where $\frac{1}{2} < \nu_0 < \frac{3}{2}$. It can be shown that the contribution to the transverse fields from the path E is zero. This is not true for the individual functions $V_1(\underline{r}, s)$ and $V_2(\underline{r}, s)$. When equations 5.17 and 5.18 are employed to calculate ξ_{θ} and ξ_{ϕ} , however, it is found that the portion of $V_1(\underline{r}, s)$ which is due to the integration along E is canceled by the like portion of $V_2(\underline{r}, s)$. As

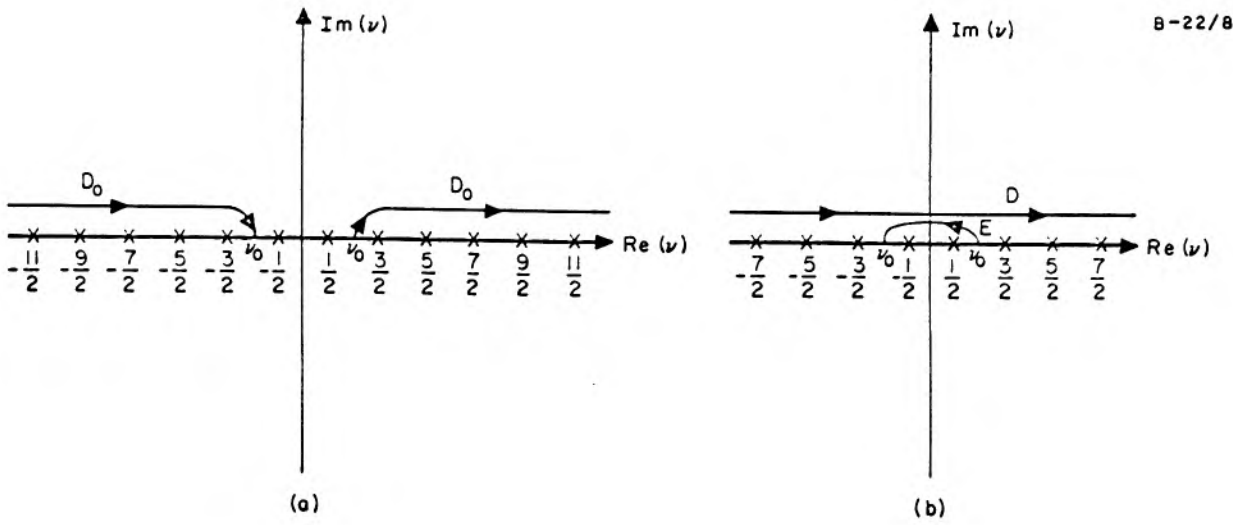


Fig. 5.3 Equivalent contours

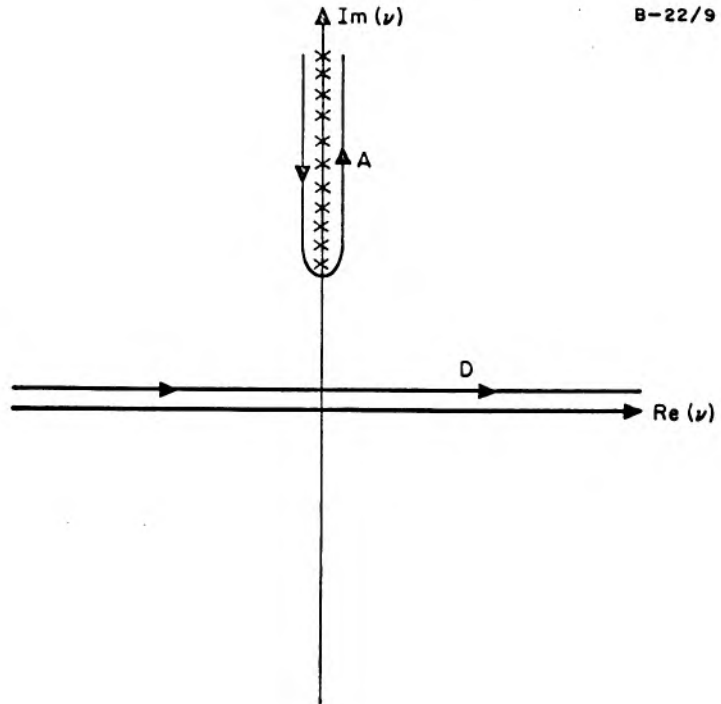


Fig. 5.4 Contour for residue series calculation

a result, it is convenient to define a new set of functions $I_1(\underline{r}, s)$ and $I_2(\underline{r}, s)$ which do not involve the integral along E .

$$I_1(\underline{r}, s) = e^{i\frac{3\pi}{4}} \int_D (-1)^\nu \frac{\nu}{\nu^2 - \frac{1}{4}} \left[j_{\nu - \frac{1}{2}}(iR) - \frac{j_{\nu - \frac{1}{2}}(i\rho)}{h_{\nu - \frac{1}{2}}^{(1)}(i\rho)} h_{\nu - \frac{1}{2}}^{(1)}(iR) \right] \frac{P_{\nu - \frac{1}{2}}^1(-\cos \theta)}{\cos \nu \pi} d\nu \quad (5.23)$$

$$I_2(\underline{r}, s) = \frac{e^{i\frac{3\pi}{4}}}{R} \int_D (-1)^\nu \frac{\nu}{\nu^2 - \frac{1}{4}} \left[[iRh_{\nu - \frac{1}{2}}^{(1)}(iR)]' - \frac{[i\rho j_{\nu - \frac{1}{2}}(i\rho)]'}{[i\rho h_{\nu - \frac{1}{2}}^{(1)}(i\rho)]'} [iRh_{\nu - \frac{1}{2}}^{(1)}(iR)]' \right] \frac{P_{\nu - \frac{1}{2}}^1(-\cos \theta)}{\cos \nu \pi} d\nu \quad (5.24)$$

The transverse electric fields can be expressed in terms of these functions by equations which are identical with 5.17 and 5.18 except $V_1(\underline{r}, s)$ and $V_2(\underline{r}, s)$ are replaced by $I_1(\underline{r}, s)$ and $I_2(\underline{r}, s)$ respectively. The equations 5.23 and 5.24 are the desired integral representations of the original harmonic series.

5.3.2 Identification of the various terms in the wavefront expansion. It has been indicated that a hint as to the form of the wavefront expansion can be obtained from an investigation of the behavior of the field transforms for large values of s . In order to simplify matters, the investigation will be limited to a discussion of the asymptotic behavior of the scalar quantity $I_1(\underline{r}, s)$ which is defined in the

preceding section. The behavior of $I_2(\underline{r},s)$, $\xi_\theta(\underline{r},s)$ and $\xi_\phi(\underline{r},s)$ will be deduced from that of $I_1(\underline{r},s)$

An idea of asymptotic form of $I_1(\underline{r},s)$ can be obtained by considering the behavior of its integrand for large s . The integrand behaves in exactly the same manner as the terms in the original harmonic series did for large s . The significant regions of the ν plane are determined by those values of ν for which $\nu \sim i\rho$. The asymptotic form of $I_1(\underline{r},s)$ for large s is therefore very closely related to the asymptotic value of the integrand of 5.23 for large ν . This provides a very important clue as to the nature of the desired decomposition of $I_1(\underline{r},s)$. Each term in the wavefront expansion has an exponent which accounts for the time delay associated with that term. Consequently, the wavefront expansion should involve a series of terms each of which has a different asymptotic exponent. It is not possible to express the Bessel and Hankel functions in a series of terms of the form indicated above. The angular function $P_{\nu - \frac{1}{2}}^1(-\cos \theta)/\cos \nu\pi$, however, does possess such an asymptotic expansion. A complete decomposition of this function into a series of terms, each of which has a different asymptotic exponent, can be obtained from equations A-3.2 and A-3.8 of Appendix III. The proposed expansion of the angular function is given by the relation

$$\frac{P_{\nu - \frac{1}{2}}^1(-\cos \theta)}{\cos \nu\pi} = \frac{2i}{\pi} Q_{\nu - \frac{1}{2}}^1(\cos \theta - i0) + \frac{2i}{\pi} \sum_{p=1}^{\infty} (-1)^p \left[Q_{\nu - \frac{1}{2}}^1(\cos \theta + i0) + Q_{\nu - \frac{1}{2}}^1(\cos \theta - i0) \right] e^{12p\pi\nu} \quad (5.25)$$

The asymptotic behavior of the function $Q_{\nu - \frac{1}{2}}^1(\cos \theta \pm i0)$ is obtained as indicated in equation A-3.9. It is noted that each term in 5.25 has a different asymptotic exponent.

The discussion in the preceding paragraph leads to the conclusion that the wavefront expansion of the fields scattered by a sphere can be obtained by replacing the angular function which appears in the integral representations 5.23 and 5.24 by the expansion defined in equation 5.25. The proposed wavefront expansion of $I_1(\underline{r}, s)$ can be written

$$I_1(\underline{r}, s) = \sum_{m=0}^{\infty} (-1)^m I_{1m}(\underline{r}, s, -) + \sum_{m=1}^{\infty} (-1)^m I_{1m}(\underline{r}, s, +) \quad (5.26)$$

where

$$I_{1m}(\underline{r}, s, \pm) = -\frac{2}{\pi} e^{i\frac{\pi}{4}} \int_D (-1)^\nu \frac{\nu}{\nu - \frac{1}{4}} \left[j_{\nu - \frac{1}{2}}(iR) - \frac{j_{\nu - \frac{1}{2}}(i\rho)}{h_{\nu - \frac{1}{2}}^{(1)}(i\rho)} h_{\nu - \frac{1}{2}}^{(1)}(iR) \right] e^{i2m\pi\nu} Q_{\nu - \frac{1}{2}}^1(\cos \theta \pm i0) d\nu \quad (5.27)$$

It will be demonstrated in the subsequent portions of this paper that the expansion defined by equations 5.26 and 5.27 is the required wavefront expansion.

5.4 Derivation of the Asymptotic Estimates of the Transforms for Large s

The Tauberian theorem given in Chapter II, Section 2.3, will be employed to simplify the problem of inverting the transforms of the field vectors in the vicinity of the wavefronts. This will necessitate an

explicit knowledge of the asymptotic form of these transforms for large s . It will be sufficient to consider the behavior of $I_1(\underline{r}, s)$ since the results for $I_2(\underline{r}, s)$ can be deduced from those for $I_1(\underline{r}, s)$.

The dependence of $I_1(\underline{r}, s)$ on the variable s is entirely contained in the bracketed quantity in 5.27. The asymptotic behavior of this quantity can be determined from the results of Appendix I. The calculation of the asymptotic expansion of $I_{1m}(\underline{r}, s, \pm)$ for large s is simplified if it is assumed that $\arg s = 0$. On the path of integration in the s plane $\arg s \neq 0$, but the asymptotic expansion of $I_m(\underline{r}, s, \pm)$ obtained along the line $\arg s = 0$ can be analytically continued on to the path of integration ($\operatorname{Re} s > 0$). The analytic continuation is legitimate since the asymptotic expansions employed for the Hankel and Bessel functions in 5.27 are valid in the entire angular domain $-\frac{3}{2} < \arg s < \frac{\pi}{2}$.

It will be shown that the asymptotic expansion of the functions $I_{1m}(\underline{r}, s, \pm)$, $m \neq 0$, can be obtained by evaluating equation 5.27 by the calculus of residues. It is demonstrated that these terms correspond to the diffracted rays of a generalized geometrical optics. The behavior of the $m = 0$ term of the wavefront expansion is dependent upon the position of the observer. In the deep shadow zone the asymptotic expansion of $I_{10}(\underline{r}, s, -)$ is obtained in the same way as the higher order wavefront terms. In the illuminated region the residue series expression for $I_{10}(\underline{r}, s, -)$ converges extremely slowly. The appropriate technique of evaluation in this region is the saddle point method. It is found that the function $I_{10}(\underline{r}, s, -)$ can be divided into two wavefront terms in the illuminated region. One of these terms corresponds

to the incident wavefront and the other describes the geometrically reflected field. In the transitional region between the deep shadow and the illuminated region $I_{10}(\underline{r}, s, -)$ is again expressed as the sum of two terms. One of these terms corresponds to a conventional knife edge type diffraction phenomena and the other is a correction term which accounts for the non-zero radius of curvature of the sphere at the shadow boundary.

5.4.1 The deep shadow region. The integrand of the integral in equation 5.27 vanishes on the infinite arc in the upper half of the v plane. This behavior is insured by the particular combination of Bessel and Hankel functions which appear in the integrand. It was for this reason that we chose to consider the transforms of the total field rather than the scattered field alone. Since the integrands of the integral expressions for the wavefront term $I_{1m}(\underline{r}, s, \pm)$ vanish on the infinite arc, the contour D can be deformed into a new contour which encircles the singularities of the integrands in the upper half plane. The only singularities of $I_{1m}(\underline{r}, s, \pm)$ in the upper half of the v plane are the simple poles associated with the zeros of the Hankel function $H_v^1(i\rho)$. Figure 5.4 illustrates the location of these zeros and the deformation of the contour D into a new contour A which encircles the zeros of $H_v^1(i\rho)$ in the upper half plane.

A straightforward evaluation of the integral around the contour A by Cauchy's theorem yields the following residue series expression for the wavefront terms $I_{1m}(\underline{r}, s)$.

$$I_{lm}(\underline{r}, s, \pm) = 2e^{\frac{i3\pi}{4}} \sum_{\nu_l} (-i)^{\nu_l} \frac{\nu_l}{\nu_l - \frac{1}{4}} \frac{H_{\nu_l}^{(2)}(i\rho)}{\frac{\partial}{\partial \nu_l} H_{\nu_l}^{(1)}(i\rho)} h_{\nu_l - \frac{1}{2}}^{(1)}(i\rho) \times$$

$$\times e^{\frac{i2\pi\nu_l}{\nu_l - \frac{1}{2}}} Q_{\nu_l - \frac{1}{2}}^1(\cos \theta \pm i0) \quad (5.28)$$

where ν_l is the l^{th} zero of the Hankel function $H_{\nu - \frac{1}{2}}^{(1)}(i\rho)$. A slightly more useful form of this equation can be obtained by applying the Wronskian relation

$$H_{\nu}^{(1)}(i\rho) H_{\nu}^{(2)'}(i\rho) - H_{\nu}^{(1)'}(i\rho) H_{\nu}^{(2)}(i\rho) = -\frac{4}{\pi\rho} \quad (5.29)$$

When 5.29 is employed to eliminate the Hankel function of the second kind in 5.28, we obtain

$$I_{lm}(\underline{r}, s, \pm) = \frac{8e^{\frac{i3\pi}{4}}}{\pi\rho} \sum_{\nu_l} (-i)^{\nu_l} \frac{\nu_l}{\nu_l - \frac{1}{4}} \frac{\partial \nu_l / \partial (i\rho)}{[H_{\nu_l}^{(1)}(i\rho)]^2} h_{\nu_l - \frac{1}{2}}^{(1)}(iR) \times$$

$$\times e^{\frac{i2\pi\nu_l}{\nu_l - \frac{1}{2}}} Q_{\nu_l - \frac{1}{2}}^1(\cos \theta \pm i0) \quad (5.30)$$

The residue series expression which is given in equation 5.30 is exact. An asymptotic expansion of this series for large values of s can be obtained if the quantities ν_l , $H_{\nu_l}^{(1)'}(i\rho)$ and $Q_{\nu_l - \frac{1}{2}}^1(\cos \theta \pm i0)$ are replaced by their asymptotic expansions. The necessary expansions can be obtained from Appendices I and III.

$$\lim_{s \gg 1} v_l = 1 \left[\rho + \alpha_l \left(\frac{\rho}{2}\right)^{1/3} + \frac{1}{60} \alpha_l^2 \left(\frac{\rho}{2}\right)^{-1/3} + O(\rho^{-1}) \right], \quad (5.31)$$

$$\lim_{s \gg 1} H_{v_l}^{(1)'}(i\rho) = -4 \left(\frac{1 - z_l^2}{4z_l^2 \zeta_l} \right)^{1/4} \frac{e^{i\pi/3}}{z_l^{1/2} v_l^{2/3}} A_1'(v_l^{2/3} \zeta_l e^{i\frac{2\pi}{3}}) \left[1 + O(\rho^{-2/3}) \right] \quad (5.32)$$

$$\lim_{s \gg 1} Q_{v_l - \frac{1}{2}}^1(\cos \theta + i0) = \left(\frac{\pi v_l}{2 \sin \theta} \right)^{1/2} e^{-i v_l \theta - i\frac{\pi}{4}} \left[1 + O\left(\frac{1}{\rho \sin \theta}\right) \right] \quad (5.33)$$

$$\lim_{s \gg 1} Q_{v_l - \frac{1}{2}}^1(\cos \theta - i0) = \left(\frac{\pi v_l}{2 \sin \theta} \right)^{1/2} e^{+i v_l \theta - i\frac{3\pi}{4}} \left[1 + O\left(\frac{1}{\rho \sin \theta}\right) \right] \quad (5.34)$$

where

$$z_l \equiv \frac{i\rho}{v_l},$$

$$\alpha_l = l^{\text{th}} \text{ zero of the Airy function } A_1(-\alpha)$$

$$\frac{2}{3} \zeta_l^{3/2} = \ln \left(\frac{1 + (1 - z_l^2)^{1/2}}{z_l} \right) - (1 - z_l^2)^{1/2},$$

and a prime indicates a differentiation with respect to the argument of the primed quantity. When the expansions given in 5.31 - 5.34 are substituted in 5.30, the following asymptotic estimates are obtained

$$\lim_{s \gg 1} {}_{lm} I_{lm}(r, s, -) = \frac{e^{i\frac{3\pi}{4}}}{2\left(\frac{\rho}{2}\right)^{1/6} (\pi \sin \theta)^{1/2}} \sum_{\alpha_l} \frac{e^{i v_l (2m\pi + \theta - \frac{\pi}{2})}}{[A_1'(-\alpha_l)]^2} \times$$

$$\times h_{v_l - \frac{1}{2}}^{(1)}(iR) \left[1 + O(\rho^{-2/3} + (\rho \sin \theta)^{-1}) \right] \quad (5.35)$$

$$\lim_{s \gg 1} I_{1m}(\underline{r}, s, +) = \frac{e^{i\frac{5\pi}{4}}}{2(\frac{\rho}{2})^{1/6}(\pi \sin \theta)^{1/2}} \sum_{\alpha_\ell} \frac{e^{i\nu_\ell(2m\pi - \theta - \frac{\pi}{2})}}{[A_1'(-\alpha_\ell)]^2} \times h_{\nu_\ell}^{(1)} - \frac{1}{2}(iR) \left[1 + O(\rho^{-2/3} + (\rho \sin \theta)^{-1}) \right] \quad (5.36)$$

Likewise the asymptotic estimates for the functions $I_{2m}(\underline{r}, s, \pm)$ are given by

$$\lim_{s \gg 1} I_{2m}(\underline{r}, s, -) = \frac{e^{-i\frac{\pi}{4}}}{2(\frac{\rho}{2})^{1/6}(\pi \sin \theta)^{1/2}} \sum_{\beta_p} \frac{e^{i\nu_p(2m\pi + \theta - \frac{\pi}{2})}}{\beta_p [A_1(-\beta_p)]^2} \times \frac{[iRh_{\nu_p}^{(1)} - \frac{1}{2}(iR)]'}{R} \left[1 + O(\rho^{-2/3} + (\rho \sin \theta)^{-1}) \right] \quad (5.37)$$

$$\lim_{s \gg 1} I_{2m}(\underline{r}, s, +) = \frac{e^{i\frac{\pi}{4}}}{2(\frac{\rho}{2})^{1/6}(\pi \sin \theta)^{1/2}} \sum_{\beta_p} \frac{e^{i\nu_p(2m\pi - \theta - \frac{\pi}{2})}}{\beta_p [A_1(-\beta_p)]^2} \times \frac{[iRh_{\nu_p}^{(1)} - \frac{1}{2}(iR)]'}{R} \left[1 + O(\rho^{-2/3} + (\rho \sin \theta)^{-1}) \right] \quad (5.38)$$

where β_p is the p^{th} zero of the Airy function $A_1'(-\beta)$. The first fifty-six values of α_ℓ , $A_1'(-\alpha_\ell)$, β_p , $A_1(-\beta_p)$ have been tabulated by Logan (5). These tables are given in Appendix II. A number of observations concerning the properties of the expansions 5.35 - 5.38 are made in the following sub-sections.

5.4.1a Near Field

In the near field ($r \sim a$) the argument of the Hankel function $h_{\nu_\ell - \frac{1}{2}}^{(1)}(iR)$ is of the same order as the order ν_ℓ . The appropriate asymptotic form is then given by the Airy function approximation

$$h_{\nu_\ell - \frac{1}{2}}^{(1)}(iR) = \left(\frac{2\pi}{R}\right)^{1/2} \frac{e^{-i\frac{3\pi}{4}}}{\left(\frac{\rho}{2}\right)^{1/3}} A_1(-\alpha_{\ell r}) \left[1 + \mathcal{O}(\rho^{-4/3})\right] \quad (5.39)$$

The parameter $\alpha_{\ell r}$ is defined by the relation

$$\nu_\ell = i \left[R + \alpha_{\ell r} \left(\frac{R}{2}\right)^{1/3} + \frac{1}{60} \alpha_{\ell r}^2 \left(\frac{R}{2}\right)^{1/3} + \mathcal{O}(R^{-1}) \right] \quad (5.40)$$

If the two expressions for ν_ℓ given in equations 5.31 and 5.40 are equated, the parameter $\alpha_{\ell r}$ can be expressed in terms of α_ℓ . It is found that

$$\alpha_{\ell r} = \alpha_\ell - \frac{R - \rho}{\left(\frac{\rho}{2}\right)^{1/3}} + \mathcal{O}(\rho^{-2/3}) \quad (5.41)$$

Consequently, the form of the asymptotic estimate of $h_{\nu_\ell - \frac{1}{2}}^{(1)}(iR)$ which is appropriate in the near field can be written

$$h_{\nu_\ell - \frac{1}{2}}^{(1)}(iR) = \left(\frac{2\pi}{R}\right)^{1/2} \frac{e^{-i\frac{3\pi}{4}}}{\left(\frac{\rho}{2}\right)^{1/3}} A_1 \left(\frac{R - \rho}{\left(\frac{\rho}{2}\right)^{1/3}} - \alpha_\ell \right) \left[1 + \mathcal{O}(\rho^{-2/3})\right] \quad (5.42)$$

Likewise, the estimate for $[iR h_{\nu_\ell - \frac{1}{2}}^{(1)}(iR)]'/R$ can be written

$$[i h_{\nu_\ell - \frac{1}{2}}^{(1)}(iR)]'/R = \left(\frac{2\pi}{R}\right)^{1/2} \frac{e^{i\frac{3\pi}{4}}}{\left(\frac{\rho}{2}\right)^{1/3}} A_1' \left(\frac{R - \rho}{\left(\frac{\rho}{2}\right)^{1/3}} - \beta_p \right) \left[1 + \mathcal{O}(\rho^{-2/3})\right] \quad (5.43)$$

Substitution of equations 5.42 and 5.43 in equations 5.35 - 5.38 will yield asymptotic estimates of the functions $I_{1m}(\underline{r}, s, \pm)$, $I_{2m}(\underline{r}, s, \pm)$ in the near field.

5.4.1b Far Field

The far field will be defined as that region of space in which the Debye type asymptotic expansions given in equations A-1.50 - A-1.59 are valid. The Debye approximation yields the relation

$$h_{\nu - \frac{1}{2}}^{(1)}(iR) = \frac{e^{-i\frac{3\pi}{4}}}{R(-i \sinh \gamma)^{1/2}} e^{iR[\sinh \gamma - \gamma \cosh \gamma]} \left[1 + O(R \sinh \gamma)^{-1} \right] \quad (5.44)$$

where γ is defined such that $\nu = iR \cosh \gamma$. The necessity of employing the more accurate Airy function estimate in the near field is now evident. In the near field the parameter $\gamma \rightarrow 0$. Consequently the error term in 5.44 becomes very large. An idea of the extent of the near field region can be obtained by defining this region as extending out to the point at which $R \sin \gamma = \rho^{2/3}$. At this point the error in the Debye form and the Airy integral form is equal. The transition is found to occur when $R \sim \rho + \text{constant} \times \rho^{1/3}$.

A convenient form of the relation 5.44 is

$$h_{\nu - \frac{1}{2}}^{(1)}(iR) = \frac{e^{-i\frac{3\pi}{4}}}{R^{1/2}(R^2 - \rho^2)^{1/4}} e^{-(R^2 - \rho^2)^{1/2} - i\nu_\ell \cos^{-1} \frac{\rho}{R}} \left[1 + O\left(\frac{\rho^{4/3}}{R^2}\right) \right] \quad (5.45)$$

This equation is obtained by using the relation $\cosh \gamma = \frac{\nu_\ell}{iR}$ with ν_ℓ being given by equation 5.31. Similarly, the following asymptotic

estimate of $[iR h_{\nu_\ell - \frac{1}{2}}^{(1)}(iR)]'/R$ can be obtained

$$[iR h_{\nu_\ell - \frac{1}{2}}^{(1)}(iR)]'/R = \frac{e^{i\frac{\pi}{4}}}{R^{1/2}(R^2 - \rho^2)^{1/4}} e^{-(R^2 - \rho^2)^{1/2} - i\nu_\ell \cos^{-1} \frac{\rho}{R}} \left[1 + O\left(\frac{\rho^{4/3}}{R}\right)\right] \quad (5.46)$$

Substitution of equations 5.45 and 5.46 in equations 5.35 - 5.38 will yield asymptotic estimates of the functions $I_{1m}(\underline{r}, s, \pm)$, $I_{2m}(\underline{r}, s, \pm)$ in the far field.

5.4.1c Fields in the Vicinity of the
Focal Line $\theta = \pi$

In the asymptotic expansions 5.35 - 5.38 the order of the error is given by the quantity $(\rho^{-2/3} + (\rho \sin \theta)^{-1})$. It is noted, the second term in this expression becomes very large when $\theta \sim \pi$. Consequently the expansions 5.35 - 5.38 are not useful in the region $\theta \sim \pi$. It will subsequently be demonstrated that equations 5.35 - 5.38 describe the amplitude of the waves which travel along the rays of a generalized geometric optics. The difficulty in the region $\theta \sim \pi$ is related to the presence of a caustic of the ray system along the line $\theta = \pi$.

The asymptotic expansions which are appropriate in the vicinity of the caustic can be obtained by writing the angular function in $I_1(\underline{r}, s)$ and $I_2(\underline{r}, s)$ in the form

$$\frac{P^{1/2}}{\cos \nu\pi} = 2P^{1/2} (-\cos \theta)^{\nu - \frac{1}{2}} \sum_{m=0}^{\infty} (-1)^m e^{i(2m+1)\pi\nu} \quad (5.47)$$

The wavefront expansion of $I_1(\underline{r}, s)$ is then written in the form

$$I_1(\underline{r}, s) = \sum_{m=0}^{\infty} (-1)^m I_{1m}^c(\underline{r}, s) , \quad (5.48)$$

where

$$I_{1m}^c(\underline{r}, s) = 2e^{i\frac{3\pi}{4}} \int_D (-1)^v \frac{v}{v^2 - \frac{1}{4}} \left[j_{v - \frac{1}{2}}(iR) - \frac{j_{v - \frac{1}{2}}(i\rho)}{h_{v - \frac{1}{2}}^{(1)}(i\rho)} h_{v - \frac{1}{2}}^{(1)}(iR) \right] e^{i(2m+1)\pi v} P_{v - \frac{1}{2}}^1(-\cos \theta) dv \quad (5.49)$$

This expansion must be employed in the region $\pi - \theta < \rho^{-1/3}$ if it is desired that the order of the error term in the asymptotic estimates for the wavefront terms be less than $\rho^{-2/3}$.

The wavefront terms $I_{1m}^c(\underline{r}, s)$ can be evaluated by the calculus of residues in exactly the same way as the terms $I_{1m}(\underline{r}, s, \pm)$ were evaluated. Two asymptotic expansions which are quite useful in the region $\pi - \theta < \rho^{-1/3}$ are (17)

$$P_{v - \frac{1}{2}}^1(-\cos \theta) = -\frac{v}{\sin \frac{\theta}{2}} J_1(2v \cos \frac{\theta}{2}) + O(\pi - \theta)^2 \quad (5.50)$$

$$\frac{\partial}{\partial \theta} P_{v - \frac{1}{2}}^1(-\cos \theta) = v^2 J_0(2v \cos \frac{\theta}{2}) - \frac{v}{2 \sin^2 \frac{\theta}{2} \cos \frac{\theta}{2}} J_1(2v \cos \frac{\theta}{2}) + O(\pi - \theta)^2 \quad (5.51)$$

The explicit forms of the residue series for $\pi - \theta < \rho^{-1/3}$ are given by the relations

$$I_{1m}^c(\underline{r}, s) = \frac{e^{i\frac{3\pi}{4}}}{2(\frac{\rho}{2})^{2/3}} \sum_{\alpha_\ell} \frac{e^{i\nu_\ell(2m+\frac{1}{2})\pi}}{[A'_1(-\alpha_\ell)]^2} h_{\nu_\ell-\frac{1}{2}}^{(1)}(i\rho) P_{\nu_\ell-\frac{1}{2}}^1(-\cos \theta) \times [1 + O(\rho^{-2/3+(\pi-\theta)^2})] \quad (5.52)$$

$$I_{2m}^c(\underline{r}, s) = \frac{e^{-i\frac{\pi}{4}}}{2(\frac{\rho}{2})^{2/3}} \sum_{\beta_p} \frac{e^{i\nu_p(2m+\frac{1}{2})\pi}}{\beta_p [A'_1(-\beta_p)]^2} \frac{[iR h_{\nu_p-\frac{1}{2}}^{(1)}(iR)]'}{R} \times P_{\nu_p-\frac{1}{2}}^1(-\cos \theta) [1 + O(\rho^{2/3+(\pi-\theta)^2})] \quad (5.53)$$

5.4.1d A Physical Interpretation of the Residue Series

It was stated in Section 5.3.2 that each of the terms $I_{1m}(\underline{r}, s)$ in the expansion of $I_1(\underline{r}, s)$ corresponded to a particular wavefront term in a ray representation of the diffraction process. The validity of this statement is easily established by an investigation of the asymptotic expansions given in equations 5.35 - 5.38. Consider the quantity $I_{1m}(\underline{r}, s, -)$. In the far field the exponent of the ℓ^{th} term in the residue series 5.35 is given by

$$-(R^2 - \rho^2)^{1/2} + i\nu_\ell \left[2m\pi + \theta - \left(\frac{\pi}{2} + \cos^{-1} \frac{a}{R} \right) \right] = -s T_m(\underline{r}, -) - \left[\alpha_\ell \left(\frac{\rho}{2} \right)^{1/3} + \frac{1}{60} \alpha_\ell^2 \left(\frac{\rho}{2} \right)^{-1/3} \right] \delta_m^- + O(\rho^{-1}) \quad (5.54)$$

where

$$T_m(\underline{r}, -) = \frac{1}{c} \left[(r^2 - a^2)^{1/2} + a \delta_m^- \right] ,$$

$$\delta_m^\mp = 2m\pi \pm \theta - \left(\frac{\pi}{2} + \cos^{-1} \frac{a}{r} \right) . \quad (5.56)$$

The function $T_m(\underline{r}, -)$ is readily interpreted as the time delay for a wave which encircles the sphere m times in a clockwise direction and then leaves the sphere at the point defined by the tangent line from (r, θ, ϕ) to the sphere. The quantity $(a\delta_m^-)$ is equal to the distance that the wave travels on the surface of the sphere. The quantity $[\alpha_{\rho}(\frac{\rho}{2})^{1/3} + \frac{1}{60} \alpha_{\rho}^2(\frac{\rho}{2})^{-1/3}] \delta_m^-$ describes the dispersion of the wave as it travels on the surface of the sphere. The exponent of the quantity $I_{1m}(\underline{r}, s, +)$ can be interpreted in a similar manner. It is found that this function yields a wave with a time delay and dispersion which correspond to a wave which has encircled the sphere $m-1$ times in a counter-clockwise direction. Figure 5.5 illustrates the ray system determined from the functions $I_{1m}(\underline{r}, s, \pm)$.

The directional properties of the vector field transforms derived from the functions $I_{1m}(\underline{r}, s, \pm)$ and $I_{2m}(\underline{r}, s, \pm)$ lend further support to the ray interpretation. The vector field transforms derived from these functions are contained in the plane transverse to the ray direction. As an example consider the far fields derived from $I_{1m}(\underline{r}, s, -)$, $I_{2m}(\underline{r}, s, -)$ and $I_{3m}(\underline{r}, s, -)$. The scalar function $I_{3m}(\underline{r}, s, -)$ is included here because the contribution of $\xi_{rm}(\underline{r}, s, -)$ to the net field must be taken into account. The ϕ component of the vector field

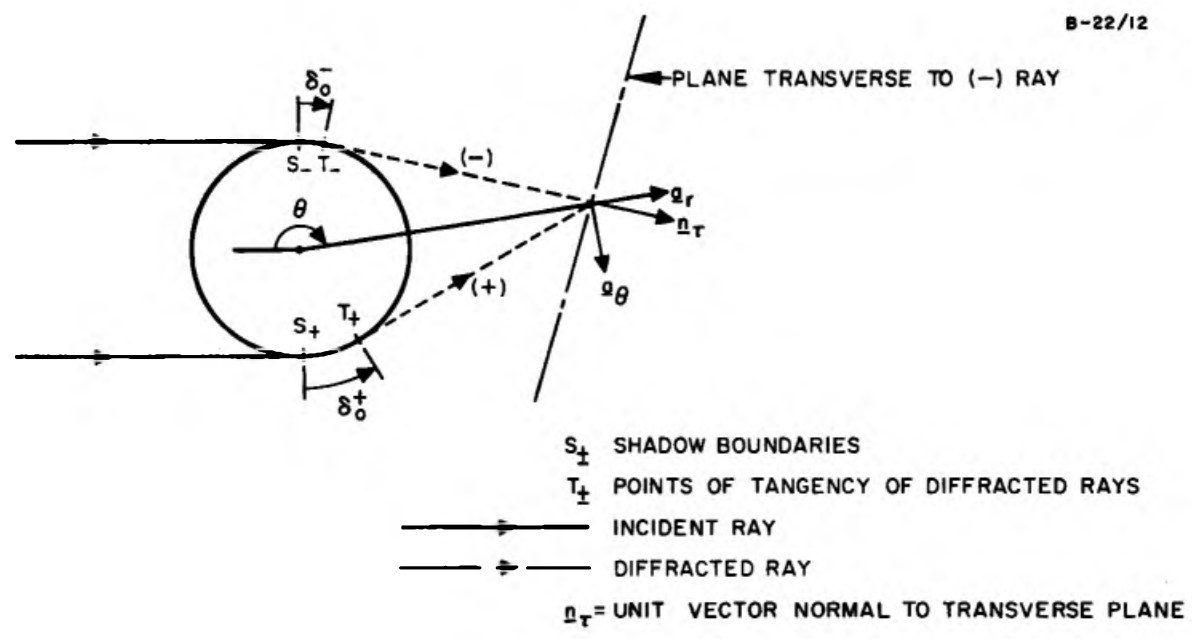


Fig. 5.5 Generalized ray system for a sphere

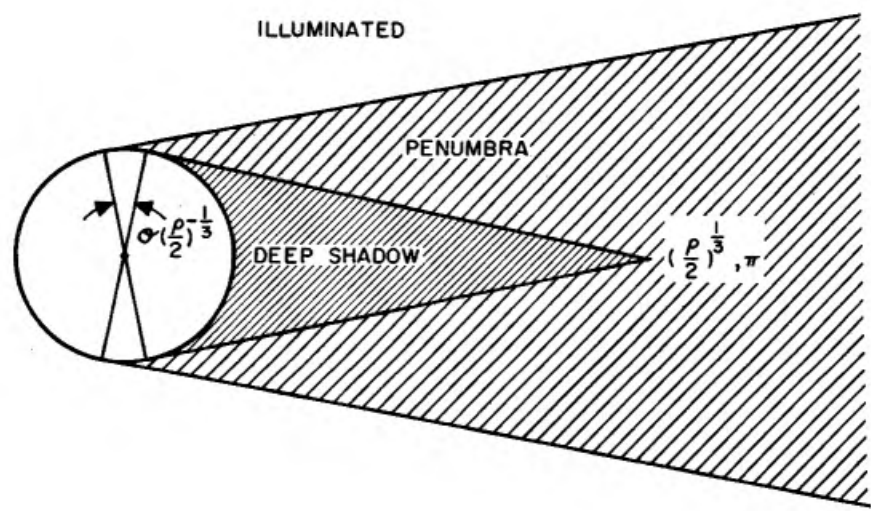


Fig. 5.6 Scattering zones

transform is wholly contained in the transverse plane so we need consider only the vector addition of $\xi_{\theta m}(\underline{r}, s, -)$ and $\xi_{r m}(\underline{r}, s, -)$. These field quantities are given by the relations

$$\xi_{\theta m}(\underline{r}, s, -) = e^{-\rho} \left[\frac{I_{1m}(\underline{r}, s, -)}{\sin \theta} + \frac{\partial}{\partial \theta} I_{2m}(\underline{r}, s, -) \right] \cos \phi \quad (5.57)$$

$$\xi_{r m}(\underline{r}, s, -) = e^{-\rho} I_{3m}(\underline{r}, s, -) \cos \phi \quad (5.58)$$

It can easily be shown that the asymptotic estimate of $I_{3m}(\underline{r}, s, -)$ is given by the relation

$$\lim_{s \gg 1} I_{3m}(\underline{r}, s, -) = -\frac{a}{r} \lim_{s \gg 1} \frac{\partial}{\partial \theta} I_{2m}(\underline{r}, s, -) \quad (5.59)$$

The relations 5.35 and 5.37 also reveal that the asymptotic form of $\xi_{\theta m}(\underline{r}, s, -)$ is given by

$$\lim_{s \gg 1} \xi_{\theta m}(\underline{r}, s, -) = e^{-\rho} \lim_{s \gg 1} \frac{\partial}{\partial \theta} I_{2m}(\underline{r}, s, -) \left[1 + O(\rho^{-1}) \right] \quad (5.60)$$

The component of the field transform normal to the transverse plane is given by

$$\underline{n}_{\tau} \cdot \underline{\xi}_m(\underline{r}, s, -) = \frac{a}{r} \xi_{\theta m}(\underline{r}, s, -) + \xi_{r m}(\underline{r}, s, -) \left[1 + O\left(\frac{a}{r}\right)^2 \right] \quad (5.61)$$

When relations 5.58-5.60 are substituted in the above equation, it is found that, to the accuracy of our calculations, the normal component of the vector field derived from $I_{im}(\underline{r}, s, -)$ ($i=1,2,3$) is zero. Thus the fields derived from the scalar functions $I_{im}(\underline{r}, s, -)$ ($i=1,2,3$) not only

have the proper time delay but they also satisfy the condition that they be contained in the plane transverse to the ray direction. This, of course, implies that the Poynting vector is in the ray direction.

5.4.1e Convergence of the Residue Series

The convergence of the residue series 5.35 - 5.38 is governed by the exponential factors $\exp[-(\frac{\rho}{2})^{1/3} \alpha_{\ell} \delta_m^{\pm}]$ and $\exp[-(\frac{\rho}{2})^{1/3} \beta_p \delta_m^{\pm}]$. Since the zeros of the Airy functions are of the order unity or greater, the magnitude of the bracketed term in these exponentials is of the order $(\frac{\rho}{2})^{1/3} \delta_m^{\pm}$. Consequently, unless $\delta_m^{\pm} \sim 0$, the residue series will converge quite rapidly when $s \gg 1$. It was noted in the previous section that δ_m^{\pm} is the angular distance traveled on the sphere by the m^{th} wavefront. As a result, it is obvious that the residue series expansions for $\lim_{s \gg 1} I_{1m}(\underline{r}, s, \pm)$ and $\lim_{s \gg 1} I_{2m}(\underline{r}, s, \pm)$ will always converge rapidly if $m \neq 0$. Actually, the quantity δ_0^+ is also large enough to insure a rapid convergence for zero plus terms. The deep shadow is defined as the region in which the quantity δ_0^- for the zero minus wave is large enough to insure convergence.

The specification of a particular minimum value of δ_0^- for which the residue series converges sufficiently rapidly is rather arbitrary. A reasonable choice is

$$(\delta_0^-)_{\min} \sim (\frac{\rho}{2})^{-1/3} \quad . \quad (5.62)$$

At this angular distance the ratio of the magnitude of the tenth and the first terms in the residue series is

$$\begin{aligned} \text{tenth term/first term} &= e^{-(\alpha_{10} - \alpha_1)} \left[\frac{A_1'(-\alpha_1)}{A_1'(-\alpha_{10})} \right]^2 \\ &= 1.12 \times 10^{-5} \quad , \end{aligned} \tag{5.63}$$

for the series $I_{10}(\underline{r}, s, -)$, and

$$\begin{aligned} \text{tenth term/first term} &= e^{-(\beta_{10} - \beta_1)} \frac{\beta_1}{\beta_{10}} \left[\frac{A_1(-\beta_1)}{A_1(-\beta_{10})} \right]^2 \\ &= 3.02 \times 10^{-6} \end{aligned} \tag{5.64}$$

for the series $I_{20}(\underline{r}, s, -)$. Consequently, if $\delta_0^- \geq (\frac{\rho}{2})^{-1/3}$, an accuracy of one part in 10^5 is obtained by summing ten terms.

The condition $\delta_0^- \geq (\frac{\rho}{2})^{-1/3}$ defines a conical region which will henceforth be termed the deep shadow. This region is shown in Figure 5.6 which also illustrates the other regions of interest in this problem. A simple trigonometrical calculation reveals that the vertex of the conical shadow zone is located at the point $(r, \theta) = ((\frac{\rho}{2})^{1/3} a, \pi)$. It is rather interesting that the deep shadow zone as defined here from rigorous diffraction theory is of much smaller extent than the like region defined on the basis of physical optics. Brillouin has considered the extent of the shadow region in the steady state scattering by a sphere (18). He employed physical optics approximations and obtained a vertex distance of the order $(ka)a$. The present results are consistent, however, with work of Fok pertaining to the width of the penumbra region in steady state problems (19). Fok obtains a penumbra width of the order $(ka/2)^{-1/3} a$ which implies a vertex distance of the order $(ka/2)^{1/3} a$.

5.4.2 The illuminated region. The illuminated region can be somewhat loosely defined as the angular domain defined by the condition $\delta_0^- < 0$. In this region the residue series representations of $\lim_{s \gg 1} I_{10}(\underline{r}, s, -)$ and $\lim_{s \gg 1} I_{20}(\underline{r}, s, -)$ converge very slowly. The physical reason for this slow convergence of the residue series representation is related to the fact that the nature of the waves described by the scalar functions $I_{10}(\underline{r}, s, -)$ and $I_{20}(\underline{r}, s, -)$ changes as the observation point is moved from the deep shadow to the illuminated region. In the deep shadow the waves result from a diffraction process. The residue series representation is appropriate for waves which arise from diffraction. The waves in the illuminated region, however, can also originate from the incident signal and a reflection of the incident signal. It will be shown in this section that the portions of $I_{10}(\underline{r}, s, -)$ and $I_{20}(\underline{r}, s, -)$ which yield the incident wave can be identified. When this is done, the remaining portions of $I_{10}(\underline{r}, s, -)$ and $I_{20}(\underline{r}, s, -)$ will be evaluated by the saddle point method.

5.4.2a Separation of the Incident Field

The portion of $I_{10}(\underline{r}, s)$ which is associated with the incident wave can be identified by the writing of this function in the form

$$I_{10}(\underline{r}, s, -) = I_{10}^i(\underline{r}, s, -) + I_{10}^a(\underline{r}, s, -) \quad (5.65)$$

where

$$I_{10}^i(\underline{r}, s, -) = -\frac{2}{\pi} e^{i\frac{\pi}{4}} \int_{D_1} (i)^v \frac{v}{v^2 - \frac{1}{4}} J_{v - \frac{1}{2}}(iR) Q_{v - \frac{1}{2}}^1(\cos \theta - i0) dv$$

$$- \frac{2}{\pi} e^{i\frac{\pi}{4}} \int_{D_2} (-i)^v \frac{v}{v^2 - \frac{1}{4}} J_{v - \frac{1}{2}}(iR) Q_{v - \frac{1}{2}}^1(\cos \theta - i0) dv \quad (5.66)$$

$$\begin{aligned}
 I_{10}^4(\underline{r}, s, -) &= \frac{2}{\pi} e^{i\frac{\pi}{4}} \int_{D_1} (i)^{\nu} \frac{\nu}{\nu - \frac{1}{4}} \frac{j_{-\nu - \frac{1}{2}}(i\rho)}{h_{-\nu - \frac{1}{2}}^{(1)}(i\rho)} h_{\nu - \frac{1}{2}}^{(1)}(iR) Q_{\nu - \frac{1}{2}}^1(\cos \theta - i0) d\nu \\
 &+ \frac{2}{\pi} e^{i\frac{\pi}{4}} \int_{D_2} (-i)^{\nu} \frac{\nu}{\nu - \frac{1}{4}} \frac{j_{\nu - \frac{1}{2}}(i\rho)}{h_{\nu - \frac{1}{2}}^{(1)}(i\rho)} h_{\nu - \frac{1}{2}}^{(1)}(iR) Q_{\nu - \frac{1}{2}}^1(\cos \theta - i0) d\nu .
 \end{aligned} \tag{5.67}$$

The contour D_1 is that portion of D for which $\text{Re}(\nu) < 0$ and the contour D_2 is the portion for which $\text{Re}(\nu) > 0$. The term $I_{10}^1(\underline{r}, s, -)$ is related to the incident field. This relationship is revealed if the angular function $Q_{\nu - \frac{1}{2}}^1(\cos \theta - i0)$ is replaced by an expression obtained from Appendix III

$$Q_{\nu - \frac{1}{2}}^1(\cos \theta - i0) = \frac{\pi}{2i} \frac{P_{\nu - \frac{1}{2}}^1(-\cos \theta)}{\cos \nu \pi} - \frac{\pi}{2} P_{\nu - \frac{1}{2}}^1(\cos \theta) \frac{e^{i\nu\pi}}{\cos \nu \pi} . \tag{5.68}$$

When 5.68 is substituted in 5.66 and ν is replaced by $-\nu$ in the integral over D_1 which contains $P_{\nu - \frac{1}{2}}^1(-\cos \theta)$, the function $I_{10}^1(\underline{r}, s, -)$ assumes the form

$$\begin{aligned}
 I_{10}^1(\underline{r}, s, -) &= e^{i\frac{3\pi}{4}} \int_{C'} (-i)^{\nu} \frac{\nu}{\nu - \frac{1}{4}} j_{\nu - \frac{1}{2}}(iR) \frac{P_{\nu - \frac{1}{2}}^1(-\cos \theta)}{\cos \nu \pi} d\nu + \\
 &+ e^{i\frac{\pi}{4}} \int_{D_1} (i)^{\nu} \frac{\nu}{\nu - \frac{1}{4}} j_{-\nu - \frac{1}{2}}(iR) P_{\nu - \frac{1}{2}}^1(\cos \theta) \frac{e^{i\nu\pi}}{\cos \nu \pi} d\nu + \\
 &+ e^{i\frac{\pi}{4}} \int_{D_2} (-i)^{\nu} \frac{\nu}{\nu - \frac{1}{4}} j_{\nu - \frac{1}{2}}(iR) P_{\nu - \frac{1}{2}}^1(\cos \theta) \frac{e^{i\nu\pi}}{\cos \nu \pi} d\nu
 \end{aligned} \tag{5.69}$$

The first term in 5.69 is the exact integral representation of the portion of the incident field derived from $I_{10}(\underline{r}, s, -)$. An asymptotic evaluation of the second and third terms in 5.69 has revealed that their contribution to the asymptotic expansion $\lim_{s \gg 1} I_{10}(\underline{r}, s, -)$ is negligible in comparison with the incident field terms and the contribution from $I_{10}(\underline{r}, s, -)$. As a result, it appears that the function $I_{10}(\underline{r}, s, -)$ can be interpreted as being associated with the wave reflected from the surface of the sphere. The function $I_{20}(\underline{r}, s, -)$ can be divided in the same manner with the portion $I_{20}^{\Delta}(\underline{r}, s, -)$ being given by

$$\begin{aligned}
 I_{20}^{\Delta}(\underline{r}, s, -) = & \frac{2e^{i\frac{\pi}{4}}}{\pi R} \int_{D_1} (i)^{\nu} \frac{\nu}{\nu^2 - \frac{1}{4}} \frac{[i\rho j^{-\nu - \frac{1}{2}}(i\rho)]'}{[i\rho h^{(1)}(i\rho)]'_{\nu - \frac{1}{2}}} [iRh^{(1)}(iR)]'_{\nu - \frac{1}{2}} \\
 & \times Q^{\frac{1}{\nu - \frac{1}{2}}}(\cos \theta - i0) d\nu + \\
 & + \frac{2e^{i\frac{\pi}{4}}}{\pi R} \int_{D_2} (-i)^{\nu} \frac{\nu}{\nu^2 - \frac{1}{4}} \frac{[i\rho j^{-\nu - \frac{1}{2}}(i\rho)]'}{[i\rho h^{(1)}(i\rho)]'_{\nu - \frac{1}{2}}} [iRh^{(1)}(iR)]'_{\nu - \frac{1}{2}} \cdot Q^{\frac{1}{\nu - \frac{1}{2}}}(\cos \theta - i0) d\nu .
 \end{aligned}
 \tag{5.70}$$

5.4.2b Expression of $I_{10}^{\Delta}(\underline{r}, s, -)$ and $I_{20}^{\Delta}(\underline{r}, s, -)$
in a Form Suitable for Saddle Point Integration

When s is very large the integral representations of the functions $I_{10}^{\Delta}(\underline{r}, s, -)$ and $I_{20}^{\Delta}(\underline{r}, s, -)$ can be evaluated by the saddle point method. The asymptotic expansions of the Bessel and Hankel functions which are given in Appendix I are useful in the conversion of equations 5.67 and 5.70 into forms which are suitable for saddle point integration. The appropriate expansions are:

a) $h_{\nu-\frac{1}{2}}^{(1)}(i\rho)$, $[i\rho h_{\nu-\frac{1}{2}}^{(1)}(i\rho)]'$; along all portions of D_1 and D_2 ,

$$h_{\nu-\frac{1}{2}}^{(1)}(i\rho) = \left(\frac{\pi}{2i\rho}\right)^{1/2} \frac{1}{\left(-\frac{\nu\pi i \tanh \gamma}{2}\right)^{1/2}} e^{i\rho[\sinh \gamma - \gamma \cosh \gamma] - i\frac{\pi}{4}} \\ \left[1 + \frac{1}{\nu \tanh \gamma} \left(\frac{1}{8} - \frac{5 \coth^2 \gamma}{24}\right) + \mathcal{O}\left(\frac{1}{\nu^2 \zeta^3}\right)\right], \quad (5.71)$$

$$[i\rho h_{\nu-\frac{1}{2}}^{(1)}(i\rho)]' = \left(\frac{\pi i\rho}{2}\right)^{1/2} \frac{\sinh \gamma}{\left(-\frac{\nu\pi i \tanh \gamma}{2}\right)^{1/2}} e^{i\rho[\sinh \gamma - \gamma \cosh \gamma] - i\frac{\pi}{4}} \\ \left[1 + \frac{1}{\nu \tanh \gamma} \left(\frac{5}{8} - \frac{5 \coth^2 \gamma}{24} + \frac{1}{2 \sinh^2 \gamma}\right) + \mathcal{O}\left(\frac{1}{\nu^2 \zeta^3}\right)\right] \quad (5.72)$$

b) $j_{\nu-\frac{1}{2}}(i\rho)$, $[i\rho j_{\nu-\frac{1}{2}}(i\rho)]'$; along D_2 ,

$$2j_{\nu-\frac{1}{2}}(i\rho) = \left(\frac{\pi}{2i\rho}\right)^{1/2} \frac{1}{\left(-\frac{\nu\pi i \tanh \gamma}{2}\right)^{1/2}} e^{-i\rho[\sinh \gamma - \gamma \cosh \gamma] + i\frac{\pi}{4}} \\ \left[1 - \frac{\left(\frac{1}{8} - \frac{5 \coth^2 \gamma}{24}\right)}{\nu \tanh \gamma} + \mathcal{O}\left(\frac{1}{\nu^2 \zeta^3}\right)\right] \quad (5.73)$$

$$[2 i\rho j_{\nu-\frac{1}{2}}(i\rho)]' = \left(\frac{\pi i\rho}{2}\right)^{1/2} \frac{\sinh \gamma}{\left(-\frac{\nu\pi \tanh \gamma}{2}\right)^{1/2}} e^{-i\rho[\sinh \gamma - \gamma \cosh \gamma] - i\frac{3\pi}{4}} \\ \left[1 - \frac{\left(\frac{5}{8} - \frac{5 \coth^2 \gamma}{24} + \frac{1}{2 \sinh^2 \gamma}\right)}{\nu \tanh \gamma} + \mathcal{O}\left(\frac{1}{\nu^2 \zeta^3}\right)\right]. \quad (5.74)$$

c) $e^{i\nu\pi} j_{-\nu - \frac{1}{2}}(i\rho)$, $e^{i\nu\pi} [i\rho j_{-\nu - \frac{1}{2}}(i\rho)]'$; along D_1 these expansions

are identical with those given respectively in equations 5.73 and 5.74.

In all of the above equations the parameter γ is defined by the relations

$$\nu = i\rho \cosh \gamma \quad (5.75)$$

$$\gamma = \beta + i\alpha, \quad 0 < \alpha < \pi, \quad -\infty < \beta < \infty.$$

The expansions for the Hankel functions of argument iR can be obtained from equations 5.71 and 5.72 if ρ is replaced by R and γ by γ_0 .

The parameter γ_0 is defined by

$$\nu = iR \cosh \gamma_0 \quad (5.76)$$

$$\gamma_0 = \beta_0 + i\alpha_0, \quad 0 < \alpha_0 < \pi, \quad -\infty < \beta_0 < \pi.$$

The asymptotic expansions of $I_{10}^{\Delta}(\underline{r}, s, -)$ and $I_{20}^{\Delta}(\underline{r}, s, -)$ are obtained by replacing the Bessel and Hankel functions in their integrands with the asymptotic expansions given in 5.71 - 5.74. When

$Q_{\nu - \frac{1}{2}}^1(\cos \theta - i0)$ is written in the form given in A-3.9, we obtain

$$\lim_{s \gg 1} I_{10}^{\Delta}(\underline{r}, s, -) = \frac{e^{-i\frac{3\pi}{4}}}{R(2\pi \sin \theta)^{1/2}} \int_{D_1 + D_2} \frac{W(\nu, \theta)}{(-1 \sinh \gamma_0)^{1/2}} e^{-2\rho u}$$

$$\left[1 + \frac{1}{\nu} \left(\Psi_1(\gamma, \gamma_0, \theta) - \frac{13 \cos \theta}{8 \sin \theta} - \frac{1}{4} \right) + \mathcal{O} \left(\frac{1}{\nu^2} \right) \right] d\nu \quad (5.77)$$

$$\lim_{s \gg 1} I_{20}^{\Delta}(\underline{r}, s, -) = \frac{e^{-i\frac{3\pi}{4}}}{R(2\pi \sin \theta)^{1/2}} \int_{D_1 + D_2} (-i \sinh \gamma_0)^{1/2} W(\nu, \theta) e^{-i2\rho U} \left[1 + \frac{1}{\nu} \left(\Psi_2(\gamma, \gamma_0, \theta) - \frac{13 \cos \theta}{8 \cos \theta} - \frac{1}{4} \right) + O\left(\frac{1}{\nu^2}\right) \right] d\nu \quad (5.78)$$

where

$$W(\nu, \theta) = \frac{\Gamma(\nu - \frac{1}{2})}{\Gamma(\nu)} {}_2F_1\left(\frac{3}{2}, -\frac{1}{2}; \nu+1; -\frac{ie^{i\theta}}{2 \sin \theta}\right), \quad (5.79)$$

$$U(\nu, \theta) = \sinh \gamma - \left(\gamma - \frac{i(\frac{\pi}{2} - \theta)}{2}\right) \cosh \gamma - \frac{R}{2\rho} (\sinh \gamma_0 - \gamma_0 \cosh \gamma_0) \quad (5.80)$$

$$\Psi_1(\gamma, \gamma_0, \theta) = -\frac{1}{4 \tanh \gamma} + \frac{5}{12 \tanh^3 \gamma} + \frac{1}{8 \tanh \gamma_0} - \frac{5}{24 \tanh^3 \gamma_0} + \frac{13 \cos \theta}{8 \sin \theta} \quad (5.80a)$$

$$\Psi_2(\gamma, \gamma_0, \theta) = -\frac{5}{4 \tanh \gamma} + \frac{5}{12 \tanh^3 \gamma} - \frac{\cosh \gamma}{\sinh^3 \gamma} + \frac{5}{8 \tanh \gamma_0} - \frac{5}{24 \tanh^3 \gamma_0} + \frac{\cosh \gamma_0}{2 \sinh^3 \gamma_0} + \frac{13 \cos \theta}{8 \sin \theta} \quad (5.80b)$$

5.4.2c Determination of the Saddle Points

For large values of the parameter ρ , the behavior of the integrals 5.77 and 5.78 is very closely related to the variation of the function $U(\nu, \theta)$ along the contour of integration. The first step in the saddle point method of integration is to investigate the topography of $\text{Im} U(\nu, \theta)$ in the complex ν plane. $U(\nu, \theta)$ is an analytic function everywhere in the finite ν plane and as a result its real and imaginary parts have no maximums or minimums. The points at which $\frac{\partial}{\partial \nu} U(\nu, \theta) = 0$

are saddle points and the real and imaginary parts of $\mathcal{U}(v, \theta)$ at neighboring points increase or decrease depending upon the location of these points relative to the saddle point. There is a path on which $\text{Im } \mathcal{U}(v, \theta)$ decreases at a maximum rate. This path is called the path of steepest descent. It will subsequently be shown that the steepest paths are defined by the condition $\text{Re } \mathcal{U}(v, \theta) = \text{constant}$. The general idea of the saddle point method is to deform the original contour of integration into a new contour which traverses the saddle points on the paths of steepest descent.

The derivative of $\mathcal{U}(v, \theta)$ is given by the expression

$$\frac{\partial}{\partial v} \mathcal{U}(v, \theta) = - \frac{1}{2i\rho} \left[2\gamma - \gamma_0 - i\left(\frac{\pi}{2} - \theta\right) \right] \quad . \quad (5.81)$$

It is convenient to express the variable γ_0 in the form

$$\gamma_0 = i \cos^{-1}\left(\frac{\rho}{R} \cosh \gamma\right) = i \left[\frac{\pi}{2} - \sin^{-1}\left(\frac{\rho}{R} \cosh \gamma\right) \right] \quad . \quad (5.82)$$

When 5.82 is substituted in 5.81 and the result equated to zero, the following relation is obtained for the saddle point $v_s = i\rho \cosh \gamma_s$

$$2\gamma_s = i \left[\pi - \theta - \sin^{-1}\left(\frac{\rho}{R} \cosh \gamma\right) \right] \quad . \quad (5.83)$$

The determination of the values of γ and γ_0 at which $\frac{\partial}{\partial v} \mathcal{U}(v, \theta)$ vanishes is facilitated if the physical meaning of the exponent in equations 5.77 and 5.78 is recalled. This exponent is related to the time delay of the reflected wave. Consequently, if the function $\mathcal{U}(v, \theta)$ is evaluated at the point where $\frac{\partial}{\partial v} \mathcal{U}(v, \theta) = 0$, the

time delay for the reflected wave is minimized. In order for the time delay to be a minimum, the reflected wave must travel along the ray paths determined by optics. Consider the ray system depicted in Figure 5.7. The incident ray strikes the sphere at an angle ξ to the normal and is reflected at the surface such that the angle of incidence and reflection are equal. It is intuitively obvious that the parameters γ_s and γ_{os} are related in some way to the angles defined by the ray system in Figure 5.7. A clue to the nature of this correspondence can be obtained by considering the far-field limit of equation 5.83.

$$\lim_{R \rightarrow \infty} \gamma_s = i\left(\frac{\pi - \theta}{2}\right) .$$

If this result is interpreted in light of the geometric optics path shown in Figure 5.7, it appears that $-i\gamma_s$ is the angular distance from $\theta = \frac{\pi}{2}$ to the point at which the incident ray strikes the reflecting surface. In terms of the angle of incidence ξ , the above condition yields

$$-i\gamma_s = \frac{\pi}{2} - \xi . \quad (5.84)$$

The validity of equation 5.84 can be ascertained by checking to see if the expression given for γ_s satisfies equation 5.83. When this is done, the following equation is obtained.

$$R \sin (2\xi - \theta) = \rho \sin \xi . \quad (5.85)$$

The ray system depicted in Figure 5.7 does satisfy 5.85. Consequently the relation 5.84 is the desired solution for γ_s . The value of γ_{os}

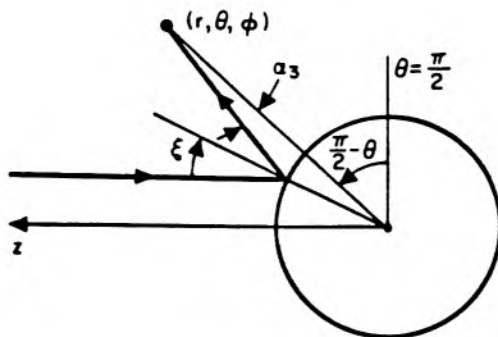


Fig. 5.7 Ray system

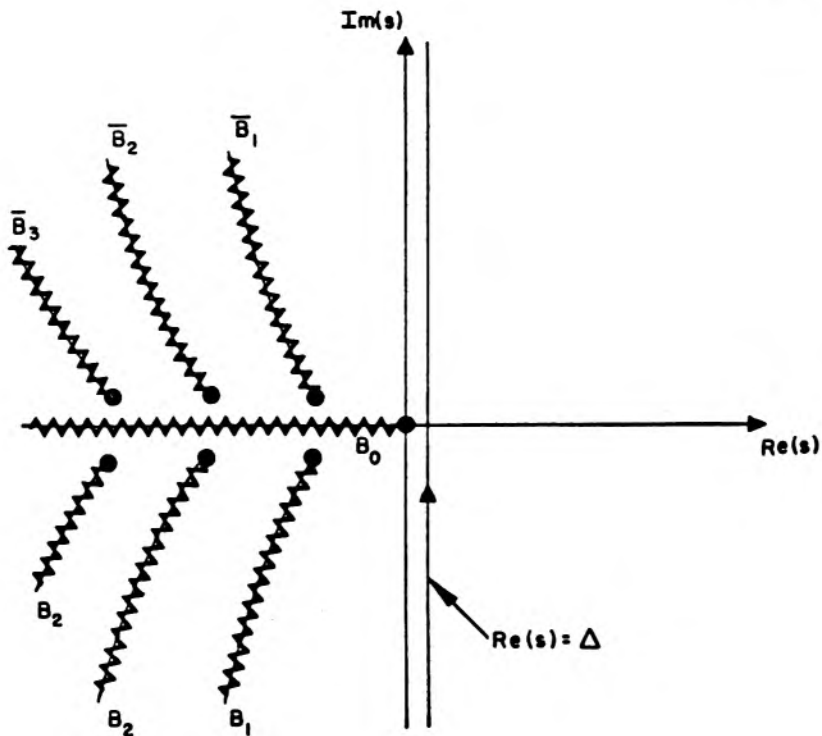


Fig. 5.8 Distribution of the singularities of $I_{im}(\underline{r}, s, \pm)$ ($i = 1, 2$)

is easily obtained from 5.81 and 5.84.

$$-i\gamma_{os} = \frac{\pi}{2} - (2\xi - \theta) = \frac{\pi}{2} - \alpha_3 \quad . \quad (5.86)$$

5.4.2d The Path of Steepest Descent

The location of the path of steepest descent (or ascent) can easily be determined if the basic definition of an analytic function is recalled. An analytic function of a complex variable has a unique derivative at a point independent of the direction along which the derivative is taken. Consider the derivative of $\mathcal{U}(v, \theta)$ in an arbitrary direction h .

$$\frac{\partial}{\partial h} \mathcal{U}(v, \theta) = \frac{\partial}{\partial h} [\text{Re } \mathcal{U}(v, \theta) + i \text{Im } \mathcal{U}(v, \theta)] \quad . \quad (5.87)$$

The absolute value of $\frac{\partial}{\partial h} \mathcal{U}(v, \theta)$ is given by

$$\left| \frac{\partial}{\partial h} \mathcal{U}(v, \theta) \right|^2 = \left| \frac{\partial}{\partial h} \text{Re } \mathcal{U}(v, \theta) \right|^2 + \left| \frac{\partial}{\partial h} \text{Im } \mathcal{U}(v, \theta) \right|^2 = C \quad (5.88)$$

where C is independent of the direction h . In view of equation 5.88, it is apparent that the rate of change of $\text{Im } \mathcal{U}(v, \theta)$ is maximized if the direction h is chosen such that $\frac{\partial}{\partial h} \text{Re } \mathcal{U}(v, \theta) = 0$, i.e., $\text{Re } \mathcal{U}(v, \theta) = \text{a constant}$. The real part of $\mathcal{U}(v, \theta)$ can be obtained from equation 5.80

$$\begin{aligned} \text{Re } \mathcal{U}(v, \theta) = & \cos \alpha \left[\sinh \beta - \left(\beta - \frac{\beta_0}{2} \right) \cosh \beta \right] \\ & + \sin \alpha \sinh \beta \left[\alpha - \frac{\alpha_0}{2} - \left(\frac{\pi}{2} - \theta \right) \right] - \frac{R}{2\rho} \sinh \beta_0 \cos \alpha_0 \quad . \end{aligned} \quad (5.89)$$

At the saddle point defined by equations 5.84 and 5.86, the real part of $\mathcal{U}(v, \theta)$ is zero. Consequently, the path of steep descent (or ascent) is defined by the condition

$$\begin{aligned} \cos \alpha \left[\sinh \beta - \left(\beta - \frac{\beta_0}{2} \right) \cosh \beta \right] + \sin \alpha \sinh \beta \left[\alpha - \frac{\alpha_0}{2} - \left(\frac{\pi}{2} - \theta \right) \right] - \\ - \frac{R}{2\rho} \sinh \beta_0 \cos \alpha_0 = 0 \quad . \end{aligned} \quad (5.90)$$

The above relation is far too involved to obtain a point by point description of the steepest descent contour. The general characteristics of this curve, however, are easily determined. For large positive values of β and β_0 , equation 5.90 can be written

$$\begin{aligned} \operatorname{Re} \mathcal{U}(v, \theta) \sim \cosh \beta \left[\cos \alpha \left(1 - \beta + \frac{\beta_0}{2} - \frac{\cos \alpha_0}{2 \cos \alpha} \right) \right. \\ \left. + \sin \alpha \left(\alpha - \frac{\alpha_0}{2} - \left(\frac{\pi}{2} - \theta \right) \right) \right] = 0 \quad . \end{aligned} \quad (5.91)$$

It is evident from equation 5.91 that as β goes to plus infinity on the path of steepest descent, α approaches the value $\frac{\pi}{2} - 0$. Likewise, it can be shown that α approaches the value $\frac{\pi}{2} - 0$ when β goes to minus infinity. The line $\alpha = -\left(\frac{\pi}{2} - 0\right)$ also satisfies the condition 5.90 when β is large. The integration in equations 5.77 and 5.79 is performed, however, on the sheet $0 < \alpha < \pi$ of the multiple-valued function $\mathcal{U}(v, \theta)$. Consequently the steepest curve which is asymptotic to $\alpha = -\left(\frac{\pi}{2} - 0\right)$ is not acceptable.

It can also be shown that the path of steepest descent does not lie below the line $\alpha = \frac{\pi}{2}$. On the line $\alpha = \frac{\pi}{2}$ the real part of $\mathcal{U}(v, \theta)$ is given by

$$\operatorname{Re} \mathcal{U}(v, \theta) = \frac{\theta}{2} \sinh \beta \quad . \quad (5.92)$$

In order for the path of descent to be below the line $\alpha = \frac{\pi}{2}$ there must be at least two zeros on this line. (It was shown above that the path is asymptotic to $\alpha = \frac{\pi}{2} - 0$ for β large). The only zero of 5.92, however, is the one at $\beta = 0$. Thus the path of steepest descent is located in the region $0 < \alpha < \frac{\pi}{2}$.

In the above discussion, the contour which satisfies 5.90 and which is asymptotic to $\alpha = \frac{\pi}{2} - 0$ when β is large has been rather loosely called a path of steepest descent. This is not entirely obvious since the condition $\operatorname{Re} \mathcal{U}(v, \theta) = 0$ simply defines the steepest curves, descent and ascent. The path of steepest descent is defined by the additional condition

$$\lim_{\beta \rightarrow \pm \infty} \operatorname{Im} \mathcal{U}(v, \theta) = -\infty \quad .$$

The quantity $\operatorname{Im} \mathcal{U}(v, \theta)$ is given by the expression

$$\begin{aligned} \operatorname{Im} \mathcal{U}(v, \theta) = & \sin \alpha \left(\cosh \beta - \left(\beta - \frac{\beta_0}{2} \right) \sinh \beta \right) - \\ & - \cos \alpha \cosh \beta \left(\alpha - \frac{\alpha_0}{2} - \left(\frac{\frac{\pi}{2} - \theta}{2} \right) \right) - \frac{R}{2\rho} \sin \alpha_0 \cosh \beta_0. \end{aligned} \quad (5.93)$$

When β becomes a large positive number, equation 5.93 can be written

$$\begin{aligned} \lim_{\beta \gg 1} \operatorname{Im} \mathcal{U}(v, \theta) \sim & \cosh \beta \left[\sin \alpha \left(1 - \beta + \frac{\beta_0}{2} - \frac{\sin \alpha_0}{2 \sin \alpha} \right) - \right. \\ & \left. - \cos \alpha \left(\alpha - \frac{\alpha_0}{2} - \left(\frac{\frac{\pi}{2} - \theta}{2} \right) \right) \right] \quad . \end{aligned} \quad (5.94)$$

It is readily apparent from 5.94 that $\lim_{\beta \rightarrow \infty} \text{Im} \mathcal{U}(v, \theta) = -\infty$ when $\alpha = \frac{\pi}{2} - 0$. Likewise, it can easily be shown that the condition for large negative values of β is also satisfied when $\alpha = \frac{\pi}{2} - 0$. Consequently, the path which passes through the point v_g and is asymptotic to the line $\alpha = \frac{\pi}{2} - 0$ when $\beta \rightarrow \pm \infty$ is the required path of steepest descent.

5.4.2e A Limitation on the Applicability of the Saddle Point Method

The asymptotic expansions of the Bessel and Hankel functions, 5.71 through 5.74, which were employed to obtain the integral representations of $\lim_{s \gg 1} I_{10}^{\circ}(\underline{r}, s, -)$ and $\lim_{s \gg 1} I_{20}^{\circ}(\underline{r}, s, -)$ have an error term of the order $(v_g^2 \zeta_s^3)^{-1}$. The parameter ζ is small when $v \sim i\rho$. The portion of the steepest descent path which is closest to this region is that in the vicinity of $v = v_g$. Consequently a reasonable criteria for judging the accuracy of the asymptotic expansions obtained from the saddle point calculation is the magnitude of the quantity $v_g^2 \zeta_s^3$. The error certainly will be considerable if $v_g^2 \zeta_s^3 \leq \mathcal{O}(1)$. The physical significance of the above condition can be obtained by considering the expansion of ζ for $v \sim i\rho$. The following expansion is obtained from A-1.4 by writing ζ as a power series in $(1 - i\rho/v)$ and equating the terms on each side of the equation

$$\zeta = 2^{1/3} \left[(1 - i\rho/v) + \frac{3}{10}(1 - i\rho/v)^2 + \frac{41}{175}(1 - i\rho/v)^3 + \dots \right] \quad (5.95)$$

The quantity v_g is approximately equal to $i\rho$ when $\zeta_g \sim 0$. The order relation $v_g^2 \zeta_s^3 \leq \mathcal{O}(1)$ then implies that $\zeta_g \sim \mathcal{O}(\rho^{-2/3})$. When ζ

in equation 5.95 is replaced by $O(\rho^{-2/3})$, the following relation is obtained for v_s

$$v_s < 1 \left[\rho - O(\rho^{1/3}) \right] . \quad (5.96)$$

The position of the saddle point v_s is given by equation 5.75 with $\gamma = 1(\frac{\pi}{2} - \xi)$ where ξ is the angle of incidence. When the magnitude of v_s determined in this way is substituted in 5.96, it is found that the angle of incidence must satisfy the condition

$$\xi < \frac{\pi}{2} - O(\rho^{-1/3}) . \quad (5.97)$$

Physically, the above condition implies that the saddle point method will be highly inaccurate for rays which are reflected at grazing incidence.

The illuminated region will be defined as the exterior of the cone generated by the tangents to the surface of the sphere at the specular point defined by the condition $\xi = \frac{\pi}{2} - O(\rho^{-1/3})$. The specular point defined by this condition is given by $\theta = \frac{\pi}{2} - O(\rho^{-1/3})$. This result is consistent with the steady state work of V. A. Fok who predicts a region of transition between the illuminated region and the shadow region of width $(\frac{ka}{2})^{-1/3} a$ (19). In the transition region the currents on the scattering object are not given by the geometrical optics current. Since the saddle point calculation is simply a higher order geometrical optics approximation, it is reasonable to expect the results of this method to be highly inaccurate in the transition region. The geometry of the illuminated region is depicted in Figure 5.6.

5.4.2f A New Variable of Integration

If the path of steepest descent satisfies the conditions discussed in the previous section, it is possible to replace the original contour $D_1 + D_2$ by the steepest path. On the steepest path the function $\mathcal{U}(v, \theta)$ is a purely imaginary function. The evaluation of the integral along the path of steepest descent is facilitated if the variable of integration v is replaced by a new variable which is real on this path. Consider the variable τ defined by the relation

$$-i\tau(v) \equiv \mathcal{U}(v, \theta) - \mathcal{U}(v_g, \theta) \quad . \quad (5.98)$$

Since $\mathcal{U}(v, \theta)$ is purely imaginary on the path of steepest descent, it is apparent that the variable $\tau(v)$ is real on this path. Also it is obvious that $\tau(v_g) = 0$ and $\tau(\pm \infty) = + \infty$.

In order to express the integrands of the integrals 5.77 and 5.78 in terms of the new variable $\tau(v)$, it is necessary to know the inverse function $v(\tau)$. The first step in the determination of $v(\tau)$ is to express the function $\tau(v)$ in a power series in powers of $(v - v_g)$. This expansion can be obtained by expanding $\mathcal{U}(v, \theta)$ in a Taylor series about $v = v_g$.

$$2i\tau(v) = a_2(\mu - \mu_g)^2 + a_3(\mu - \mu_g)^3 + a_4(\mu - \mu_g)^4 + \dots \quad , \quad (5.99)$$

where

$$\mu \equiv v/i\rho \quad (5.100)$$

$$a_2 = \frac{1}{\sinh \gamma_g} - \frac{1}{2 \frac{R}{\rho} \sinh \gamma_{0g}} \equiv \frac{i L}{r \sinh \gamma_{0g} \sinh \gamma_g} \quad (5.101)$$

$$a_3 = -\frac{\cosh \gamma_B}{3 \sinh^3 \gamma_B} + \frac{1}{6\left(\frac{R}{\rho}\right)^2} \frac{\cosh \gamma_{OS}}{\sinh^3 \gamma_{OS}}, \quad (5.102)$$

$$a_4 = \frac{1 + 2 \cosh^2 \gamma_B}{12 \sinh^5 \gamma_B} - \frac{1}{24\left(\frac{R}{\rho}\right)^3} \frac{1 + 2 \cosh^2 \gamma_{OS}}{\sinh^5 \gamma_{OS}}, \quad (5.103)$$

$$a_5 = -\frac{3 \cosh \gamma_B + 2 \cosh^3 \gamma_B}{20 \sinh^7 \gamma_B} + \frac{1}{40\left(\frac{R}{\rho}\right)^4} \frac{3 \cosh \gamma_{OS} + 2 \cosh^3 \gamma_{OS}}{\sinh^7 \gamma_{OS}}. \quad (5.104)$$

Equation 5.99 can be inverted to obtain a power series expansion of $(\mu - \mu_B)$ in powers of $\pm (2i\tau/a_2)^{1/2}$. The plus and minus signs are associated with the fact that $(v - v_B)$ is a multivalued function of τ . The integration along the path of steepest descent in the v plane is transformed into an integration around a branch cut in the τ plane. This branch cut is located on the positive real axis in the τ plane. The square root is taken plus on one side of the cut and minus on the other. The following expansion is obtained for $(\mu - \mu_B)$ when the square root is taken plus

$$\mu - \mu_B = w - b_1 w^2 + (2b_1^2 - b_2) w^3 + (5b_1 b_2 - b_3 - 5b_1^3) w^4 + \dots, \quad (5.105)$$

where

$$w \equiv (2i\tau/a_2)^{1/2}, \quad (5.106)$$

$$b_1 = \frac{a_3}{2a_2} \quad (5.107)$$

$$b_2 = \frac{a_4}{2a_2} - \frac{1}{2} \left(\frac{a_3}{2a_2} \right)^2, \quad (5.108)$$

$$b_3 = \frac{a_5}{2a_2} - \frac{a_3 a_4}{4a_2^2} + \frac{1}{2} \left(\frac{a_3}{2a_2} \right)^3. \quad (5.109)$$

On the other side of the branch cut $\mu - \mu_s$ is given by 5.105 with w replaced by $-w$.

In terms of the new variable τ , each of the integrals 5.77 and 5.78 is of the type

$$I = \int_0^{\infty} \left[\left(f(v) \frac{dv}{d\tau} \right)_+ - \left(f(v) \frac{dv}{d\tau} \right)_- \right] e^{-2\rho\tau} d\tau, \quad (5.110)$$

where the (+) refers to the topside of the cut and the (-) refers to the bottom side. The integral in 5.110 is of the Laplace type and its asymptotic expansion for large values of ρ is well known (20). An asymptotic expansion of 5.110 can be obtained by expanding the bracketed function in a power series about the point $\tau = 0$. In this region the function $W(v, \theta)$ which appears in the integrands of 5.77 and 5.78, can be replaced by its asymptotic expansion for large v . When this is done, it is found that the evaluation of 5.77 and 5.78 by the above procedure will require a knowledge of the expansions of $v^{\pm \frac{1}{2}} \frac{dv}{d\tau}$ and $(i \sinh \gamma_0)^{\pm \frac{1}{2}}$ in terms of the variable τ .

The expansion of $v^{\pm \frac{1}{2}} \frac{dv}{d\tau}$ can be obtained from 5.87 by a complicated inversion procedure. The results are

$$\left(v^{\frac{1}{2}} \frac{dv}{d\tau} \right)_+ = i\rho \left(\frac{1v_s}{2a_s\tau} \right)^{1/2} \left[1 + c_1 w + c_2 w^2 + \dots \right], \quad (5.111)$$

$$\left(v^{-1/2} \frac{dv}{d\tau} \right)_+ = i\rho \left(\frac{1}{2v_s a_s \tau} \right)^{1/2} \left[1 + d_1 w + d_2 w^2 + \dots \right], \quad (5.112)$$

where

$$c_1 = \frac{1}{2\mu_s} - 2b_1, \quad (5.113)$$

$$c_2 = 3(2b_1^2 - b_2) - \frac{3b_1}{2\mu_s} - \frac{1}{8\mu_s^2}, \quad (5.114)$$

$$d_1 = -\frac{1}{2\mu_s} - 2b_1, \quad (5.115)$$

$$d_2 = 3(2b_1^2 - b_2) + \frac{3b_1}{2\mu_s} + \frac{3}{8\mu_s^2}. \quad (5.116)$$

On the underside of the branch cut $(v^{\pm \frac{1}{2}} \frac{dv}{d\tau})$ are given by 5.111 and 5.112 with the coefficient of the even powers of w replaced by their negatives.

The expansion of $(-i \sinh \gamma_0)^{\pm \frac{1}{2}}$ can be obtained if the function $\sinh \gamma_0$ is written in the form

$$\sinh \gamma_0 = (\cosh^2 \gamma_0 - 1)^{1/2} = \left[\left(\frac{v}{1R} \right)^2 - 1 \right]^{1/2}. \quad (5.117)$$

When 5.105 is employed in conjunction with 5.117, the following series are obtained for $(-i \sinh \gamma_0)^{\pm 1/2}$.

$$(-i \sinh \gamma_0)_+^{1/2} = (-i \sinh \gamma_{os})^{1/2} [1 + e_1 w + e_2 w^2 + \dots] \quad (5.118)$$

$$(-i \sinh \gamma_0)_+^{-1/2} = (-i \sinh \gamma_{os})^{-1/2} [1 + f_1 w + f_2 w^2 + \dots] \quad (5.119)$$

where

$$e_1 = \frac{2\mu_s}{N^2} \quad (5.120)$$

$$e_2 = -\frac{6\mu_s^2}{N^4} + \frac{1}{N^2} (1 - 2\mu_s b_1) \quad , \quad (5.121)$$

$$f_1 = -\frac{2\mu_s}{N^2} \quad , \quad (5.122)$$

$$f_2 = \frac{10\mu_s^2}{N^4} - \frac{1}{N^2} (1 - 2\mu_s b_1) \quad , \quad (5.123)$$

with N defined by the relation

$$N \equiv \frac{2R \sinh \gamma_{0s}}{\rho} \quad . \quad (5.124)$$

The expansions on the underside of the branch cut can be obtained by replacing w by $-w$ in equations 5.118 and 5.119.

The coefficients $\Psi_i(\gamma, \gamma_0, \theta)$ ($i = 1, 2$) of the terms in v^{-1} in equations 5.77 and 5.78 can be replaced by their values at the saddle point $v = v_s$. This is legitimate since the higher order terms in the expansion of these coefficients about $\tau = 0$ yield terms of the order or less than the order of the error term $O\left(\frac{1}{v^2 \xi^3}\right)$.

When written in the form 5.110, the integrals 5.77 and 5.78 become

$$\lim_{s \gg 1} I_{10}^4(\underline{r}, s, -) = \frac{D(\xi, \theta, a, r)}{\rho \sin \xi} e^{-R \cos(2\xi - \theta) + 2\rho \cos \xi} M_1(a, \theta, s) \quad (5.125)$$

$$\lim_{s \gg 1} I_{20}^4(\underline{r}, s, -) = \frac{\cos(2\xi - \theta) D(\xi, \theta, a, r)}{\rho \sin \xi} e^{-R \cos(2\xi - \theta) + 2\rho \cos \xi} M_2(a, \theta, s) \quad (5.126)$$

$$M_1(a, \theta, s) = \left(\frac{2\rho}{\pi}\right)^{1/2} \int_0^{\infty} \frac{e^{-2\rho\tau}}{\tau^{1/2}} \left[1 + \frac{\Psi_1(r_s, r_{os}, \theta)}{v_s} + \right. \\ \left. + (d_2 + f_2 + d_1 f_1) \frac{2i}{a_2} \tau + O\left((v_s^2 \xi^3)^{-1} + \tau^2\right) \right] d\tau \quad (5.127)$$

$$M_2(a, \theta, s) = \left(\frac{2\rho}{\pi}\right)^{1/2} \int_0^{\infty} \frac{e^{-2\rho\tau}}{\tau^{1/2}} \left[1 + \frac{\Psi_2(r_s, r_{os}, \theta)}{v_s} + \right. \\ \left. + (d_2 + e_2 + d_1 e_1) \frac{2i}{a_2} \tau + O\left((v_s^2 \xi^3)^{-1} + \tau^2\right) \right] d\tau \quad (5.128)$$

$$D(\xi, \theta, a, r) = \left(\frac{a^2 \sin \xi \cos \xi}{2r L \sin \theta} \right)^{1/2} = \text{geometrical optics divergence factor for a sphere} \quad (5.129)$$

$$L = r \cos(2\xi - \theta) - \frac{a}{2} \cos \xi = \text{distance from the caustic of the geometrical optics ray system} \quad (5.130)$$

The physical interpretation of these equations is quite obvious. The time delay in 5.125 and 5.126 corresponds to the delay associated with a wave which is reflected from the sphere at the specular point. Furthermore, the factor $D(\xi, \theta, a, r)$ which appears in these equations is the divergence factor for rays which are reflected from a sphere. The explicit evaluation of $M_1(a, \theta, s)$ and $M_2(a, \theta, s)$ can be easily obtained to yield the relations

$$M_1(a, \theta, s) = 1 + \frac{\Psi_1(r_s, r_{os}, \theta)}{v_s} + \frac{i(d_2 + f_2 + d_1 f_1)}{2\rho a_2} + O\left(\frac{1}{\rho^2 \cos^6 \xi}\right) \quad (5.131)$$

$$M_2(a, \theta, s) = 1 + \frac{\Psi_2(r_s, r_{os}, \theta)}{v_s} + \frac{i(d_2 + e_2 + d_1 e_1)}{2\rho a_2} + O\left(\frac{1}{\rho^2 \cos^6 \xi}\right) \quad (5.132)$$

The asymptotic expansions of $I_{10}^{\Delta}(\underline{r}, s, -)$ and $I_{20}^{\Delta}(\underline{r}, s, -)$ given in this section will yield valid representations of both the near and far field values of the transforms of the field vectors in the illuminated region.

5.4.3 The penumbra. In the transitional region between the deep shadow and the illuminated region, the asymptotic expansions of the functions $I_{10}(\underline{r}, s, -)$ and $I_{20}(\underline{r}, s, -)$ cannot be obtained by either of the methods discussed in the preceding sections. The physical reason for this is the fact that the waves in the penumbra are of a different nature than those in either of the other two regions. The waves in the penumbra are excited by the currents in the vicinity of the shadow boundary. The fields which result from these currents are similar in nature to those which occur in the knife edge diffraction problem. It will be found that each of the scalar functions $I_{10}(\underline{r}, s, -)$ and $I_{20}(\underline{r}, s, -)$ can be divided into two terms. The asymptotic expansion of one of these terms yields a result which can be interpreted in terms of the conventional knife edge diffraction phenomena. The asymptotic expansion of the other term yields a result which can be interpreted as a background correction to the knife edge field. The origin of this term is the non-zero radius of curvature of the sphere at the shadow boundary.

The saddle point analysis of the asymptotic form of integral representations of $I_{10}^{\Delta}(\underline{r}, s, -)$ and $I_{20}^{\Delta}(\underline{r}, s, -)$ has demonstrated that the value of these integrals in the illuminated region is related to the behavior of their integrands in the vicinity of the point $\nu \sim i\rho \sin \xi$. This indicates that the asymptotic value of these

integrals in the penumbra ($\xi \sim \frac{\pi}{2}$) is related to the behavior of their integrands in the region $\nu \sim i\rho$. The contour D will therefore be deformed into a path which passes through the point $\nu = i\rho$. A suitable choice for this new contour is the path A which was employed in the residue series calculation. Asymptotic expansions of $I_{10}(\underline{r}, s, -)$ and $I_{20}(\underline{r}, s, -)$ will be obtained by expanding their integrands about the point $\nu = i\rho$. The results obtained in this fashion will be reasonably accurate since the most significant contribution to the original integrals comes from the region $\nu \sim i\rho$.

The asymptotic approximations appropriate to the region $\nu \sim i\rho$ can be obtained from Appendices I and III. A summary of these results follows:

a)
$$\frac{j_{\nu - \frac{1}{2}}(i\rho)}{h^{(1)}_{\nu - \frac{1}{2}}(i\rho)}, \frac{[i\rho j_{\nu - \frac{1}{2}}(i\rho)]'}{[i\rho h^{(1)}_{\nu - \frac{1}{2}}(i\rho)]'}$$
; in the right half of the ν plane

these functions can be represented in the form given in equations A-1.20 through A-1.23.

$$\frac{j_{\nu - \frac{1}{2}}(i\rho)}{h^{(1)}_{\nu - \frac{1}{2}}(i\rho)} = \frac{e^{\frac{i\pi}{3}}}{2} \frac{A_1(\nu^{2/3}\zeta)}{A_1(\nu^{2/3}\zeta e^{\frac{i2\pi}{3}})} [1 + O(\rho^{-4/3})], \quad (5.133)$$

$$\frac{[i\rho j_{\nu - \frac{1}{2}}(i\rho)]'}{[i\rho h^{(1)}_{\nu - \frac{1}{2}}(i\rho)]'} = \frac{e^{-\frac{i\pi}{3}}}{2} \frac{A_1'(\nu^{2/3}\zeta)}{A_1'(\nu^{2/3}\zeta e^{\frac{i2\pi}{3}})} [1 + O(\rho^{-2/3})]. \quad (5.134)$$

In the left half of the ν plane, the appropriate approximations are obtained from A-1.24 - A-1.27.

$$\frac{j_{\nu - \frac{1}{2}}(i\rho)}{h_{\nu - \frac{1}{2}}^{(1)}(i\rho)} = \frac{1}{2} - \frac{e^{-\frac{i\pi}{3}}}{2} \frac{A_1(\nu, 2/3 \zeta)}{A_1(\nu, 2/3 \zeta e^{-i2\pi/3})} [1 + O(\rho^{-4/3})] \quad (5.135)$$

$$\frac{[i\rho j_{\nu - \frac{1}{2}}(i\rho)]'}{[i\rho h_{\nu - \frac{1}{2}}^{(1)}(i\rho)]'} = \frac{1}{2} - \frac{e^{\frac{i\pi}{3}}}{2} \frac{A_1'(\nu, 2/3 \zeta)}{A_1'(\nu, 2/3 \zeta e^{-i2\pi/3})} [1 + O(\rho^{-2/3})] \quad (5.136)$$

- b) $h_{\nu - \frac{1}{2}}^{(1)}(iR)$, $[iRh_{\nu - \frac{1}{2}}^{(1)}(iR)]'$; it will be assumed in the present calculation that $r \gg a$. The asymptotic expansions in the near field can be obtained from a calculation similar to that employed by Fok in the steady state problem (21). The approximations given in equations 5.45 and 5.46 will be adequate for the portions of $I_{10}(\underline{r}, s, -)$ and $I_{20}(\underline{r}, s, -)$ which involve the Airy functions in 5.133 - 5.136. In the integrals which result from the factor $1/2$ in 5.135 and 5.136, however, the more accurate Debye approximations must be employed.
- c) $Q_{\nu - \frac{1}{2}}^1(\cos \theta - i0)$; the angular function will be replaced by the first term in its asymptotic expansion for large values of ν . The explicit form of this term can be obtained from equation A-3.9.

When the above asymptotic expansions are substituted in the integral representations of $I_{10}(\underline{r}, s, -)$ and $I_{20}(\underline{r}, s, -)$ we obtain

$$\lim_{s \gg 1} I_{10}(\underline{r}, s, -) = I_{10}^k(\underline{r}, s, -) + \frac{e^{\frac{i3\pi}{4}}}{R(2\pi \sin \theta)^{1/2}} e^{-(R^2 - \rho^2)^{\frac{1}{2}} - \rho \delta_0^-} I_{10}^b(\underline{r}, s, -) \quad (5.137)$$

$$\lim_{s \gg 1} I_{20}(\underline{r}, s, -) = I_{20}^k(\underline{r}, s, -) + \frac{e^{-i\frac{\pi}{4}}}{R(2\pi \sin \theta)^{1/2}} e^{-(R^2 - \rho^2)^{1/2} - \rho \delta_0^-} I_{20}^b(\underline{r}, s, -) \quad (5.138)$$

where

$$I_{10}^k(\underline{r}, s, -) = - \lim_{s \gg 1} e^{i\frac{\pi}{4}} \int_{\rho}^{\infty} (-1)^v \frac{v}{v^2 - \frac{1}{4}} h^{(1)}(iR) Q_{v - \frac{1}{2}}^1(\cos \theta - i0) dv \quad (5.139)$$

$$I_{10}^b(\underline{r}, s, -) = \left[e^{i\frac{\pi}{3}} \int_{A_2} e^{-\delta_0^- w} \frac{A_1(v^{2/3} \zeta)}{A_1(v^{2/3} \zeta e^{i2\pi/3})} v^{-1/2} dv - e^{-i\frac{\pi}{3}} \int_{A_1} e^{-\delta_0^- w} \frac{A_1(v^{2/3} \zeta)}{A_1(v^{2/3} \zeta e^{-i2\pi/3})} v^{-1/2} dv \right] (1 + O(\rho^{-2/3})) \quad (5.140)$$

$$I_{20}^k(\underline{r}, s, -) = \frac{1}{R} \frac{\partial}{\partial R} (R I_{10}^k(\underline{r}, s)) \left(1 + O\left(\frac{\rho}{R}\right)^2 \right) , \quad (5.141)$$

$$I_{20}^b(\underline{r}, s, -) = \left[e^{-i\frac{\pi}{3}} \int_{A_2} e^{-\delta_0^- w} \frac{A_1'(v^{2/3} \zeta)}{A_1'(v^{2/3} \zeta e^{i2\pi/3})} v^{-1/2} dv - e^{i\frac{\pi}{3}} \int_{A_1} e^{-\delta_0^- w} \frac{A_1'(v^{2/3} \zeta)}{A_1'(v^{2/3} \zeta e^{-i2\pi/3})} v^{-1/2} dv \right] (1 + O(\rho^{-2/3})) . \quad (5.142)$$

The variable w in equations 5.140 and 5.142 is defined by the relation $v = i(\rho + w)$. The superscript k terms in equations 5.137 and 5.138 yield the knife edge type diffraction results whereas the superscript b terms yield the background correction to the knife edge terms.

5.4.3a Evaluation of the Knife Edge Type Diffraction Terms:

The integral in 5.139 will be evaluated by a saddle point calculation. In this calculation the function $h_{\nu - \frac{1}{2}}^{(1)}(iR)$ will be replaced by the following Debye approximation in the entire range of integration.

$$h_{\nu - \frac{1}{2}}^{(1)}(iR) = \frac{e^{-R[\sin \alpha - \alpha \cos \alpha] - i\frac{3\pi}{4}}}{R(\sin \alpha)^{1/2}} (1 + O(R \sin \alpha)^{-1}) \quad (5.143)$$

where

$$\nu = iR \cos \alpha .$$

This is a valid approximation if $r \gg a$. When this is done and $Q_{\nu - \frac{1}{2}}^1(\cos \theta - i0)$ is replaced by the first term in its asymptotic expansion, $I_{10}^k(\underline{r}, s, -)$ assumes the form

$$I_{10}^k(\underline{r}, s, -) \sim \frac{e^{-i\frac{\pi}{4}}}{R(2\pi \sin \theta)^{1/2}} \int_{i\rho}^{\infty} (\nu \sin \alpha)^{-1/2} e^{-Rh(\alpha, \theta)} d\nu \quad (5.144)$$

where

$$h(\alpha, \theta) = \sin \alpha - (\alpha - (\theta - \frac{\pi}{2})) \cos \alpha . \quad (5.145)$$

The function $h(\alpha, \theta)$ has a saddle point at $\alpha = \theta - \frac{\pi}{2}$. An expansion of the integrand of 5.144 about this point yields the result

$$I_{10}^k(\underline{r}, s, -) \sim \frac{e^{R \cos \theta}}{R \sin \theta} \pi^{-1/2} \int_{-v_0}^{\infty} e^{-v^2} dv \quad (5.146)$$

where

$$v_0 = \left(\frac{s}{c}\right)^{1/2} \frac{r \sin \theta - a}{(-2r \cos \theta)^{1/2}} . \quad (5.147)$$

The result expressed in equations 5.146 and 5.147 is easily interpreted as a knife edge type diffraction phenomena. The parameter v_0 is a measure of the distance from the shadow boundary. When $v_0 \gg 1$ the integral in 5.146 is approximately equal to $\pi^{1/2}$ and the resultant value of $I_{10}^k(\underline{r}, s, -)$ is readily shown to be equivalent to the portion of the incident field derivable from $I_1(\underline{r}, s)$. In the vicinity of the shadow boundary v_0 is small and the Fresnel integral in 5.116 oscillates rapidly. The value of $I_{10}^k(\underline{r}, s, -)$ at the geometrical shadow boundary is equal to one-half of the incident field derivable from $I_1(\underline{r}, s)$. The explicit form of $I_{10}^k(\underline{r}, s, -)$ in these two cases is

$$I_{10}^k(\underline{r}, s, -) \sim \frac{e^{R \cos \theta}}{R \sin \theta} \left[1 - \frac{\exp \left[\frac{(R \sin \theta - \rho)^2}{2R \cos \theta} \right]}{2 \left(\frac{s\pi}{c} \right)^{1/2} \frac{r \sin \theta - a}{(-2r \cos \theta)^{1/2}}} \left(1 + \mathcal{O} \left(\frac{2R \cos \theta}{(R \sin \theta - \rho)^2} \right) \right) \right]$$

(5.148)

$$I_{10}^k(\underline{r}, s, -) \sim \frac{e^{R \cos \theta}}{R \sin \theta} \left[\frac{1}{2} + \left(\frac{s}{c} \right)^{1/2} \frac{r \sin \theta - a}{(-2\pi r \cos \theta)^{1/2}} + \mathcal{O} \left(\frac{(R \sin \theta - \rho)^2}{2R \cos \theta} \right) \right]$$

(5.149)

In the region $-v_0 \gg 1$ the function $I_{10}^k(\underline{r}, s, -)$ is given by the second term in 5.148.

5.4.3b Evaluation of the Background Terms:

The integrals in $I_{10}^b(\underline{r}, s, -)$ and $I_{20}^b(\underline{r}, s, -)$ are evaluated in a manner which is quite similar to a saddle point calculation. The contours A_2 and A_1 are deformed into new contours which are chosen

such that the most significant contribution to the resultant integrals comes from the region $v \sim i\rho$. The original paths are not of this type since the integrands have an infinite number of poles in the immediate vicinity of A_2 and A_1 . The paths which satisfy the requirement are defined by the conditions $\arg v^{2/3}\xi = 0$ and $\arg v'^{2/3}\xi = 0$. On these contours the magnitude of the integrands decreases at a maximum rate for large values of $u \equiv v^{2/3}\xi$ or $v'^{2/3}\xi$ (rate of decrease $\sim \exp(-\frac{4}{3}u^{3/2})$). The integrals are then evaluated by expanding their integrands in power series about $u = 0$ and integrating term by term.

The integrand of $I_{10}^b(\underline{r}, s, -)$ can be expanded in a power series about $u = 0$ if it is noted that for $v \sim i\rho$

$$w = \left(\frac{\rho}{2}\right)^{1/3} e^{\pm i\frac{\pi}{3}} u + \frac{1}{60} e^{\pm i\frac{2\pi}{3}} \left(\frac{\rho}{2}\right)^{-1/3} + .1490\left(\frac{\rho}{2}\right)^{-1} + O(\rho^{-4/3}) \quad (5.150)$$

where the + sign is taken on the path obtained from A_1 and the - sign on the path obtained from A_2 . With the assistance of this expression we can write $I_{10}^b(\underline{r}, s, -)$ in the form

$$I_{10}^b(\underline{r}, s, -) = \frac{e^{i\frac{\pi}{4}}}{2^{1/2}} \left(\frac{\rho}{2}\right)^{-1/6} \left[\int_0^{\infty} \exp\left[-\xi e^{-i\frac{\pi}{3}} u\right] \frac{A_1(u)}{A_1(ue^{i2\pi/3})} du + \int_0^{\infty} \exp\left[-\xi e^{i\frac{\pi}{3}} u\right] \frac{A_1(u)}{A_1(ue^{-i2\pi/3})} du \right] (1 + O(\rho^{-1/3})) \quad (5.151)$$

where

$$\xi \equiv \left(\frac{\rho}{2}\right)^{1/3} \delta_0^- \quad . \quad (5.152)$$

It is noted that the second integral in 5.151 is the complex conjugate of the first. Consequently, it is possible to write

$$I_{10}^b(\underline{r}, s, -) = 2^{1/2} e^{i\frac{\pi}{4}} \left(\frac{\rho}{2}\right)^{-1/6} \operatorname{Re} \int_0^{\infty} \exp \left[-\xi e^{-i\frac{\pi}{3}} u \right] \frac{A_1(u)}{A_1(ue^{i2\pi/3})} du (1 + \mathcal{O}(\rho^{-1/3})) \quad (5.153)$$

In the penumbra region the parameter ξ is small. An asymptotic estimate of $I_{10}^b(\underline{r}, s, -)$ for small ξ can be obtained by replacing the exponential factor in 5.153 by its Taylor series expansion about $u = 0$. This yields the result

$$I_{10}^b(\underline{r}, s, -) = 2^{3/2} e^{i\frac{\pi}{4}} \left(\frac{\rho}{2}\right)^{-1/6} \operatorname{Re} \sum_{n=0}^N \Omega_{1n} e^{i(2n-1)\frac{\pi}{3}} \frac{\xi^n}{n!} (1 + \mathcal{O}(\rho^{-1/3})) \quad (5.154)$$

where

$$\Omega_{1n} = \int_0^{\infty} u^n \frac{A_1^2(u)}{F_1^2(u)} du + i \int_0^{\infty} u^n \frac{A_1(u) B_1(u)}{F_1^2(u)} du \quad (5.155)$$

$$F_1^2(u) = A_1^2(u) + B_1^2(u) .$$

The integrals in 5.155 have been calculated numerically for $n = 1$ to 20 to five significant figures (22). The function $I_{20}^b(\underline{r}, s, -)$ can be evaluated in a similar manner. The asymptotic estimate of this function for small ξ is

$$I_{20}^b(\underline{r}, \underline{s}, -) = 2^{3/2} e^{i\frac{\pi}{4}} \left(\frac{\rho}{2}\right)^{-1/6} \operatorname{Re} \sum_{n=0}^N \Omega_{2n} e^{i(2n-1)\frac{\pi}{3}} \frac{\xi^n}{n!} (1 + \mathcal{O}(\rho^{-1/3})) \quad (5.156)$$

where

$$\Omega_{2n} = \int_0^{\infty} u^n \frac{A_1'^2(u)}{F_1'^2(u)} du + i \int_0^{\infty} u^n \frac{A_1'(u) B_1'(u)}{F_1'^2(u)} du \quad (5.157)$$

$$F_1'^2(u) = A_1'^2(u) + B_1'^2(u) \quad .$$

The integrals in Ω_{2n} have also been tabulated in reference (22). For future reference the values of Ω_{10} and Ω_{11} ($i = 1, 2$) are given below

$$\begin{aligned} \Omega_{10} &= .092361 + i.30900, & \Omega_{11} &= .029547 + i.17071, \\ \Omega_{20} &= .15095 + i.40149, & \Omega_{21} &= .058235 + i.23627. \end{aligned} \quad (5.158)$$

5.5 Behavior of the Fields in the Vicinity of the Wavefronts

In this section asymptotic estimates of the fields in the vicinity of the wavefronts will be obtained by a term by term inversion of the asymptotic expansion of the field transforms. These results will then be employed to indicate the time variation of the scattering processes. It is shown that the types of waves observed at a stationary point in space change as time progresses. The penumbra and the caustic region in the vicinity of the line $\theta = \pi$ are initially of zero extent. These regions expand with increasing time. An indication of the rate of this growth is obtained by a consideration of the error terms in the asymptotic expansions of the fields.

5.5.1 The initial behavior of the fields in the deep shadow.

Asymptotic expansions of the transforms of the transverse fields can be obtained from equations 5.17, 5.18 and 5.35 - 5.37 . If the far-field approximations for the Hankel functions are employed, the θ component of the transform of the $m = 0$ term in the wavefront expansion can be written

$$\lim_{s \gg 1, r/a \gg 1} \xi_{\theta_0}(\underline{r}, s, -) = - \frac{a \cos \phi}{2r(\pi \sin \theta)^{1/2}} \frac{e^{-(R^2 - \rho^2)^{1/2} - \rho(\delta_0^- + 1)}}{(\rho/2)^{1/6}}$$

$$\sum_{\alpha_l} \frac{e^{-(\frac{\rho}{2})^{1/3} \beta_p \delta_0^-}}{\beta_p [A_1(-\beta_p)]^2} \left[1 + \mathcal{O}(\rho^{-1/3} \delta_0^- + (\rho \sin \theta)^{-1} + (R^2 - \rho^2)^{-1/2}) \right] \quad (5.159)$$

The time function associated with this transform can be obtained by applying the inversion operator defined in equation 2.2. The inversion integrals which result from the operation can be evaluated by the saddle point method. Friedlander has obtained a rather general result for integrals of this type (23).

$$\frac{1}{2\pi i} \int_{-i\infty+\Delta}^{+i\infty+\Delta} s^{-n} \exp(Ts - \alpha s^{1/3}) ds = \frac{3^{1/4}(6n-1)}{2\pi^{1/2}} \alpha^{1/4} (3-6n) T^{1/4} (6n-s)$$

$$\mathcal{U}(T) \exp \left[- \frac{2(\alpha/3)^{3/2}}{T^{1/2}} \right] \left[1 + \mathcal{O}\left(\frac{T^{1/2}}{\alpha^{3/2}}\right) \right] \quad (5.160)$$

With the assistance of this equation, the inversion of 5.159 can be written in the form

$$\lim_{T_0^- \text{ small}} \underline{E}_{\theta_0}(\underline{r}, t) = - \frac{a(\delta_0^-)^{1/2}}{4\pi r(\sin \theta)^{1/2}} (T_0^-)^{-1} \mathcal{U}(T_0^-) \Psi(\beta_p, \delta_0^-, T_0^-) \cos \phi \quad (5.161)$$

where

$$T_0^- \equiv t - \frac{(r^2 - a^2)^{1/2} - a(\delta_0^- + 1)}{c} = \text{time measured from the arrival of the wavefront} \quad (5.162)$$

$$\begin{aligned} \Psi(\beta_p, \delta_0^-, T_0^-) = \sum_{\beta_p} \frac{1}{\beta_p^{1/2} [A_1(-\beta_p)]^2} \exp \left[- \frac{2(\delta_0^- \beta_p/3)^{3/2}}{(2cT_0^-/a)^{1/2}} \right] \left[1 + \right. \\ \left. + \mathcal{O} \left[\left(\frac{2cT_0^-}{a} \right)^{1/2} \left((\delta_0^-)^{-3/2} + \delta_0^- \right) + \frac{1}{\delta_0^-} \left(\frac{2cT_0^-}{a} \right)^{3/2} \left(\frac{1}{\sin \theta} + \right. \right. \right. \\ \left. \left. \left. + \frac{a}{(r^2 - a^2)^{1/2}} \right) \right] \right] \quad (5.163) \end{aligned}$$

In the earlier portions of this chapter, it was shown that a change in the rate of convergence of a particular mathematical representation of a wave phenomena indicated that the wave process itself was changing. In view of this, the result expressed in equations 5.161-5.163 yields the following facts about the wave behavior in the shadow.

- (a) The form of the exponential factor in $\Psi(\beta_p, \delta_0^-, T_0^-)$ indicates that the representation given in 5.161 converges slowly for $\frac{cT_0^-}{a} \gtrsim (\delta_0^-)^3$. This suggests that the wave processes associated with the shadow region are contained within a cone generated by the tangents to the surface of the sphere at the points $(r, \theta, \phi) = (a, \frac{\pi}{2} + \mathcal{O}(\frac{cT_0^-}{a})^{1/3}, \phi)$. At $T_0^- = 0$ the shadow region obviously occupies the entire geometrical shadow.

(b) The order of the error terms in 5.163 also yields some information about the wave phenomena in the region behind the sphere. The behavior of the order term $\left(\frac{2cT_0^-}{a}\right)^{1/2} \delta_0^-^{-3/2}$ merely substantiates the conclusions of (a). Some additional information, however, can be obtained from the terms involving the factor $\left(\frac{2cT_0^-}{a}\right)^{3/2}$. The term in $(\sin \theta)^{-1}$ indicates that the extent of the caustic region in the vicinity of the ray $\theta = \pi$ is of the order $\pi - \theta \lesssim O\left(\frac{2cT_0^-}{a}\right)^{3/2} / \delta_0^-$. Likewise, the extent of the far-field zone is indicated by the order of the term in $a/(r^2 - a^2)^{1/2}$. It is found that the far field can be defined by the condition $(r^2 - a^2)^{1/2}/a \gtrsim O\left(\frac{2cT_0^-}{a}\right)^{3/2} / \delta_0^-$.

The above discussion indicates that the nature of the waves observed at a given point behind the sphere changes with time. A point (r, θ, ϕ) which is initially in the far-field portion of the shadow might eventually be in the near-field portion of the caustic region.

5.5.2 The initial behavior of the fields in the illuminated region. Asymptotic expansions of the transverse field transforms in the illuminated region can be obtained from the results of Section 5.4.2f. In the far field, the θ component of the field transform assumes the form

$$\lim_{s \gg 1, r/a \gg 1} \xi_{\theta 0}^*(\underline{r}, s, -) = -\frac{a \cos \phi}{2r} e^{-R + 2\rho \cos \frac{\theta}{2} - \rho} \left[1 - \frac{1}{2\rho \cos^3 \frac{\theta}{2}} + O(\rho^2 \cos^6 \frac{\theta}{2})^{-1} \right]. \quad (5.164)$$

The analytic continuation of this result into the real frequency domain ($\rho \rightarrow ika$) yields a result which is identical with the steady state calculation of Logan (24). This provides a convenient check on the correctness of the more general results of Section 5.4.2f.

Application of the inversion operator 2.2 to equation 5.164 yields the following asymptotic estimate of the small time behavior of $\underline{E}_{\theta_0}(\underline{r}, s)$.

$$\lim_{T_0^* \text{ small}} \underline{E}_{\theta_0}(\underline{r}, t) = -\frac{a \cos \phi}{2r} \left[\delta(T_0^*) - \left(\frac{2a}{c} \cos^3 \frac{\theta}{2}\right)^{-1} \mathcal{U}(T_0^*) + \mathcal{O}\left(\frac{c}{a} \frac{cT_0^*}{a} \cos^{-6} \xi\right) \right], \quad (5.165)$$

where

$$T_0^* \equiv t - \frac{r + a - 2a \cos \frac{\theta}{2}}{c}. \quad (5.166)$$

The order term in 5.165 indicates that the extent of the illuminated region at small times is approximately given by the relation $0 \leq 2\xi \leq \pi - \mathcal{O}\left(\frac{cT_0^*}{a}\right)^{1/6}$, (ξ = angle of incidence).

5.5.3 The initial behavior of the fields in the penumbra. The transforms of the fields in the vicinity of the geometrical shadow can be obtained from the results of Section 5.4.3. The far-field values of the transforms of the θ component of the field are given by the relations

$$\lim_{s \gg 1, r/a \gg 1} \xi_{\theta_0}^k(\underline{r}, s, -) = \cos \theta \cos \phi e^{R \cos \theta - \rho} \int_{-v_0}^{\infty} e^{-v^2} dv \quad (5.167)$$

$$\lim_{s \gg 1, r/a \gg 1} \xi_{\theta_0}^b(\underline{r}, s, -) = - \frac{2a \cos \phi}{r(\pi \sin \theta)^{1/2}} \frac{e^{-(R^2 - \rho^2)^{1/2} - \rho(\delta_0^- + 1)}}{(\rho/2)^{1/6}} \times$$

$$\times \left[0.42316 - 0.17528 \delta_0^- \left(\frac{\rho}{2}\right)^{1/3} + \mathcal{O}\left(\left(\rho \delta_0^-\right)^2 + \rho^{-\frac{1}{3}}\right) \right] \quad (5.168)$$

where v_0 is defined by equation 5.147. These transforms can easily be inverted to obtain the following asymptotic estimates of the θ component of the field

$$\lim_{h \ll 1, r \sin \theta - a > 0} E_{\theta_0}^k(\underline{r}, t) = \cos \theta \cos \phi \left[\delta\left(t + \frac{z - a}{c}\right) - \frac{\mathcal{U}(T_0^k)}{2\pi} \left(\frac{c}{T_0^k}\right)^{\frac{1}{2}} \frac{(-2r \cos \theta)^{1/2}}{r \sin \theta - a} \left[1 + \mathcal{O}(h)\right] \right] \quad (5.169)$$

$$\lim_{h \gg 1} E_{\theta_0}^k(\underline{r}, t) = \frac{1}{2} \cos \theta \cos \phi \left[\delta\left(t + \frac{z - a}{c}\right) - \frac{\mathcal{U}(T_0^k)}{\pi} \frac{c}{(cT_0^k)^{3/2}} \frac{r \sin \theta - a}{(-2r \cos \theta)^{1/2}} \left[1 + \mathcal{O}(h^{-1})\right] \right] \quad (5.170)$$

$$\lim_{h \ll 1, r \sin \theta - a < 0} E_{\theta_0}^k(\underline{r}, t) = + \cos \theta \cos \phi \frac{\mathcal{U}(T_0^k)}{2\pi} \left(\frac{c}{T_0^k}\right)^{1/2} \frac{(-2r \cos \theta)^{1/2}}{a - r \sin \theta} (1 + \mathcal{O}(h)) \quad (5.171)$$

where

$$T_0^k \equiv t + \frac{z - a}{c} + \frac{(r \sin \theta - a)^2}{2r \cos \theta} \quad (5.172)$$

$$h \equiv \frac{cT_0^k r \cos \theta}{(r \sin \theta - a)^2} \quad , \quad (5.173)$$

and

$$\begin{aligned} \lim_{T_0^- \text{ small}} E_{\theta 0}^b(\underline{r}, t) = & - \frac{4\Gamma(\frac{1}{6}) a \cos \phi}{r(\pi \sin \theta)^{1/2}} \frac{c}{a} \mathcal{U}(T_0^-) \left(\frac{a}{2cT_0^-}\right)^{\frac{5}{6}} \left[0.42316 + \right. \\ & \left. + \mathcal{O} \left(\delta_0^- \left(\frac{a}{2cT_0^-}\right)^{1/3} + \left(\frac{2cT_0^-}{a}\right)^{1/3} \right) \right] \end{aligned} \quad (5.174)$$

where T_0^- is defined by equation 5.162. The error terms again indicate that the wave processes observed at a particular point in space change in time. The knife edge terms can be interpreted as cylindrical waves whereas all of the other waves are spherical. The error term in 5.174 indicates that the background type fields exist only when

$\left(\frac{2cT_0^-}{a}\right)^{1/3} \gtrsim \delta_0^-$. This implies that the width of the penumbra is of the order $\left(\frac{2cT_0^-}{a}\right)^{1/3}$ at T_0^- . The penumbral width determined here is in accord with the results of Section 5.5.1 concerning the extent of the shadow.

5.6 Large Time Behavior of the Fields

It was originally planned to evaluate the large time behavior of the field vectors by means of a term by term inversion of the wavefront expansion. The results obtained in this manner, however, have recently been found to be unsatisfactory. One of the reasons for this difficulty is probably associated with the fact that the large time behavior of the impulse response is related to the low frequency characteristics of the scatterer. The appropriate mathematical description of the low frequency wave behavior is the harmonic series representation and not the wavefront expansion.

The inversion of the transforms of the transverse field components can be obtained by a term by term inversion of the harmonic series representations given in equations 5.13 and 5.14. The n^{th} terms in these series have poles at the zeros of the Hankel functions $h_n^{(1)}(i\rho)$ and $[i\rho h_n^{(1)}(i\rho)]'$. The first few zeros of these Hankel functions are given in the following table (25)

n	$h_n^{(1)}(i\rho_m) = 0$	$[i\rho_e h_n^{(1)}(i\rho_e)]' = 0$
1	-1	$e^{\pm i \frac{2\pi}{3}}$
2	$-1 \pm i0.86$	- 1.60 - 0.70 \pm i1.81
3	-2.26 $-1.87 \pm i1.75$	- 2.17 \pm i0.87 - 0.83 \pm i12.77

It is noted that the real part of the zeros becomes more negative as the order n increases. Consequently, the higher order terms in the

residue series expansion of $E_\theta(\underline{r}, t)$ and $E_\phi(\underline{r}, t)$ can be neglected when $t \gg 1$. The explicit form of the residue series expansion of $E_\theta(\underline{r}, t)$ is

$$E_\theta(\underline{r}, t) = + \frac{ci}{a} \sum_{n=1}^{\infty} (-1)^n \frac{2n+1}{n(n+1)} \left[\sum_{m=1}^n e^{\rho_m \left(\frac{ct}{a} - 1\right)} \frac{j_n(i\rho_m)}{[h_n^{(1)}(i\rho_m)]'} h_n^{(1)}\left(i \frac{r}{a} \rho_m\right) \frac{P_n^1(\cos \theta)}{\sin \theta} + \sum_{e=1}^{n+1} e^{\rho_e \left(\frac{ct}{a} - 1\right)} \frac{[i\rho_e j_n(i\rho_e)]'}{[i\rho_e h_n^{(1)}(i\rho_e)]''} \frac{[i \frac{r}{a} \rho_e h_n^{(1)}(i \frac{r}{a} \rho_e)]'}{\rho_e \frac{r}{a}} \frac{\partial}{\partial \theta} P_n^1(\cos \theta) \right] \cos \phi. \quad (5.175)$$

When $t \gg 1$ equation 5.175 can be approximated by the residue at the pole $\rho_e = e^{\pm i2\pi/3}$. This yields

$$\lim_{\frac{cT}{a} \gg 1} E_\theta(\underline{r}, t) = - \frac{2 \cos \theta \cos \phi}{\frac{r}{c}} e^{-cT/2a} \cdot \text{Re} \left[\frac{e^{+i(\sqrt{3} \frac{cT}{2a} + \frac{\pi}{3})}}{(1 - i \frac{1}{\sqrt{3}})} \left[1 + \frac{a}{r} e^{-i \frac{2\pi}{3}} + \left(\frac{a}{r}\right)^2 e^{-i \frac{4\pi}{3}} \right] \right] + O(e^{-0.70 \frac{cT}{a}}). \quad (5.176)$$

$$\text{where } T \equiv t - \frac{r - a}{c}. \quad (5.177)$$

Although there has been insufficient time to fully investigate the wavefront treatment of a pulse modulated carrier signal, it is felt that

this problem can be handled most efficiently by a wavefront expansion approach when $ka \gg 1$. In this problem, the large time behavior of the scattered fields is predominately of an optical nature and the wavefront expansion should adequately describe the fields. The wavefront expansion for this problem can be obtained from the results of equation 5.27. The inversion of each term in this expansion can be obtained at large times by deforming the contour $\text{Re}(s) = \Delta$ into the left half plane. Aside from any singularities associated with the source function, the singularities of a typical wavefront term are depicted in Figure 5.8. The branch cut B_0 along the negative real axis accounts for the fact that the Bessel and Hankel functions in the integrands of $I_{im}(\underline{r}, s, \pm)$ ($i = 1, 2$) are multiple valued in the s plane. The curved branch cuts B_j, \bar{B}_j ($j = 1, 2, \dots$) result from the fact that the integrands of the wavefront integrals are singular along these lines. These lines are the loci of the zeros of the Hankel functions $h_{\nu - \frac{1}{2}}^{(1)}(i\rho)$ and $[i p h_{\nu - \frac{1}{2}}^{(1)}(i\rho)]'$ as ν varies from $-\infty$ to ∞ along the real axis in the ν plane. It can be shown that the singularities which result in the wavefront terms are of a logarithmic nature. At large times the significant contribution to inversion of $I_{im}(\underline{r}, s, \pm)$ comes from the branch point integration along the negative real axis. Consequently, it should be possible to obtain an asymptotic expansion of the time behavior of the fields by expanding the transform functions $I_{im}(\underline{r}, s, \pm)$ in the vicinity of the branch point $s = 0$ and integrating the results term by term.

VI SUMMARY AND CONCLUSIONS

A general technique for the solution of pulse scattering from finite obstacles is formulated. The essential feature of this formulation is the identification and separate consideration of the individual terms in a wavefront expansion of the field transforms. Each wavefront term is associated with a particular ray of a generalized geometrical optics. An estimate of the behavior of the fields in the vicinity of the wavefronts is obtained by means of a Tauberian theorem. The wave behavior at a large times after the arrival of the wavefront is obtained by deforming the contour of Laplace transform inversion integral into the left half of the s plane. The most significant contribution on the deformed path is the one which originates from the singularity closest to the imaginary axis. In general this singularity can be either a pole or a branch point.

The reflection of a delta pulse from a semi-infinite conducting dielectric is considered. The results of this problem are employed to determine the significance of the dispersive effect of a finite conductivity in a scattering obstacle. It is found that the wave distortion is negligible for all metallic conductors. A significant distortion may result, however, when a signal is scattered by an obstacle whose composition is somewhat like dry earth. It is reasonable to expect, for instance, that a signal scattered by one of the planets or the moon would be distorted as a result of their finite conductivity.

The transmission of a delta pulse through a conducting dielectric slab is considered. This problem demonstrates the usefulness of the

wavefront expansion technique. The results are pertinent to problems of shielding by thin sheets. Estimates of the large and small time behavior of the impulse response are given. If a more complete description of the transmitted field is desired, the integral representation of this quantity can easily be evaluated by numerical methods.

The scattering of a delta pulse by a smooth sphere is treated in considerable detail. The individual wavefront terms are identified and considered separately. The error terms in the asymptotic expansions of the field quantities are employed to indicate the general time behavior of wave phenomena. It is found that the nature of the waves changes in time. This is particularly true in the vicinity of the shadow boundary. Initially the penumbra is of zero extent. It subtends an angular region of the order $(\frac{2cT}{a})^{1/3}$ at a time T after the arrival of the diffracted wavefront. The rates of growth of the caustic region in the vicinity of the focal line $\theta = \pi$ and the near field zone are also obtained by an interpretation of the error terms. The saddle point calculation of asymptotic behavior of the field transforms in the illuminated region can be analytically continued into the real frequency domain ($\rho \rightarrow ika$) to yield a result which is useful in the steady state scattering problem. The asymptotic expansion of the reflected fields obtained in this way is valid in both the near and the far field regions.

Some difficulty was experienced in the attempt to obtain the large time behavior of the impulse response of the sphere by a separate consideration of each term in the wavefront expansion. This problem is undoubtedly associated with the fact that the large time behavior of the impulse response is related to the low frequency characteristics of the

sphere. The appropriate mathematical formulation of the low frequency wave behavior is the harmonic series and not the optical expansion. It appears that the wavefront expansion technique must be restricted to those problems whose steady state behavior is predominantly of an optical nature. The transmission problem considered in Chapter IV is of this type. A problem which merits additional attention is the scattering of a c.w. wave with a unit step function envelope. When the carrier wavelength is large compared to the radius of the sphere, the steady state response to this signal is optical in nature. A wavefront analysis should simplify the task of interpreting the results of this problem in a physically meaningful way.

APPENDIX I

ASYMPTOTIC EXPANSIONS OF THE HANKEL FUNCTIONS $H_\nu^{(1,2)}(i\rho)$

The evaluation of the integrals which result from the transformation of the harmonic series representation of the fields scattered from a sphere to the equivalent integral representations requires a knowledge of the behavior of the Hankel functions $H_\nu^{(1,2)}(i\rho)$ in the complex ν plane. Our task is considerably simplified since we shall be satisfied with an asymptotic solution of the field integrals for large values of the quantity $|i\rho|$. In this case, a knowledge of the asymptotic behavior of the Hankel functions for large values of $|\nu|$ is sufficient. In the following section the asymptotic expansions of Olver will be employed to obtain the necessary approximations (1,2). We will restrict the discussion to the case where $\arg \rho = 0$.

Olver Approximation

The Hankel functions $H_\nu^{(1,2)}(i\rho)$ satisfy the differential equation

$$\frac{\partial^2 H_\nu^{(1,2)}(i\rho)}{\partial \rho^2} + \frac{1}{\rho} \frac{\partial H_\nu^{(1,2)}(i\rho)}{\partial \rho} - \left(1 + \frac{\nu^2}{\rho^2}\right) H_\nu^{(1,2)}(i\rho) = 0 \quad (\text{A-1.0})$$

If ρ is replaced by μz , where μ is defined by the relation $\nu = i\mu$ the above equation assumes the form

$$\frac{\partial^2 H_\nu^{(1,2)}(\nu z)}{\partial z^2} + \frac{1}{z} \frac{\partial H_\nu^{(1,2)}(\nu z)}{\partial z} + \nu^2 \left(1 - \frac{1}{z^2}\right) H_\nu^{(1,2)}(\nu z) = 0 \quad (\text{A-1.1})$$

The solution of A-1.1 is given by Olver in terms of the Airy integrals $A_{\frac{1}{2}}(\nu^{2/3} \zeta(z) e^{i\frac{2\pi}{3}})$ and $A_{\frac{1}{2}}(\nu^{2/3} \zeta(z) e^{-i\frac{2\pi}{3}})$ respectively for $H_\nu^{(1)}(\nu z)$ and $H_\nu^{(2)}(\nu z)$. In the angular domain $-\frac{\pi}{2} < \arg \nu < \frac{\pi}{2}$, $-\pi < \arg z < \pi$ he obtains the results

$$H_v^{(1)}(vz) \sim \frac{2e^{-\frac{1\pi}{3}}}{v^{1/3}} \left(\frac{4\zeta(z)}{1-z^2} \right)^{1/4} \left\{ A_1(v^{2/3}\zeta(z)e^{\frac{i2\pi}{3}}) \sum_{s=0}^{\infty} \frac{A_s(\zeta)}{v^{2s}} + \right. \\ \left. + e^{\frac{i2\pi}{3}} \frac{A_1'(v^{2/3}\zeta(z)e^{\frac{i2\pi}{3}})}{v^{4/3}} \sum_{s=0}^{\infty} \frac{B_s(\zeta)}{v^{2s}} \right\}, \quad (A-1.2)$$

$$H_v^{(2)}(vz) \sim \frac{2e^{\frac{1\pi}{3}}}{v^{1/3}} \left(\frac{4\zeta(z)}{1-z^2} \right)^{1/4} \left\{ A_1(v^{2/3}\zeta(z)e^{-\frac{2\pi}{3}}) \sum_{s=0}^{\infty} \frac{A_s(\zeta)}{v^{2s}} + \right. \\ \left. + e^{-\frac{2\pi}{3}} \frac{A_1'(v^{2/3}\zeta(z)e^{-\frac{2\pi}{3}})}{v^{4/3}} \sum_{s=0}^{\infty} \frac{B_s(\zeta)}{v^{2s}} \right\}. \quad (A-1.3)$$

The prime in the above equations indicates a differentiation with respect to the argument of the primed quantity. The functions $\zeta(z)$, $A_s(\zeta)$, and $B_s(\zeta)$ are defined as follows:

$$\zeta(z) \left(\frac{d\zeta}{dz} \right)^2 \equiv \frac{1-z^2}{z^2}, \quad (A-1.4)$$

$$A_0(\zeta) \equiv 1, \quad (A-1.5)$$

$$B_s(\zeta) \equiv \frac{1}{2} \zeta^{-1/2} \int_0^{\zeta} t^{-1/2} [f(t) A_s(t) - A_s''(t)] dt, \quad (A-1.6)$$

$$A_{s+1}(\zeta) \equiv -\frac{1}{2} B_s'(\zeta) + \frac{1}{2} \int f(\zeta) B_s(\zeta) d\zeta, \quad (A-1.7)$$

$$f(\zeta) \equiv -\frac{\dot{z}^2}{4z^2} + \dot{z}^{1/2} \frac{d^2}{d\zeta^2} (\dot{z}^{-1/2}), \quad \dot{z} \equiv \frac{dz}{d\zeta}. \quad (A-1.8)$$

It is evident that the set of equations A-1.4 - A-1.8 forms a recursive system, which in theory, will yield all of the coefficients appearing in the asymptotic expansions A-1.2 and A-1.3.

The asymptotic expansions for $H_v^{(1,2)'}(vz)$ can be obtained by differentiating equations A-1.2 and A-1.3 term by term with respect to vz .

The equations which result are

$$H_v^{(1)'}(vz) \sim -2e^{-\frac{1\pi}{3}} \psi(\zeta) \left\{ \frac{A_1(v^{2/3} \zeta e^{i\frac{2\pi}{3}})}{v^{4/3}} \sum_{s=0}^{\infty} \frac{C_s(\zeta)}{v^{2s}} + \right. \\ \left. + e^{i\frac{2\pi}{3}} \frac{A_1'(v^{2/3} \zeta e^{i\frac{2\pi}{3}})}{v^{2/3}} \sum_{s=0}^{\infty} \frac{D_s(\zeta)}{v^{2s}} \right\}, \quad (\text{A-1.9})$$

$$H_v^{(2)'}(vz) \sim -2e^{i\frac{\pi}{3}} \psi(\zeta) \left\{ \frac{A_1(v^{2/3} \zeta e^{-i\frac{2\pi}{3}})}{v^{4/3}} \sum_{s=0}^{\infty} \frac{C_s(\zeta)}{v^{2s}} + \right. \\ \left. + e^{-i\frac{2\pi}{3}} \frac{A_1'(v^{2/3} \zeta e^{-i\frac{2\pi}{3}})}{v^{2/3}} \sum_{s=0}^{\infty} \frac{D_s(\zeta)}{v^{2s}} \right\} \quad (\text{A-1.10})$$

where

$$C_s(\zeta) \equiv (\zeta)A_s(\zeta) + A_s'(\zeta) + \zeta B_s(\zeta), \quad (\text{A-1.11})$$

$$D_s(\zeta) \equiv A_s(\zeta) + \chi(\zeta) B_{s-1}(\zeta) + B_{s-1}'(\zeta), \quad (\text{A-1.12})$$

$$\chi(\zeta) \equiv \frac{\phi'(\zeta)}{\phi(\zeta)}; \quad \phi(\zeta) \equiv \left(\frac{4\zeta}{1-z} \right)^{1/4} = \left(-\frac{2}{z} \frac{dz}{d\zeta} \right)^{1/2}, \quad (\text{A-1.13})$$

$$\psi(\zeta) \equiv \frac{2}{z\phi(\zeta)}. \quad (\text{A-1.14})$$

Asymptotic expansions which are valid in the angular range $\frac{\pi}{2} < \arg v < \frac{3\pi}{2}$ can be obtained from equations for A-1.2, 1.3, 1.9, and 1.10 by applying the appropriate continuation formulas for the Hankel functions. The desired continuation formulas are obtained from the following relations quoted by Watson (3).

$$H_{\nu}^{(2)}(ue^{m\pi i}) = \frac{\sin(m+1)\pi}{\sin \nu\pi} H_{\nu}^{(2)}(u) + e^{i\nu\pi} \frac{\sin m\nu\pi}{\sin \nu\pi} H_{\nu}^{(1)}(u) , \quad (\text{A-1.15})$$

$$H_{-\nu}^{(2)}(u) = e^{-i\nu\pi} H_{\nu}^{(2)}(u) , \quad (\text{A-1.16})$$

$$J_{\nu}(u) = e^{-im\pi\nu} J_{\nu}(ue^{im\pi}) . \quad (\text{A-1.17})$$

If $m=-1$, $u \equiv \nu z$, and $\nu' \equiv e^{-i\pi}\nu$, the first two of the above equations yield the relation

$$H_{\nu}^1(\nu z) = -H_{\nu'}^{(2)}(\nu' z) . \quad (\text{A-1.18})$$

Likewise, equation A-1.17 in conjunction with the definition of the Hankel functions yields

$$H_{\nu}^{(2)}(\nu z) = 2J_{\nu'}(\nu' z) + e^{i2\nu\pi} H_{\nu'}^{(2)}(\nu' z) . \quad (\text{A-1.19})$$

Equations A-1.2, 1.3, 1.9, 1.10, 1.18 and 1.19 define the Hankel functions in the entire ν plane.

Explicit Form of the Asymptotic Approximations in the Various Regions of the ν Plane

The asymptotic evaluation of the diffraction integrals becomes quite unwieldy if a large number of terms are required in the expansion.

Luckily, however, the first two terms in this expansion will be sufficient for our purposes. Consequently, it is necessary to retain only the first two terms in the asymptotic approximations given in the previous section.

When this is done the following expressions are obtained for the various Hankel functions

$$H_{\nu}^{(1)}(\nu z) = \frac{2e^{-i\frac{\pi}{3}}}{\nu^{1/3}} \left(\frac{4\zeta}{1-z^2}\right)^{1/4} \left\{ A_1(\nu^{2/3} \zeta e^{i\frac{2\pi}{3}}) + e^{i\frac{2\pi}{3}} \frac{A_1'(\nu^{2/3} \zeta e^{i\frac{2\pi}{3}}) B_0(\zeta)}{\nu^{4/3}} + \right. \\ \left. + O(\nu^{-2}) \right\} \quad (A-1.20)$$

$$H_{\nu}^{(2)}(\nu z) = \frac{2e^{i\frac{\pi}{3}}}{\nu^{1/3}} \left(\frac{4\zeta(z)}{1-z^2}\right)^{1/4} \left\{ A_1(\nu^{2/3} \zeta(z) e^{-i\frac{2\pi}{3}}) \right. \\ \left. + e^{-i\frac{2\pi}{3}} \frac{A_1'(\nu^{2/3} \zeta(z) e^{-i\frac{2\pi}{3}}) B_0(\zeta)}{\nu^{4/3}} + O(\nu^{-2}) \right\} \quad (A-1.21)$$

$$H_{\nu}^{(1)'}(\nu z) = -\frac{2e^{-i\frac{\pi}{3}} \psi(\zeta)}{\nu^{2/3}} \left\{ e^{i\frac{2\pi}{3}} A_1'(\nu^{2/3} \zeta e^{i\frac{2\pi}{3}}) + \right. \\ \left. + \frac{A_1(\nu^{2/3} \zeta e^{i\frac{2\pi}{3}})}{\nu^{2/3}} C_0(\zeta) + O(\nu^{-2}) \right\} \quad (A-1.22)$$

$$H_{\nu}^{(2)'}(\nu z) = -\frac{2e^{i\frac{\pi}{3}} \psi(\zeta)}{\nu^{2/3}} \left\{ e^{-i\frac{2\pi}{3}} A_1'(\nu^{2/3} \zeta e^{-i\frac{2\pi}{3}}) + \right. \\ \left. + \frac{A_1(\nu^{2/3} \zeta e^{-i\frac{2\pi}{3}}) C_0(\zeta)}{\nu^{2/3}} + O(\nu^{-2}) \right\} \quad (A-1.23)$$

The above equations are valid, of course, only in the angular range $-\frac{\pi}{2} < \text{ang } \nu < \frac{\pi}{2}$. Similar approximations valid in the remainder of the ν plane can be obtained from A-1.20 - 1.23 by means of the continuation formulas A1.18, 1.19. The resulting asymptotic expansions are

$$H_v^{(1)}(vz) = -\frac{2e^{\frac{i\pi}{3}}}{v^{1/3}} \left(\frac{4\zeta}{1-z^2}\right)^{1/4} \left\{ A_1(v^{2/3}\zeta e^{-\frac{i2\pi}{3}}) + e^{-\frac{i2\pi}{3}} \frac{A_1'(v^{2/3}\zeta e^{-\frac{i2\pi}{3}}) B_0(\zeta)}{v^{4/3}} + O(v^{-2}) \right\} \quad (A-1.24)$$

$$H_v^{(2)}(vz) = \frac{2e^{\frac{i\pi}{3}}}{v^{1/3}} \left(\frac{4\zeta}{1-z^2}\right)^{1/4} \left\{ e^{-\frac{i\pi}{3}} A_1(v^{2/3}\zeta) + e^{12v\pi} A_1(v^{2/3}\zeta e^{-\frac{i2\pi}{3}}) + \frac{\left[e^{-\frac{i\pi}{3}} A_1'(v^{2/3}\zeta) + e^{12v\pi} e^{-\frac{i2\pi}{3}} A_1'(v^{2/3}\zeta e^{-\frac{i2\pi}{3}}) \right] B_0(\zeta)}{v^{4/3}} + O(v^{-2}) \right\} \quad (A-1.25)$$

$$H_v^{(1)'}(vz) = -\frac{2e^{\frac{i\pi}{3}}\psi(\zeta)}{v^{2/3}} \left\{ e^{-\frac{i2\pi}{3}} A_1'(v^{2/3}\zeta e^{-\frac{i2\pi}{3}}) + \frac{A_1(v^{2/3}\zeta e^{-\frac{i2\pi}{3}}) C_0(\zeta)}{v^{2/3}} + O(v^{-2}) \right\} \quad (A-1.26)$$

$$H_v^{(2)'}(vz) = \frac{2\psi(\zeta)}{v^{2/3}} \left\{ A_1'(v^{2/3}\zeta) + e^{-\frac{i\pi}{3}} e^{12v\pi} A_1'(v^{2/3}\zeta e^{-\frac{i2\pi}{3}}) + \frac{\left[A_1(v^{2/3}\zeta) + e^{12\pi} e^{\frac{i\pi}{3}} A_1(v^{2/3}\zeta e^{-\frac{i2\pi}{3}}) \right] C_0(\zeta)}{v^{2/3}} + O(v^{-2}) \right\} \quad (A-1.27)$$

The coefficients $B_0(\zeta)$ and $C_0(\zeta)$ which appear in equations A-1.20 through A-1.27 can be obtained from the recursion relations A-1.4 - A-1.8. These coefficients are given by the relations

$$C_0(\zeta) = \chi(\zeta) + \zeta B_0(\zeta) \quad , \quad (A-1.28)$$

$$B_0(\zeta) = -\frac{5}{48 \zeta^2} - \frac{1}{\zeta^{1/2}} \left(\frac{v}{8} - \frac{5v^3}{24} \right) \quad , \quad (A-1.29)$$

where $v \equiv (1 - z^2)^{-1/2}$.

If the distance from the point $v = i\rho$ ($\zeta = 0$) is sufficiently large, the Airy functions in equations A-1.24 - A-1.27 can be replaced by their asymptotic expansions. These expansions are summarized in Appendix II. It is noted that the explicit form of the approximations depend upon the angular domain within which the arguments of the Airy functions are located. Consequently, it is necessary to ascertain the behavior of $\arg(v^{2/3} \zeta)$ in the v plane.

The function $\zeta(z)$ is defined by the relation given in equation A-1.4. Olver has integrated this equation to obtain the result

$$\frac{2}{3} \zeta^{3/2} = \ln \frac{1 + \sqrt{1 - z^2}}{z} - \sqrt{1 - z^2} \quad . \quad (A-1.30)$$

The logarithm in equation A-1.11 is defined on the z plane cut in the manner shown in Figure A-1.0.

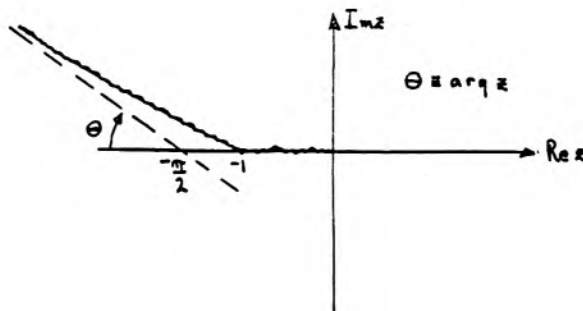


Fig. A-1.0. Branch Cut Configuration in the z Plane

If the variable z is replaced by $\operatorname{sech} \sigma$, equation A-1.30 assumes the

form

$$\frac{2}{3} \zeta^{3/2} = \sigma - \tanh \sigma \quad , \quad (\text{A-1.31})$$

$$z \equiv \operatorname{sech} \sigma \quad , \quad \sigma = \sigma_r + i\sigma_i \quad .$$

In this transformation, the domain $0 < \arg z < \pi$ is mapped conformally on the half strip $-\pi < \sigma_i < 0$, $\sigma_r > 0$, and the domain $-\pi < \arg z < 0$ is mapped on the half strip $0 < \sigma_i < \pi$, $\sigma_r > 0$. In order to facilitate a comparison with Debye's asymptotic series, it is necessary to define v by means of the relations

$$v \equiv i\rho \cosh \gamma \quad (\text{A-1.32})$$

$$\gamma = \beta + i\alpha \quad , \quad -\infty < \beta < \infty \quad , \quad 0 < \alpha < \pi \quad .$$

A comparison of this definition of v and that obtained by the relation $v = i\rho/z$ reveals that $\sigma = -\gamma$ if $\operatorname{Re}(v) > 0$, and $\sigma = \gamma$ if $\operatorname{Re}(v) < 0$. Consequently, in terms of Debye's variable γ , the function $v^{2/3} \zeta$ is representable in the form

$$v^{2/3} \zeta = \left[\frac{3i\rho}{2} \left(\sinh \gamma - \gamma \cosh \gamma \right) \right]^{2/3} \quad ,$$

for $\operatorname{Re}(v) > 0$ and $\quad (\text{A-1.33})$

$$v^{2/3} \zeta = \left[-\frac{3i\rho}{2} \left(\sinh \gamma - \gamma \cosh \gamma \right) \right]^{2/3}$$

for $\operatorname{Re}(v) < 0$. These equations can be used to obtain the behavior of $\arg(v^{2/3} \zeta)$ in the v plane. The results obtained in this manner are summarized in Figure A-1.2. In the left half plane, the function $\arg(v^{2/3} \zeta)$ varies continuously from $\pi/3$ along the line $\alpha = 0$ to $-2\pi/3$ along the line $\beta = 0$. Likewise, in the right half plane

$\arg(v^{2/3}\zeta)$ varies continuously from $\pi/3$ along $\alpha = 0$ to $4\pi/3$ along $\alpha = 0, \beta = 0$.

The above results on the behavior of $\arg(v^{2/3}\zeta)$ in the v plane, in conjunction with the asymptotic expansions A-2.9 - A-2.12, yield the following expressions for the Airy functions which appear in equations A-1.20 - A-1.27.

$$A_1(v^{2/3}\zeta e^{i\frac{2\pi}{3}}) = \frac{1}{2\pi^{1/2}v^{1/6}\zeta^{1/4}e^{i\pi/6}} e^{i\rho(\sinh\tau - \tau \cosh\tau)} L(\frac{2}{3}v\zeta^{3/2}) \quad (\text{A-1.34})$$

$$A_1'(v^{2/3}\zeta e^{i\frac{2\pi}{3}}) = -\frac{v^{1/6}\zeta^{1/4}e^{i\frac{\pi}{6}}}{2\pi^{1/2}} e^{i\rho(\sinh\tau - \tau \cosh\tau)} M(\frac{2}{3}v\zeta^{3/2}) \quad (\text{A-1.35})$$

$$A_{-1}(v^{2/3}\zeta e^{-i\frac{2\pi}{3}}) = \frac{1}{\pi^{1/2}v^{1/6}\zeta^{1/4}e^{i\pi/12}} \left[\cos(\rho[\sinh\tau - \tau \cosh\tau] + \frac{\pi}{4}) P(\frac{2}{3}v\zeta^{3/2}e^{\frac{i\pi}{2}}) - \sin(\rho[\sinh\tau - \tau \cosh\tau] + \frac{\pi}{4}) Q(\frac{2}{3}v\zeta^{3/2}e^{\frac{i\pi}{2}}) \right] \quad (\text{A-1.36})$$

$$A_{-1}'(v^{2/3}\zeta e^{-i\frac{2\pi}{3}}) = \frac{v^{1/6}\zeta^{1/4}e^{i\frac{\pi}{12}}}{\pi^{1/2}} \left[\cos(\rho[\sinh\tau - \tau \cosh\tau] + \frac{3\pi}{4}) R(\frac{2}{3}v\zeta^{3/2}e^{\frac{i\pi}{2}}) - \sin(\rho[\sinh\tau - \tau \cosh\tau] + \frac{3\pi}{4}) S(\frac{2}{3}v\zeta^{3/2}e^{\frac{i\pi}{2}}) \right] \quad (\text{A-1.37})$$

where

$$L(\frac{2}{3}v\zeta^{3/2}) = 1 + \frac{5}{72 i\rho[\sinh\tau - \tau \cosh\tau]} + \mathcal{O}\left(\frac{1}{v^2\zeta^3}\right) \quad (\text{A-1.38})$$

$$M(\frac{2}{3}v\zeta^{3/2}) = 1 - \frac{7}{72 i\rho[\sinh\tau - \tau \cosh\tau]} + \mathcal{O}\left(\frac{1}{v^2\zeta^3}\right) \quad (\text{A-1.39})$$

$$P\left(\frac{2}{3}v\zeta^{3/2}e^{i\frac{\pi}{2}}\right) = 1 + O\left(\frac{1}{v^2\zeta^3}\right), \quad (\text{A-1.40})$$

$$Q\left(\frac{2}{3}v\zeta^{3/2}e^{i\frac{\pi}{2}}\right) = -\frac{5}{72\rho[\sinh\gamma - \gamma \cosh\gamma]} + O\left(\frac{1}{v^3\zeta^{9/2}}\right), \quad (\text{A-1.41})$$

$$R\left(\frac{2}{3}v\zeta^{3/2}e^{i\frac{\pi}{2}}\right) = 1 + O\left(\frac{1}{v^2\zeta^3}\right), \quad (\text{A-1.42})$$

$$S\left(\frac{2}{3}v\zeta^{3/2}e^{i\frac{\pi}{2}}\right) = +\frac{7}{72\rho[\sinh\gamma - \gamma \cosh\gamma]} + O\left(\frac{1}{v^3\zeta^{9/2}}\right), \quad (\text{A-1.43})$$

and it is assumed that $|\arg v| < \frac{\pi}{2}$. In the angular range $\frac{\pi}{2} < \arg v < \frac{3\pi}{2}$ the Airy function approximations are of the form

$$A_1(v^{2/3}\zeta) = A_1(v^{2/3}\zeta e^{-i\frac{2\pi}{3}}) = \frac{1}{2\pi^{1/2}v^{1/6}\zeta^{1/4}e^{-i\pi/6}} \times e^{-i\rho[\sinh\gamma - \gamma \cosh\gamma]} L\left(\frac{2}{3}v\zeta^{3/2}\right), \quad (\text{A-1.44})$$

$$A_1'(v^{2/3}\zeta e^{-i\frac{2\pi}{3}}) = -\frac{v^{1/6}\zeta^{1/4}e^{-i\frac{\pi}{6}}}{2\pi^{1/2}} e^{-i\rho[\sinh\gamma - \gamma \cosh\gamma]} M\left(\frac{2}{3}v\zeta^{3/2}\right) \quad (\text{A-1.45})$$

$$A_1(v^{2/3}\zeta e^{-i\frac{2\pi}{3}}) = A_1(v^{2/3}\zeta e^{-i\frac{4\pi}{3}}) = \frac{1}{\pi^{1/2}v^{1/6}\zeta^{1/4}e^{-i\pi/12}} \times \left[\cos(\rho[\sinh\gamma - \gamma \cosh\gamma] + \frac{\pi}{4}) P\left(\frac{2}{3}v\zeta^{3/2}e^{-i\frac{\pi}{2}}\right) - \sin(\rho[\sinh\gamma - \gamma \cosh\gamma] + \frac{\pi}{4}) Q\left(\frac{2}{3}v\zeta^{3/2}e^{-i\frac{\pi}{2}}\right) \right] \quad (\text{A-1.46})$$

$$A_1'(v^{2/3} \zeta e^{-i\frac{4\pi}{3}}) = \frac{v^{1/6} \zeta^{1/4} e^{-i\frac{\pi}{12}}}{\pi^{1/2}} \left[\cos(\rho[\sinh \gamma - \gamma \cosh \gamma] + \frac{3\pi}{4}) R(\frac{2}{3} v \zeta^{3/2} e^{-i\frac{\pi}{2}}) - \sin(\rho[\sinh \gamma - \gamma \cosh \gamma] + \frac{3\pi}{4}) S(\frac{2}{3} v \zeta^{3/2} e^{-i\frac{\pi}{2}}) \right] \quad (A-1.47)$$

where

$$L(\frac{2}{3} v \zeta^{3/2}) = 1 - \frac{5}{72i\rho[\sinh \gamma - \gamma \cosh \gamma]} + \mathcal{O}\left(\frac{1}{v^2 \zeta^3}\right) \quad , \quad (A-1.48)$$

$$M(\frac{2}{3} v \zeta^{3/2}) = 1 + \frac{7}{72i\rho[\sinh \gamma - \gamma \cosh \gamma]} + \mathcal{O}\left(\frac{1}{v^2 \zeta^3}\right) \quad , \quad (A-1.49)$$

and the functions P, Q, R and S are identical with the definitions given in equations A-1.40 - A-1.43.

When the above equations are substituted in equations A-1.20 - A-1.27 the following asymptotic expansions are obtained for the Hankel functions.

$$H_v^{(1)}(vz) = \frac{1}{(-\frac{v\pi i \tanh \gamma}{2})^{1/2}} e^{i\rho[\sinh \gamma - \gamma \cosh \gamma] - i\frac{\pi}{4}} \times \left[1 + \frac{1}{v \tanh \gamma} \left(\frac{1}{8} - \frac{5 \coth^2 \gamma}{24} \right) + \mathcal{O}\left(\frac{1}{v^2 \zeta^3}\right) \right] \quad (A-1.50)$$

$$H_v^{(2)}(vz) = \frac{2e^{i\pi/2}}{(-\frac{v\pi i \tanh \gamma}{2})^{1/2}} \left[\cos(\rho[\sinh \gamma - \gamma \cosh \gamma] + \frac{\pi}{4}) + i \sin(\rho[\sinh \gamma - \gamma \cosh \gamma] + \frac{\pi}{4}) \frac{(\frac{1}{8} - \frac{5 \coth^2 \gamma}{24})}{v \tanh \gamma} + \mathcal{O}\left(\frac{1}{v^2 \zeta^3}\right) \right] \quad (A-1.51)$$

$$H_{\nu}^{(1)'}(\nu z) = \frac{\sinh \gamma}{\left(-\frac{\nu \pi i \tanh \gamma}{2}\right)^{1/2}} e^{i\rho[\sinh \gamma - \gamma \cosh \gamma] - \frac{i\pi}{4}} \times \left[1 + \frac{1}{\nu \tanh \gamma} \left(\frac{1}{8} - \frac{5 \coth^2 \gamma}{24} + \frac{1}{2 \sinh^2 \gamma} \right) + \mathcal{O}\left(\frac{1}{\nu^2 \zeta^3}\right) \right] \quad (\text{A-1.52})$$

$$H_{\nu}^{(2)}(\nu z) = \frac{2 \sinh \gamma}{\left(-\frac{\nu \pi i \tanh \gamma}{2}\right)^{1/2}} \left[\cos(\rho[\sinh \gamma - \gamma \cosh \gamma] + \frac{3\pi}{4}) + i \sin(\rho[\sinh \gamma - \gamma \cosh \gamma] + \frac{3\pi}{4}) \frac{\left(\frac{1}{8} - \frac{5 \coth^2 \gamma}{24} + \frac{1}{2 \sinh^2 \gamma}\right)}{\nu \tanh \gamma} + \mathcal{O}\left(\frac{1}{\nu^2 \zeta^3}\right) \right] \quad (\text{A-1.53})$$

where it is assumed that $0 < \arg \nu < \frac{\pi}{2}$. The analogous expansions which are valid in the angular range $\frac{\pi}{2} < \arg \nu < \pi$ are

$$H_{\nu}^{(1)}(\nu z) = \frac{2}{\left(\frac{\nu \pi i \tanh \gamma}{2}\right)^{1/2}} \left[\cos(\rho[\sinh \gamma - \gamma \cosh \gamma] + \frac{\pi}{4}) + i \sin(\rho[\sinh \gamma - \gamma \cosh \gamma] + \frac{\pi}{4}) \frac{\left(\frac{1}{8} - \frac{5 \coth^2 \gamma}{24}\right)}{\nu \tanh \gamma} + \mathcal{O}\left(\frac{1}{\nu^2 \zeta^3}\right) \right] \quad (\text{A-1.54})$$

if $\frac{\pi}{3} < \arg(\nu^{2/3} \zeta) < \pi$, and

$$H_{\nu}^{(1)}(\nu z) = \frac{1}{\left(\frac{\nu \pi i \tanh \gamma}{2}\right)^{1/2}} e^{i\rho[\sinh \gamma - \gamma \cosh \gamma] + \frac{\pi}{4}} \times \left[1 + \frac{1}{\nu \tanh \gamma} \left(\frac{1}{8} - \frac{5 \coth^2 \gamma}{24} \right) + \mathcal{O}\left(\frac{1}{\nu^2 \zeta^3}\right) \right] \quad (\text{A-1.55})$$

when $\pi < \arg(v^{2/3}\xi) < \frac{4\pi}{3}$.

$$H_v^{(2)}(vz) = - \frac{2e^{i\nu\pi}}{(\frac{\nu\pi \tanh \gamma}{2})^{1/2}} \left[\cos(\rho[\sinh \gamma - \gamma \cosh \gamma] + \nu\pi + \frac{\pi}{4}) + \right. \\ \left. + i \sin(\rho[\sinh \gamma - \gamma \cosh \gamma] + \nu\pi + \frac{\pi}{4}) \frac{(\frac{1}{8} - \frac{5 \coth^2 \gamma}{24})}{\nu \tanh \gamma} + \mathcal{O}\left(\frac{1}{\nu^2 \xi^3}\right) \right] . \quad (\text{A-1.56})$$

$$H_v^{(1)'}(vz) = - \frac{2e^{\frac{i\pi}{2} \sinh \gamma}}{(\frac{\nu\pi \tanh \gamma}{2})^{1/2}} \left[\cos(\rho[\sinh \gamma - \gamma \cosh \gamma] + \frac{3\pi}{4}) + \right. \\ \left. + i \sin(\rho[\sinh \gamma - \gamma \cosh \gamma] + \frac{3\pi}{4}) \frac{(\frac{1}{8} - \frac{5 \coth^2 \gamma}{24} + \frac{1}{2 \sinh^2 \gamma})}{\nu \tanh \gamma} + \mathcal{O}\left(\frac{1}{\nu^2 \xi^3}\right) \right] \quad (\text{A-1.57})$$

if $\frac{\pi}{3} < \arg(v^{2/3}\xi) < \pi$, and

$$H_v^{(1)'}(vz) = + \frac{\sinh \gamma}{(\frac{\nu\pi \tanh \gamma}{2})^{1/2}} e^{i\rho[\sinh \gamma - \gamma \cosh \gamma] + \frac{i\pi}{4}} \\ \left[1 + \frac{1}{\nu \tanh \gamma} \left(\frac{1}{8} - \frac{5 \coth^2 \gamma}{24} + \frac{1}{2 \sinh^2 \gamma} \right) + \mathcal{O}\left(\frac{1}{\nu^2 \xi^3}\right) \right] \quad (\text{A-1.58})$$

when $\pi < \arg(v^{2/3}\xi) < \frac{4\pi}{3}$.

$$\begin{aligned}
 H_{\nu}^{(2)'}(\nu z) &= \frac{2ie^{i\nu\pi} \sinh \gamma}{\left(\frac{\nu\pi i \tanh \gamma}{2}\right)^{1/2}} \left[\cos(\rho[\sinh \gamma - \gamma \cosh \gamma] + \nu\pi + \frac{3\pi}{4}) + \right. \\
 &\quad \left. + i \sin(\rho[\sinh \gamma - \gamma \cosh \gamma] + \nu\pi + \frac{3\pi}{4}) \frac{\left(\frac{1}{8} - \frac{5 \coth^2 \gamma}{24} + \frac{1}{2 \sinh^2 \gamma}\right)}{\nu \tanh \gamma} + \mathcal{O}\left(\frac{1}{\nu^2 \zeta^3}\right) \right]
 \end{aligned}$$

(A-1.59)

The asymptotic expansions of the Hankel functions valid in the region $\text{Im}(\nu) < 0$ are easily obtained from the above relations by means of the continuation formulas

$$\underline{H}_{\nu}^{(1)}(u) = e^{i\nu\pi} H_{\nu}^{(1)}(u) \tag{A-1.60}$$

$$\underline{H}_{\nu}^{(2)}(u) = e^{-i\nu\pi} H_{\nu}^{(2)}(u) \tag{A-1.61}$$

As ν approaches the value $i\rho$, that is, $\zeta \sim 0$, the error term $\mathcal{O}\left(\frac{1}{\nu^2 \zeta^3}\right)$ in the asymptotic expansions A-1.50 - A-1.59 rapidly increases. Consequently, the more exact approximations A-1.20 - A-1.27 must be employed in this region.

Complex Zeros of the Hankel Functions of Argument $i\rho$

The asymptotic expansions of the preceding section provide a convenient means of investigating the location of the zeros of the Hankel functions of fixed argument in the complex ν plane. If the argument $i\rho$ is very large, a good approximation to the location of the zeros can be obtained by neglecting all but the leading terms in the expansions A-1.20 - A-1.27. The zeros of the Hankel functions are then given by the zeros of the Airy integrals which appear in the leading terms.

The zeros of the Airy integrals are all real and less than zero. Consequently, it is a rather simple matter to determine the contours on which the zeros of the Hankel functions are located. It is easily deduced from equations A-1.20 - A-1.27 that the zeros of the Hankel functions of the first kind are located on the contour described by the condition $\arg(v^{2/3}\zeta) = \pi/3$. Reference to Figure A-1.2 reveals that this contour is defined by the portions of the imaginary axis for which $|v| > \rho$. The location of the zeros of the Hankel functions of the second kind are also easily determined. In the angular region $-\frac{\pi}{2} < \arg v < \frac{\pi}{2}$ these zeros are situated on the contour defined by the condition $\arg(v^{2/3}\zeta) = -\pi/3$. Likewise, in the angular region $\frac{\pi}{2} < \arg v < \frac{3\pi}{2}$ the zeros are located on the image of the above contour obtained by reflection through the origin.

For the diffraction problem, the zeros of greatest interest are the zeros of the Hankel functions of the first kind in the vicinity of the point $v = i\rho$. In this region the parameter ζ can be expanded in a power series in $(1 - z)$. The coefficients of this series can be obtained from the definition of ζ given in equation A-1.4. Inversion of this series yields the following expansion of z in powers of ζ .

$$z = 1 - 2^{-1/3}\zeta + \frac{3}{10} 2^{-2/3}\zeta^2 + \frac{1}{700} \zeta^3 + \zeta^4 \mathcal{O}(1) . \quad (\text{A-1.62})$$

Define the parameters α_m, β_m, μ_m , and $\bar{\mu}_m$ by the relations $A_1(-\alpha_m) = 0$, $A_1'(-\beta_m) = 0$, $\mu_m^{2/3}\zeta = \alpha_m$, and $\bar{\mu}_m^{2/3}\zeta = \beta_m$. In terms of these parameters, equation A-1.62 yields the relation

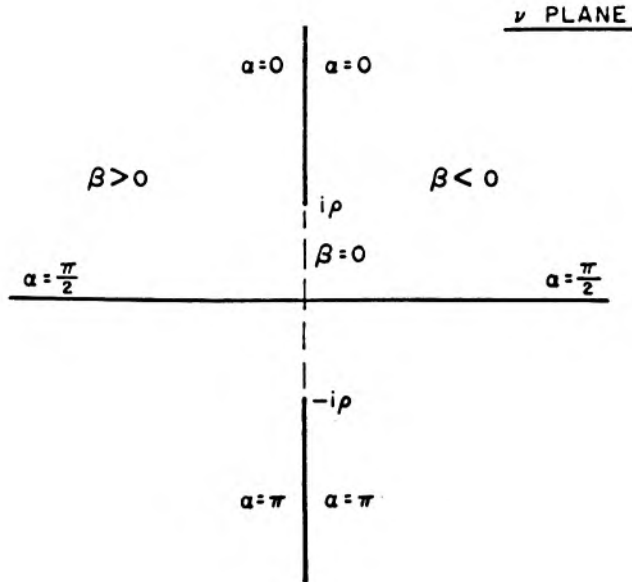


Fig. A1.1 The transformation $v = ip \cosh \gamma$

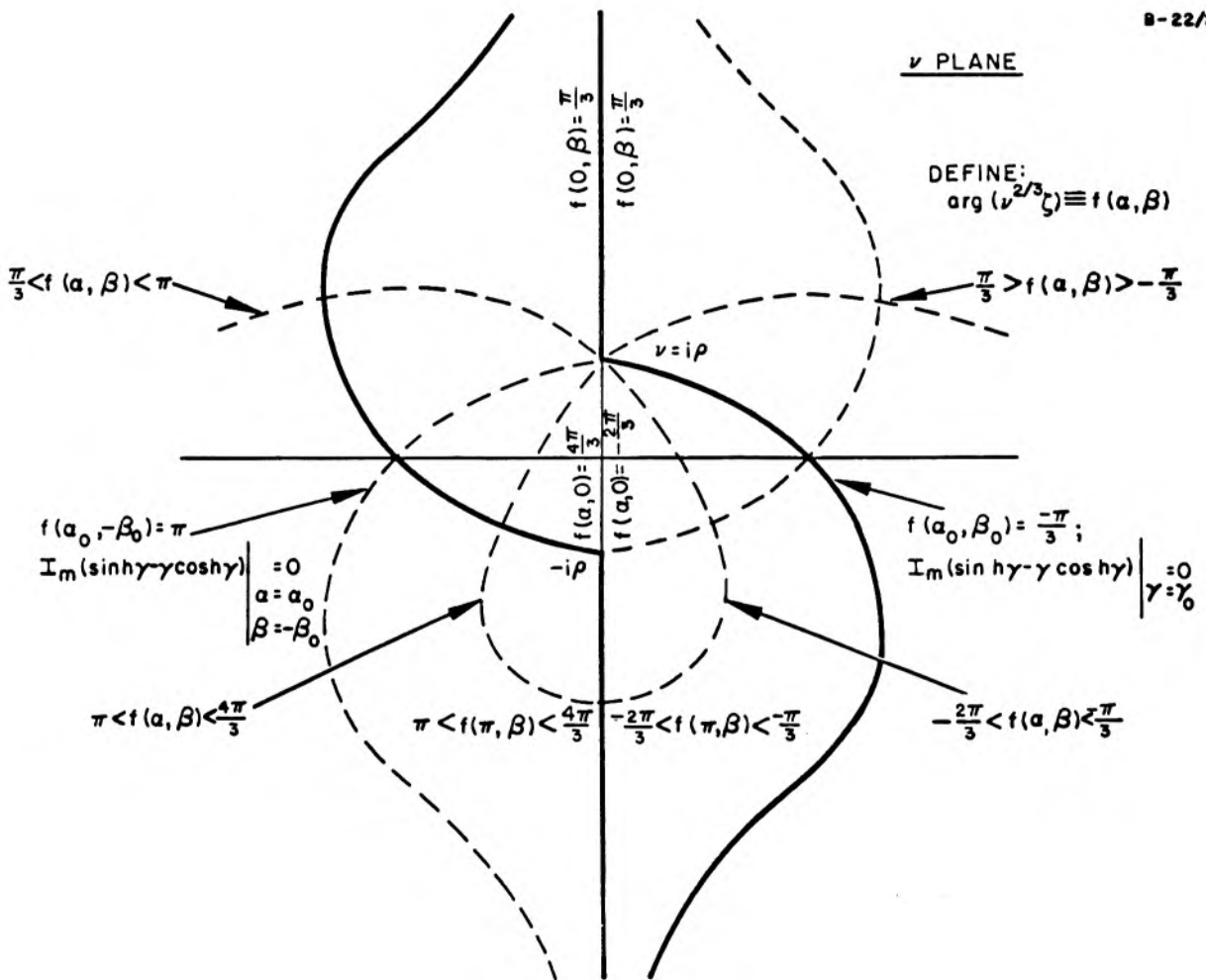


Fig. A1.2 Behavior of $\arg(v^{2/3} \zeta)$ in the v plane

$$\mu_m - \rho = \alpha_m \left(\frac{\mu_m}{2}\right)^{1/3} - \frac{3}{20} \alpha_m^2 \left(\frac{\mu_m}{2}\right)^{-1/3} - \frac{1}{1400} \alpha_m^3 \left(\frac{\mu_m}{2}\right)^{-1} + \mathcal{O}(\mu_m^{-4/3}) \quad (\text{A-1.63})$$

and a similar relation with $\bar{\mu}_m$ and β_m in place of μ_m and α_m .

Equation A-1.63 can be inverted to obtain μ_m or $\bar{\mu}_m$ in a power series in $\rho^{-2/3}$.

$$\mu_m = \rho + \alpha_m \left(\frac{\rho}{2}\right)^{1/3} + \frac{1}{60} \alpha_m^2 \left(\frac{\rho}{2}\right)^{-1/3} - 0.1490 \alpha_m^3 \left(\frac{\rho}{2}\right)^{-1} + \mathcal{O}(\rho^{-4/3}) \quad (\text{A-1.64})$$

The values of the first fifty-six roots of $A_1(-\alpha)$ and $A_1'(-\beta)$ have been tabulated in reference (5) and these tables are repeated in Appendix II.

The zeros of large magnitude can easily be obtained if the Airy functions are replaced by their trigonometric approximations. In this case, equations A-1.50 - A-1.59 are the appropriate Hankel function approximations. The zeros of the Hankel function $H_v^{(1)}(i\rho)$ are situated along the imaginary axis at the points where the argument of the trigonometric function is an odd multiple of $\frac{\pi}{2}$.

$$\rho(\sinh \beta_m - \beta_m \cosh \beta_m) + \frac{\pi}{4} = -\frac{(2m+1)\pi}{2}, \quad (\text{A-1.65})$$

where

$$v_m = i\rho \cosh \gamma_m = i\rho \cosh \beta_m,$$

$m =$ a large positive integer.

If $|v_m| \gg \rho$ these zeros are given approximately by

$$v_m \cong i \frac{(m + \frac{3}{4})\pi}{\ln \frac{(m + \frac{3}{4})\pi}{e\rho}} \quad (\text{A-1.66})$$

Likewise the large zeros of $H_{\nu}^{(1)'}(i\rho)$ are approximately given by the relation

$$\nu_m \approx i \frac{(m + \frac{5}{4})\pi}{\ln \frac{(m + \frac{5}{4})\pi}{e\rho}} \quad . \quad (A-1.67)$$

APPENDIX II

AIRY INTEGRALS

The asymptotic approximations for the Hankel functions contain Airy functions of complex argument. In order to facilitate the understanding of the asymptotic behavior of the Hankel functions, the properties of these Airy functions will be discussed. The material contained in this section is taken primarily from the work of Olver (1,2), Miller (4), and Logan (5).

The Airy integral arises as the solution of the second order differential equation

$$\frac{d^2 w}{dz^2} - zw = 0 . \tag{A-2.0}$$

In the notation of Miller, the two independent solutions of this equation are written

$$A_1(z) = \frac{1}{2\pi i} \int_{L_{31}} \exp\left(\frac{1}{3} u^3 - zu\right) du , \tag{A-2.1}$$

$$B_1(z) = \frac{1}{2\pi} \left[\int_{L_{21}} \exp\left(\frac{1}{3} u^3 - zu\right) du + \int_{L_{23}} \exp\left(\frac{1}{3} u^3 - zu\right) du \right] \tag{A-2.2}$$

where the L_{ij} is a contour originating at i and terminating at j . These contours are illustrated in Figure A-2.0.

The integral representations given in A-2.1, A-2.2 can be used to derive the following useful relations

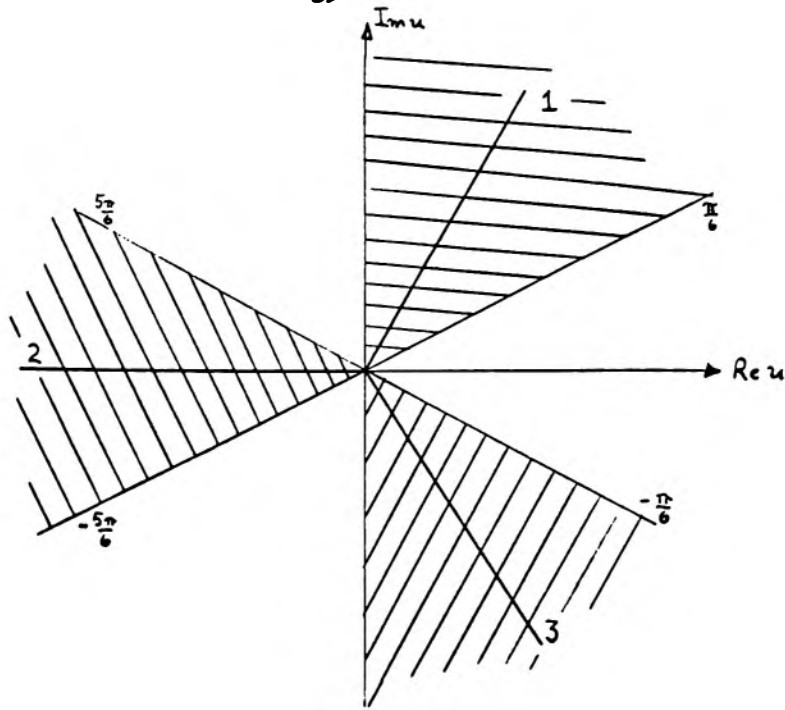


Fig. A-2.0. The Contours L_{ij}

$$A_1(z e^{\pm i \frac{2\pi}{3}}) = \frac{1}{2} e^{\pm i \frac{\pi}{3}} [A_1(z) \mp i B_1(z)] \quad (A-2.3)$$

$$A_1'(z e^{\pm i \frac{2\pi}{3}}) = \frac{1}{2} e^{\pm i \frac{\pi}{3}} [A_1'(z) \mp i B_1'(z)] \quad (A-2.4)$$

The solutions of equation A-2.0 can also be written in terms of the Bessel functions of order one-third. The relation of the Airy integrals to these Bessel functions is summarized in the following set of equations.

$$A_1(z) = \frac{z^{1/2}}{\pi \sqrt{3}} K_{1/3}(\xi) \quad , \quad (A-2.5)$$

$$A_1'(z) = \frac{z}{\pi \sqrt{3}} K_{2/3}(\xi) \quad , \quad (A-2.6)$$

$$A_1(-z) = \frac{z^{1/2}}{2 \sqrt{3}} \left(e^{i \frac{\pi}{6}} H_{1/3}^1(\xi) + e^{-i \frac{\pi}{6}} H_{1/3}^{(2)}(\xi) \right) \quad (A-2.7)$$

$$A_1'(-z) = \frac{z}{2\sqrt{3}} \left(e^{-i\frac{\pi}{6}} H_{2/3}^{(1)}(\xi) + e^{i\frac{\pi}{6}} H_{1/3}^{(2)}(\xi) \right), \quad (\text{A-2.8})$$

where

$$\xi \equiv \frac{2}{3} z^{3/2}.$$

Olver has used the above relations, in conjunction with the well-known asymptotic expansions of Bessel functions of large argument, to obtain asymptotic expansions for the Airy integrals. These expansions are repeated here.

$$\left. \begin{aligned} A_1(z) &\sim \frac{1}{2} \pi^{-1/2} z^{-1/4} e^{-\xi} L(-\xi) \\ A_1'(z) &\sim -\frac{1}{2} \pi^{-1/2} z^{1/4} e^{-\xi} M(-\xi) \end{aligned} \right\} (|\arg z| < \pi) \quad (\text{A-2.9})$$

$$A_1(-z) \sim \pi^{-1/2} z^{-1/4} \left[\cos\left(\xi - \frac{\pi}{4}\right) P(\xi) + \sin\left(\xi - \frac{\pi}{4}\right) Q(\xi) \right] \quad (\text{A-2.11})$$

$$A_1'(-z) \sim \pi^{-1/2} z^{1/4} \left[\cos\left(\xi - \frac{3\pi}{4}\right) R(\xi) + \sin\left(\xi - \frac{3\pi}{4}\right) S(\xi) \right] \quad (\text{A-2.12})$$

$$\left. \right\} (|\arg z| < \frac{2\pi}{3})$$

$$\left. \begin{aligned} B_1(z) &\sim \pi^{-1/2} z^{-1/4} e^{\xi} L(\xi) \\ B_1'(z) &\sim \pi^{-1/2} z^{1/4} e^{\xi} M(\xi) \end{aligned} \right\} (|\arg z| < \frac{\pi}{3}) \quad (\text{A-2.13})$$

$$\quad (\text{A-2.14})$$

$$B_1(-z) \sim \pi^{-1/2} z^{-1/4} \left[\cos\left(\xi + \frac{\pi}{4}\right) P(\xi) + \sin\left(\xi + \frac{\pi}{4}\right) Q(\xi) \right] \quad (\text{A-2.15})$$

$$B_1'(-z) \sim \pi^{-1/2} z^{1/4} \left[\cos\left(\xi - \frac{\pi}{4}\right) R(\xi) + \sin\left(\xi - \frac{\pi}{4}\right) S(\xi) \right] \quad (\text{A-2.16})$$

$$\left. \right\} (|\arg z| < \frac{2\pi}{3})$$

$$B_1(z e^{\pm i \frac{\pi}{3}}) \sim \left(\frac{2}{\pi}\right)^{1/2} e^{\pm i \frac{\pi}{6}} z^{-1/4} \cos\left(\xi - \frac{\pi}{4}\right) + \frac{1}{2} i \ln 2 P(\xi) + \sin\left(\xi - \frac{\pi}{4}\right) + \frac{1}{2} i \ln 2 Q(\xi) \quad (A-2.17)$$

$$B_1'(z e^{\pm i \frac{\pi}{3}}) \sim \left(\frac{2}{\pi}\right)^{1/2} e^{\mp i \frac{\pi}{6}} z^{-1/4} \left[\cos\left(\xi + \frac{\pi}{4}\right) + \frac{1}{2} i \ln 2 R(\xi) + \sin\left(\xi + \frac{\pi}{4}\right) + \frac{1}{2} i \ln 2 S(\xi) \right] \quad (A-2.18)$$

} ($|\arg z| < \frac{2\pi}{3}$)

The functions L, M, P, Q, R, and S which appear in the above equations are asymptotic expansions in terms of the variable ξ . The explicit forms of these expansions are

$$\begin{aligned} L(\xi) &\equiv \sum_{s=0}^{\infty} \frac{u_s}{\xi^s}, & P(\xi) &\equiv \sum_{s=0}^{\infty} (-1)^s \frac{u_{2s}}{\xi^{2s}}, \\ R(\xi) &\equiv \sum_{s=0}^{\infty} (-1)^s \frac{v_{2s}}{\xi^{2s}}, & M(\xi) &\equiv \sum_{s=0}^{\infty} \frac{v_s}{\xi^s}, \\ Q(\xi) &\equiv \sum_{s=0}^{\infty} (-1)^s \frac{u_{2s+1}}{\xi^{2s+1}}, & S(\xi) &\equiv \sum_{s=0}^{\infty} (-1)^s \frac{v_{2s+1}}{\xi^{2s+1}}, \end{aligned} \quad (A-2.19)$$

where the parameters u_s and v_s are defined by the relations

$$u_s \equiv \frac{(2s+1)(2s+3)(2s+5)\cdots(6s-1)}{s!(216)^s}, \quad v_s \equiv -\frac{6s+1}{6s-1} u_s.$$

The locations of the zeros of the Airy functions are also of interest. Olver proves that all possible zeros of the functions $A_1(z)$ and $A_1'(z)$ are located along the negative real axis in the z plane. The position of the first fifty-six of these zeros and the turning values at these points are given to fifteen decimal places by Logan (5). Logan's tables are repeated here in Tables A-I and A-II.

s	α_s	$A_1'(-\alpha_s)$
1	2. 33810 74104 59767	+0. 70121 08227 20691
2	4. 08794 94441 30971	-0. 80311 13696 54864
3	5. 52055 98280 97551	+0. 86520 40258 94152
4	6. 78670 80900 71759	-0. 91085 07370 49602
5	7. 94413 35871 20853	+0. 94733 57094 41568
6	9. 02265 08533 40980	-0. 97792 28085 69499
7	10. 04017 43415 58086	+1. 00437 01226 60312
8	11. 00852 43037 33263	-1. 02773 86888 20786
9	11. 93601 55632 36263	+1. 04872 06485 88189
10	12. 82877 67528 63757	-1. 06779 38591 57428
11	13. 69148 90352 10718	+1. 08530 28313 50700
12	14. 52782 99517 75335	-1. 10150 45702 77497
13	15. 34075 51359 77997	+1. 11659 61779 32656
14	16. 13268 51569 45771	-1. 13073 23104 93188
15	16. 90563 39974 29943	+1. 14403 66732 73553
16	17. 66130 01056 97057	-1. 15660 98491 16566
17	18. 40113 25992 07115	+1. 16853 47844 87525
18	19. 12638 04742 46952	-1. 17988 07298 70146
19	19. 83812 98917 21500	+1. 19070 61311 58776
20	20. 53733 29076 77567	-1. 20106 07915 19823
21	21. 22482 99436 42097	+1. 21098 75148 68287
22	21. 90136 75955 85131	-1. 22052 33738 97260
23	22. 56761 29174 96503	+1. 22970 07015 09681
24	23. 22416 50011 21681	-1. 23854 78753 29632
25	23. 87156 44555 35918	+1. 24708 99452 59407
26	24. 51030 12365 89678	-1. 25534 91404 75735
27	25. 14082 11661 48964	+1. 26334 52827 50799
28	25. 76353 14009 82756	-1. 27109 61262 18604
29	26. 37880 50521 37232	+1. 27861 76388 24258
30	26. 98698 51116 06368	-1. 28592 42371 22704
31	27. 58838 78098 82445	+1. 29302 89834 49956
32	28. 18330 55026 32645	-1. 29994 37525 11048
33	28. 77200 91652 37435	+1. 30667 93729 32094
34	29. 35475 05587 66288	-1. 31324 57481 80648
35	29. 93176 41190 86556	+1. 31965 19603 77514
36	30. 50326 86114 18505	-1. 32590 63598 38441
37	31. 06946 85851 83756	+1. 33201 66426 47702
38	31. 63055 56580 12659	-1. 33798 99181 42291
39	32. 18670 96529 52051	+1. 34383 27678 48983
40	32. 73809 96090 00269	-1. 34955 12971 47445
41	33. 28488 40819 01402	+1. 35515 11807 15907
42	33. 82721 49495 08652	-1. 36063 77026 40532
43	34. 36523 21338 63659	+1. 36601 57919 26784
44	34. 89907 02503 45312	-1. 37129 00540 34239
45	35. 42885 61927 47888	+1. 37646 47989 60084
46	35. 95471 02618 98629	-1. 38154 40663 17105
47	36. 47674 66443 74809	+1. 38653 16477 85955
48	36. 99507 38469 94501	-1. 39143 11072 66471
49	37. 50979 50920 05016	+1. 39624 57990 06725
50	38. 02100 86772 55254	-1. 40097 88839 49769
51	38. 52880 83050 94249	+1. 40563 33445 05322
52	39. 03328 33832 72514	-1. 41021 19979 25998
53	39. 53451 93007 23018	+1. 41471 75084 44110
54	40. 03259 76807 54176	-1. 41915 23983 05068
55	40. 52759 66138 89718	+1. 42371 90578 16189
56	41. 01959 08723 32490	-1. 42781 97545 15052

TABLE I - Roots and turning values of $A_1(-\alpha)$

s	β_s	$A_1(-\beta_s)$
1	1. 01879 29716 47471	+0. 53565 66560 15700
2	3. 24819 75821 79837	-0. 41901 54780 32564
3	4. 82009 92111 78736	+0. 38040 64686 28153
4	6. 16330 73556 39487	-0. 35790 79437 12292
5	7. 37217 72550 47770	+0. 34230 12444 11624
6	8. 48848 67340 19722	-0. 33047 62291 47967
7	9. 53544 90524 33547	+0. 32102 22881 94716
8	10. 52766 03969 57407	-0. 31318 53909 78682
9	11. 47505 66334 80245	+0. 30651 72938 82777
10	12. 38478 83718 45747	-0. 30073 08293 22645
11	13. 26221 89616 65210	+0. 29563 14810 01913
12	14. 11150 19704 62995	-0. 29108 16772 03539
13	14. 93593 71967 20517	+0. 28698 07069 99202
14	15. 73820 13736 92538	-0. 28325 27361 25021
15	16. 52050 38254 33794	+0. 27983 93053 60411
16	17. 28469 50502 16437	-0. 27669 44450 68930
17	18. 03234 46225 04393	+0. 27378 13856 46685
18	18. 76479 84376 65955	-0. 27107 02785 76971
19	19. 48322 16565 67231	+0. 26853 65782 82176
20	20. 18863 15094 63373	-0. 26615 98682 15709
21	20. 88192 27555 16738	+0. 26392 29929 60829
22	21. 56388 77231 98975	-0. 26181 14056 94794
23	22. 23523 22853 48913	+0. 25981 26701 51466
24	22. 89658 87388 74619	-0. 25791 60753 32572
25	23. 54852 62959 28802	+0. 25611 23337 79654
26	24. 19155 97095 26354	-0. 25439 33426 46825
27	24. 82615 64259 21155	+0. 25275 19925 76574
28	25. 45274 25617 77650	-0. 25118 20133 88409
29	26. 07170 79351 73912	+0. 24967 78484 21125
30	26. 68341 03283 22450	-0. 24823 45513 98365
31	27. 28817 91215 23985	+0. 24684 77011 60296
32	27. 88631 84087 68461	-0. 24551 33306 87119
33	28. 47810 96831 02278	+0. 24422 78676 45060
34	29. 06381 41626 38199	-0. 24298 80842 90143
35	29. 64367 48146 32016	+0. 24179 10550 23721
36	30. 21791 81244 68575	-0. 24063 41202 44844
37	30. 78675 56480 12503	+0. 23951 48554 15564
38	31. 35038 53790 83035	-0. 23843 10444 66267
39	31. 90899 29584 30463	+0. 23738 06568 33468
40	32. 46275 27462 38480	-0. 23636 18275 53143
41	33. 01182 87766 34287	+0. 23537 28399 36488
42	33. 55637 56097 89422	-0. 23441 21104 38024
43	34. 09653 90948 09138	+0. 23347 81753 92842
44	34. 63245 70546 35866	-0. 23256 96793 53833
45	35. 16425 99025 53408	+0. 23168 53648 03788
46	35. 69207 11985 10469	-0. 23082 40630 53231
47	36. 21600 81523 35199	+0. 22998 46861 64426
48	36. 73618 20799 46803	-0. 22916 62197 66428
49	37. 25269 88178 54148	+0. 22836 77166 46281
50	37. 76565 91005 38871	-0. 22758 82910 18357
51	38. 27515 89047 30879	+0. 22682 71133 87890
52	38. 78128 97640 80369	-0. 22608 34059 36628
53	39. 28413 90572 98596	+0. 22535 64383 68475
54	39. 78379 02724 68233	-0. 22464 55241 61432
55	40. 28032 32499 03719	+0. 22395 00171 79277
56	40. 77381 44056 64866	-0. 22326 93086 02552

TABLE II - Roots and turning values of $A_1'(-\beta)$

APPENDIX III

ASYMPTOTIC EXPANSION OF THE ANGULAR FUNCTION $P_{\nu-\frac{1}{2}}^1(-\cos \theta)$

The evaluation of the integral representations of the fields scattered by a sphere requires a knowledge of the asymptotic form of the associated Legendre function $P_{\nu}^1(-\cos \theta)$ for large values of the order ν . In obtaining this expansion, the following formulas taken from (6) are useful.

$$e^{-i\mu\pi} Q_{\nu}^{\mu}(\cos \theta \pm i0) = \left(\frac{\pi}{2 \sin \theta}\right)^{1/2} \frac{\Gamma(\nu+\mu+1)}{\Gamma(\nu+\frac{3}{2})} e^{\mp i[\frac{\pi}{4} + (\nu+\frac{1}{2})\theta]} {}_2F_1\left(\frac{1}{2}+\mu, \frac{1}{2}-\mu; \nu+\frac{3}{2}; \frac{\pm i e^{\mp i\theta}}{2 \sin \theta}\right) \quad (A-3.1)$$

$$i\pi e^{i\mu\pi} P_{\nu}^{\mu}(x) = - \left[e^{-\frac{i\mu\pi}{2}} Q_{\nu}^{\mu}(x+i0) - e^{+\frac{i\mu\pi}{2}} Q_{\nu}^{\mu}(x-i0) \right] \quad (A-3.2)$$

$$2e^{i\mu\pi} Q_{\nu}^{\mu}(x) = \left[e^{-\frac{i\mu\pi}{2}} Q_{\nu}^{\mu}(x+i0) + e^{+\frac{i\mu\pi}{2}} Q_{\nu}^{\mu}(x-i0) \right] \quad (A-3.3)$$

$$P_{\nu}^{\mu}(-x) = P_{\nu}^{\mu}(x) \cos \pi(\nu+\mu) - \frac{2}{\pi} Q_{\nu}^{\mu}(x) \sin \pi(\nu+\mu) \quad (A-3.4)$$

where

$${}_2F_1(\alpha, \beta, \gamma, z) = \text{Hypergeometric function} = 1 + \frac{\alpha\beta}{\gamma} \frac{z}{1!} + \frac{\alpha(\alpha+1)\beta(\beta+1)}{\gamma(\gamma+1)} \frac{z^2}{2!} + \dots$$

If μ is set equal to unity and the result is divided by $\cos \nu\pi$, equation A-3.4 becomes

$$\frac{P^1_{\nu - \frac{1}{2}}(-x)}{\cos \nu\pi} = - P^1_{\nu - \frac{1}{2}}(x) \frac{\sin \nu\pi}{\cos \nu\pi} - \frac{2}{\pi} Q^1_{\nu - \frac{1}{2}}(x) ,$$

and this can be written in the more useful form

$$\frac{P^1_{\nu - \frac{1}{2}}(-x)}{\cos \nu\pi} = - P^1_{\nu - \frac{1}{2}}(x) \left(\frac{\sin \nu\pi}{\cos \nu\pi} + \frac{1}{i} \right) - \frac{2}{\pi} \left[\frac{i\pi}{2} P^1_{\nu - \frac{1}{2}}(x) + Q^1_{\nu - \frac{1}{2}}(x) \right] \tag{A-3.5}$$

The bracketed term in A-3.5 can be evaluated with the assistance of equations A-3.2 and A-3.3.

$$\frac{i\pi}{2} P^1_{\nu - \frac{1}{2}}(x) + Q^1_{\nu - \frac{1}{2}}(x) = e^{-\frac{i\pi}{2}} Q^1_{\nu - \frac{1}{2}}(x - i0) . \tag{A-3.6}$$

Also, if $\text{Im}(\nu) > 0$, the factor $(\tan \nu\pi - i)$ can be expanded in powers of $e^{i2\nu\pi}$.

$$\tan \nu\pi - i = i2 \sum_{m=1}^{\infty} (-1)^m e^{i2m\pi\nu} . \tag{A-3.7}$$

Thus the function $\frac{P^1_{\nu - \frac{1}{2}}(-x)}{\cos \nu\pi}$ can be written in the form

$$\frac{P^1_{\nu - \frac{1}{2}}(-x)}{\cos \nu\pi} = - i2 P^1_{\nu - \frac{1}{2}}(x) \sum_{m=1}^{\infty} (-1)^m e^{i2m\pi\nu} + \frac{2i}{\pi} Q^1_{\nu - \frac{1}{2}}(x - i0) \tag{A-3.8}$$

where it is assumed that $\text{Im}(\nu) > 0$.

The explicit forms of the angular functions which appear in A3.8 can be obtained from A-3.1 and A-3.2. The functions $Q_{\nu - \frac{1}{2}}^1(\cos \theta \pm i0)$, from which all of angular functions can be derived, are given by

$$\frac{2i}{\pi} Q_{\nu - \frac{1}{2}}^1(\cos \theta \pm i0) = \left(\frac{2}{\pi \sin \theta}\right)^{1/2} \frac{\Gamma(\nu + \frac{3}{2})}{\Gamma(\nu + 1)} e^{\mp i\nu\theta \pm i\frac{\pi}{4}} {}_2F_1\left(\frac{3}{2}, -\frac{1}{2}; \nu + 1; \frac{\pm ie^{\mp i\theta}}{2 \sin \theta}\right) \quad (A-3.9)$$

The hypergeometric function ${}_2F_1(\alpha, \beta; \gamma; z)$ converges for $|z| < 1$.

Consequently, the expression defined by A-3.9 is a convergent representation of $Q_{\nu - \frac{1}{2}}^1(\cos \theta \pm i0)$ as long as $\frac{\pi}{6} < \theta < \frac{5\pi}{6}$. For other values of θ , A-3.9 is an asymptotic representation which is valid for large values of $\nu \sin \theta$.

REFERENCES

- (1) Olver, F.W.J., "The Asymptotic Solution of Differential Equations of the Second Order for Large Values of a Parameter", Phil. Trans. Roy. Soc. of London, Series A, 247, (1954-55), 307-327.
- (2) Olver, F.W.J., "The Asymptotic Expansion of Bessel Functions of Large Order", Phil. Trans. Roy. Soc. of London, Series A, 247, (1954-55), 328-368.
- (3) Watson, G.N., A Treatise on the Theory of Bessel Functions, Macmillan Company, New York (1948), 75.
- (4) Miller, J.C.P., The Airy Integral, Giving Tables of Solutions of the Differential Equation $y'' = xy$, University Press, Cambridge, (1946).
- (5) Logan, N.A., "General Research in Diffraction Theory--Vol.I", Tech. Rep. IMSD-288087, Lockheed Missiles and Space Division, Sunnyvale, California (1959).
- (6) Erdelyi, Magnus, Oberhettinger, Tricomi, Higher Transcendental Functions, Vol.I, McGraw Hill Book Co., New York (1953), 143-146.
- (7) Leontovitch, M.A., Investigations on Radiowave Propagation, Part II, Printing House of the Academy of Sciences, Moscow, 1948, 5-12. A translation is contained in ASTIA Document No. AD117276.
- (8) Keller, J.B., "A Geometrical Theory of Diffraction" contained in the book, Proceedings of Symposia in Applied Mathematics, Vol.VIII McGraw Hill Book Co., New York (1958).
- (9) Bremmer, H., van der Pol, Balthaser, Operational Calculus Based on the Two-Sided Laplace Integral, Cambridge Univ. Press, (1950).
- (10) Buchal, R.N., Keller, J.B., "Boundary Layer Problems in Diffraction Theory", Research Report No. EM-131, New York University, Institute of Mathematical Sciences, Div. of Electromagnetic Research (1959), 4.
- (11) Lighthill, M.J., Introduction to Fourier Analysis and Generalized Functions, Cambridge at the University Press, (1959), 67-68.
- (12) Weston, V.H., "Pulse Return from a Sphere", Symposium on Electromagnetic Theory, Special Supplement to the IRE Transactions on Antennas and Propagation, (1959), 43-51.
- (13) See reference (5), pages 13-15 through 13-24.
- (14) Stratton, J.A., Electromagnetic Theory, McGraw-Hill Book Company, New York (1941), 419, 564-566.

- (15) Brillouin, L., "The Scattering Cross Section of Spheres for Electromagnetic Waves", Jour. of Appl. Phys. 20, (1949), 1118.
- (16) Watson, G.N., "The Diffraction of Electric Waves by the Earth", Proc. Roy. Soc., 95A, (1918) 83-99.
- (17) Magnus, W., Oberhettinger, F., Formulas and Theorems for the Functions of Mathematical Physics, Chelsea Publishing Company, New York (1954), 72.
- (18) See reference (15), page 1110.
- (19) Fok, V.A., "The Distribution of Currents Induced by a Plane Wave on the Surface of a Conductor", Jour. of Phys. USSR, 10, (1946) 130-136. A translation of this paper is given in ASTIA Document No. AD117276.
- (20) Erdelyi, A., Asymptotic Expansions, Dover, New York (1956), 29-34.
- (21) Fok, V.A., "Fresnel Diffraction from Convex Bodies", Uspekhi Fizicheskikh Nauk, 43, (1951), 587-599. A translation of this paper is given in ASTIA Document No. AD117276.
- (22) Riley, J.A., Billings, C., "Gaussian Quadrature of Some Integrals Involving Airy Functions", Mathematical Tables and Other Aids to Computation, 13 (1959), 97.
- (23) Friedlander, F.G., Sound Pulses, Cambridge at the University Press (1958), 159-160.
- (24) Logan, N.A., "Scattering Properties of Large Spheres", Proc. of the IRE, 48 (1960), 1782.
- (25) See reference (14), page 559.